STUDIES IN THE CATALYTIC REDUCTION AND DECOMPOSITION OF

NITRIC OXIDE

by

DAVID RICHARD DAVIS M.Sc.

A Thesis presented for the Degree of

Doctor of Philosophy

in the

University of Aston in Birmingham

FEBRUARY 1976

SUMMARY

The catalytic reduction of nitric oxide by carbon monoxide was investigated using kinetic and infrared methods.

Reaction rates were monitored by mass spectrometry in a static system over a 0.5% w/w palladium and ruthenium – alumina catalysts between 250 – 500°C at a total pressure of 5 – 18 k Nm^{-2}.

The kinetics are represented by

i) Pd, $r = 2 \times 10^6 (e^{-91.2/RT}) P_{CO}^{-1} P_{NO}^2$ molecules. cm^{-2} sec^{-1}

ii) Ru, $r = 6.3 \times 10^{10} (e^{-82.4/RT}) P_{CO}^{0.22} P_{NO}^0$ molecules. cm^{-2} sec^{-1}

These equations apply for reactions containing an excess of carbon monoxide; they imply that carbon monoxide inhibits the reaction over palladium but not over ruthenium. Evidence is presented in accord with kinetic data that for palladium and reduced ruthenium the reaction proceeds through an adsorbed nitrogen atom. Under conditions of excess nitric oxide nitrous oxide is formed by, $SN\cdot + NO \rightleftharpoons S + N_2O$. In an excess of carbon monoxide surface isocyanates are formed by, $SN\cdot + CO \rightleftharpoons SNCO$. For oxidized ruthenium a reaction scheme which precludes the formation of a nitrogen atom is favoured; in this case the N – N coupling of adjacently adsorbed nitric oxide molecules is thought to occur.

The reaction between nitrous oxide and carbon monoxide was also investigated. This reaction becomes important during the reduction of an excess of nitric oxide by carbon monoxide. Over

ruthenium the decomposition of nitrous oxide is significant; this obeys first order kinetics and is inhibited by carbon monoxide. For equal reactant pressures the kinetics are represented by:-

i) Pd, $r = 4 \times 10^4 (e^{-65.1/RT}) P_{CO}^{\frac{1}{2}} P_{N_2O}^{\frac{1}{2}}$ molecules. cm.$^{-2}$ sec.$^{-1}$

ii) Ru, $r = 2.5 \times 10^4 (e^{-72.3/RT}) P_{CO}^{\sim 0} P_{N_2O}^{1}$ molecules. cm.$^{-2}$ sec.$^{-1}$

Infrared spectroscopy was used to observe the surface of a 10% w/w Pd-Al$_2$O$_3$ catalyst during the nitric oxide - carbon monoxide reaction. In reducing conditions the surface spectra contained strong absorption bands at 2250, 1640, 1575 and 1290cm^{-1}. These bands are interrelated and were assigned to isocyanate species. Experimental results indicate that an isocyanate covered surface still catalyses the reaction; the isocyanate species are relatively stable and are more likely to be formed on selected sites than to act as intermediates.

A C K N O W L E D G M E N T S

To the memory of

my father.

STUDIES IN THE CATALYTIC REDUCTION AND DECOMPOSITION OF NITRIC OXIDE

C O N T E N T S

SECTION 1

CHAPTER 1

INTRODUCTION

1.0

The 1970 Amendment of the Clean Air Act[1] imposed stringent
controls on the levels of emissions permitted from automobiles
for the 1975 model year and beyond.   The U.S. Federal standards
for 1975-1976 of 0.41 g/mile hydrocarbons, 3.4 g/mile carbon mon-
oxide and 0.40g/mile oxides of nitrogen represent a reduction of
at least 90% in the levels of pollutants from uncontrolled vehicles.
Although the oxides of nitrogen standard has recently been relaxed
to 2.0 g/mile, a considerable effort has been mounted by both
catalyst and motor vehicle manufacturers with the 0.4 g/mile oxides
of nitrogen standard as a target Table 1 [2], page 26.

**1.1 MOTOR VEHICLE EMISSIONS; PROPOSED METHODS FOR REMOVAL OF CARBON
MONOXIDE, HYDROCARBONS AND OXIDES OF NITROGEN**

These three pollutants are derived from two main sources in
the internal combustion engine, the crankcase and the combustion
chamber.   Crankcase emissions consist mainly of hydrocarbons which
are degradation products of the engine oil.   In the combustion
chamber hydrocarbons, carbon monoxide and oxides of nitrogen are
formed, the first two being incomplete combustion products.   Oxides
of nitrogen, (mainly nitric oxide) are formed in the combustion
process, following the passage of the flame front[3] and is temper-
ature dependent.   Temperatures in this region are above $2600^{\circ}K$
and are considerably higher than those required for oxidation of
hydrocarbons and carbon monoxide[4].

The extent of production of these pollutants depends upon the
condition of each individual engine, for example carburettor tuning
governs air/fuel ratios which has been shown to effect[5] the ratios
of these emissions.   The spark-ignition system also plays an im-
portant role, controlling the combustion process and can lead to
pre-ignition and detonation.   Figure 1 on page 25 shows qualitat-
ively the effect of the air/fuel ratio on emissions of hydrocarbons,
carbon monoxide and oxides of nitrogen.   The figure shows that
hydrocarbons and carbon monoxide levels decrease at first as the
air/fuel ratio increases.   At high air/fuel ratios hydrocarbon
emissions may increase again because dilution lowers the flame temp-
erature whereas excess oxygen and high flame temperatures promote
more thorough combustion.   The formation of the oxides of nitrogen
is at its peak when the fuel mixture is slightly leaner than stoich-
iometric.   Optimum conditions occur at an air/fuel ratio of about
18, corresponding to a level of 2.0g/mile for oxides of nitrogen,
for an average passenger car.   This level is considerably above the
mandatory 0.4 g/mile originally proposed by Federal law.

A variety of methods have been proposed to diminish the concen-
tration of the three main pollutants.   These methods fall into two
main categories.   The first category requires the modification of
a conventional internal combustion engine and the second a complete
re-design of this engine.   Both categories not only have inherent
technical difficulties but are also restricted to date dead-lines
and capital expenditures.   Because of these time restrictions and
cost problems the former category has received the most attention.

Effective reduction of hydrocarbons and carbon monoxide levels

have been obtained by improved carburetion and spark-ignition systems and by the incorporation of a thermal and/or a catalyst afterburner system [5,6]. The thermal afterburner can be regarded as a secondary combustion chamber in which unburnt or partially burnt hydrocarbons and carbon monoxide are treated by injecting air into a secondary chamber where the gases are still sufficiently hot to enable complete combustion. With regard to the reduction of oxides of nitrogen levels it is apparent from Figure 1 that carburetion settings required for its removal are not consistent with the maximum removal conditions of hydrocarbons and carbon monoxide. The reduction of oxides of nitrogen can be obtained by lowering the combustion temperature and by changing the compression ratio and spark tuning [5]. This also can be achieved by diluting the fuel mixtures by recirculating cooled exhaust gases. A 60% reduction of oxides of nitrogen can be obtained by this method [6].

Unfortunately there is a price to be paid for the reduction in emissions of these three pollutants. The systems described together with their variants generally lead to a reduction in the performance of the car and in some cases will also reduce fuel efficiency. A high standard of maintenance is also required for these systems to achieve maximum efficiency. [5]

Apart from the mechanical methods the use of catalytic afterburners which have been studied extensively [7,8] provides a promising short term method of reducing these three pollutants. The problem is how to manufacture afterburners of high reliability and long life. In general, catalyst and motor vehicle manufacturers have opted for

a dual bed approach. This approach requires the engine to be tuned rich to create a reducing atmosphere in which oxides of nitrogen can be removed in the first bed and then with the help of an air pump a second catalyst bed provides an oxidation process for the removal of remaining carbon monoxide or hydrocarbons.

In addition to these methods recent events in the Middle East together with a general increase in oil prices may provide a natural restraint to the overall production of these emissions.

1.2 CATALYTIC STUDIES FOR THE ELIMINATION OF OXIDES OF NITROGEN

Discussion in this section will be confined to proposed methods of the elimination of nitric oxide, since the oxidation of hydrocarbons and carbon monoxide can be accomplished with relative ease.

Fundamentally there appears to be two ways in which the removal of nitric oxide can be accomplished catalytically, either 1) by decomposition or 2) by reaction, for example with carbon monoxide. Before discussing these methods a brief review of the general properties of the nitric oxide molecule has been made in order to assess its reactivity.

1.2.1 GENERAL PROPERTIES OF NITRIC OXIDE: STABILITY

Table 2 on page 26 represents a brief description of the physical and thermodynamic properties of nitric oxide[9]. A prominent property of nitric oxide is its large thermodynamic instability with respect to elemental nitrogen and oxygen at ambient conditions. Despite the pronounced thermodynamic instability nitric oxide is kinetically extremely stable. Low reaction rates obtained for the homogeneous thermal decomposition of nitric oxide below $1000^{\circ}C$ accompanied with comparatively high activation energies, 290.7kJ

mol^{-1} [10] , 266.9 kJ mol^{-1} [11] reflect this kinetic stability. An experiment carried out by Howard and Daniels[12] serves amply as a further illustration of the kinetic stability of this unstable species. In 1917 these workers sealed nitric oxide in tubes together with a random but very wide assortment of solid catalysts. Inspection in 1958 indicated that the decomposition at room temperature was below the detection limit.

1.2.2 BONDING BEHAVIOUR OF NITRIC OXIDE

The chemisorption and nature of the subsequent bond of nitric oxide must be considered as an important step in a catalytic reaction. Since one could plausibly select metal catalysts which may prove to be active on this basis.

The nature of the bonding of the nitric oxide molecule arises from the odd electron in its structure. The molecular orbital scheme for nitrogen, oxygen and nitric oxide[13] is represented as follows.

Atomic Orbitals N	Atomic Orbitals O	Molecular Orbitals NO
2pz (↓) 2py (↑) 2px (↓) 2s (↑↓)	2px (↑) 2py (↑) 2pz (↑↓) 2s (↑↓)	σ^* 2pz ( ) π^* 2py (↑) ( ) π^*2px π 2py (↑↓) (↑↓) π2px σ 2pz (↑↓) σ^* 2s ( ) σ 2s (↑↓)

Coulson[14] gives the following molecular orbital description of the bonding in the nitric oxide molecule. The 2s electrons

on both the oxygen and nitrogen do not contribute to the bonding.
Two electrons in both the σ 2px and 2py molecular orbitals provide
a σ and a π - bond, while the remaining orbitals constitute a three
electron π -bond. The π^* 2pz orbital is antibonding and the remov-
al of the electron from this orbital results in increased bond
strength.

The molecule can form ionic or covalent bonds. As indicated
in Table 2 the low ionization potential makes for easy conversion
to the positive nitrosonium [NO]$^+$ ion and conversely by acquir-
ing an electron it can be converted to the negative nitrosyl [N=O]$^-$
ion. Nitric oxide can co-ordinate as a neutral entity by donating
a lone pair of s-electrons M.-$^\cdot$NO, by donating this pair plus the
odd electron M.- $\overset{+}{N}\equiv O.$, or by accepting an electron and forming an
electron pair bond M.-N= $\overset{+}{\underset{-}{O}}$ [15].

Simplified electronic diagrams[13] represent the changes in
electron configuration in the bonding of the nitric oxide group,
for the three modes of bonding.

covalent
$- \ddot{N} \overset{\pi}{=} \ddot{O}\colon$

cation
$[\colon N \overset{\pi}{\underset{\pi}{=}} O\colon]^+$

anion
$[\colon \dot{N} \overset{\pi}{=} \dot{O}\colon]^-$
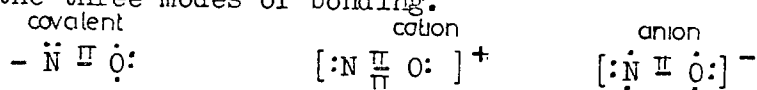
On transition metals the bonding is similar to those of
inorganic nitric oxide compounds[16][17].

A large amount of information has been gained about the nature
of the molecule on the surface from surface experiments. These
techniques include: surface infrared spectroscopy, and low energy
electron defraction (LEED). Terenin and co-workers[18] have studied
the infrared spectrum of nitric oxide adsorbed on metals, metal
oxides. These authors have assigned the bands at highest frequ-
ency to ionic species 2100-2400 cm^{-1}, for example, $\frac{NO^+}{S}$ species

having slightly lower frequences 2100 – 1800 cm^{-1} were assigned

to co-ordination type structures for example, $N \rightleftharpoons O$ co-ordina-

tive ionic

$$\overset{..}{\underset{\overline{\quad}}{S}}$$

and co-ordinative.

$$\overset{O}{\underset{\overline{\quad}}{\overset{N}{\overset{..}{S}}}}$$
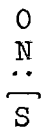
Structures giving rise to bands at lower frequencies were assigned

to species with nitrogen-oxygen double bond character

$$\overset{O}{\underset{\overline{\quad}}{\overset{\|}{\underset{\|}{N}}}} + \text{, covalent} \qquad \overset{O}{\underset{\overline{\quad}}{\overset{|}{\underset{|}{N}}}} \text{ and anionic} \qquad \overset{-}{\underset{\overline{\quad}}{N\ O}}$$
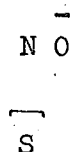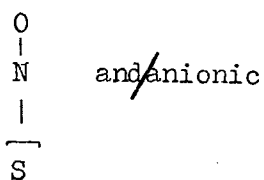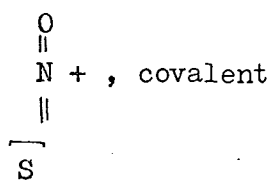
In a recent review article Shelef and Kummer[19] concluded

that in most cases the bonding of nitric oxide to the surface

the nitrogen-oxygen bond was not weakened substantially and that

the bond to the surface is mostly through the nitrogen end of the

molecule.   It was also noted that every transition metal ion has

its own predominant mode of bonding.

1.2.3 CATALYTIC DECOMPOSITION OF NITRIC OXIDE

Interest in the catalytic decomposition of nitric oxide has

arisen since the possibility of its decomposition in a catalytic

afterburner system.   The low free energies of the following de-

compositions and disproportionation reactions[20] again illustrate

the thermodynamic instability, which was discussed in section 1.2.1

(1) $2\ NO \longrightarrow N_2 + O_2$ ΔG^{o} – 172.8 kJ mol^{-1}

(2) $4\ NO \longrightarrow N_2 + 2NO_2$ ΔG^{o} – 241.8 kJ mol^{-1}

(3) $4\ NO \longrightarrow O_2 + 2N_2O$ ΔG^{o} – 136.8 kJ mol^{-1}

(4) $3\ NO \longrightarrow N_2O + NO_2$ ΔG^{o} – 102.9 kJ mol^{-1}
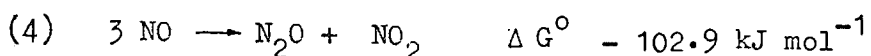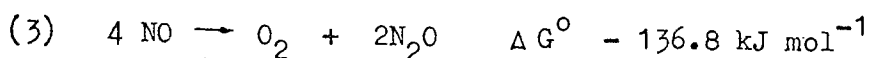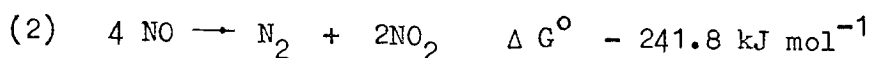
A comparison of the specific rates of decomposition of nitric

oxide to similar catalytic systems has been made by Boreskov[21].
This comparison emphasized the fact that the rate of nitric oxide
decomposition is by one or two orders of magnitude slower than the
notoriously slow oxidation of methane.

Much of the early work on the dissociation of nitric oxide
was carried out on platinum.   Table 3 on page 26   taken from
Laidler[22] indicates clearly that a number of rate laws have been
obtained.   These laws were interpreted using Langmuir-Hinshelwood
kinetic schemes.[22,23,24] and imply that the reaction is inhibited
in some way by oxygen.

There is also disagreement about its mode of decomposition.
Green and Hinshelwood[25] have suggested a unimolecular mechanism
whereas Bachman and Taylor[26] believed the reaction was bimolecular.
Sakaida et al.[28] have also suggested a bimolecular surface reaction.
A third order rate has also been proposed[20], under a homogeneous
low temperature and high pressure conditions.   The results of sub-
sequent work[29,30,31] on a variety of catalysts have shown that a
number of orders of reaction with respect to nitric oxide have been
obtained.   These orders vary from 0,1,2.   At constant temperature
the order of reaction mainly depends upon the reactant pressure,
which governs the degree of surface coverage; upon the affinity
which the reactant has for the substrate and the nature of the
bonding.   Thus it is reasonable not only to obtain different orders
of reaction between catalysts, but also on the same catalyst, de-
pending upon reaction conditions.   The interpretation of the order
becomes of prime importance when considering the mechanistic reac-
tion sequence for a reaction under a set of particular conditions.

Copper chromite, cobalt oxide and copper supported on silica
are some of the best catalysts known to catalyse this reaction[32].

The order with respect to nitric oxide for these catalysts was close to 1. It is also noteworthy that these authors obtained orders of <0.5 for commercial noble metal catalysts. Yuan[31] et al. have observed that the rate of decomposition is not only affected by temperature and pressure but also upon the diluent gas used. It was found that the rate is fastest in helium, slowest in carbon dioxide and intermediate in the presence of nitrogen. They[31] concluded reasonably that this order was the same as that of the boiling points of the gases, thus the more condensable gases carbon dioxide and nitrogen are adsorbed more readily on catalytic surfaces, thereby reducing the effective surface and poisoning the catalyst.

In an attempt to study the feasibility of using a catalyst for the heterogenous decomposition of nitric oxide in an exhaust after burner system. Shelef et al.[32] have re-investigated most of the catalysts known to be active for this decomposition. These authors have concluded that the removal of nitric oxide by this method is slow and impractical.

The feasibility of using polymer catalysts[33] for the removal of nitric oxide from exhaust emission has recently been studied by Cooper[34]. Using pyrolysed acrylonitrile co-polymer (PAN P) nitric oxide interactions were studied over a temperature range of 250 - 700°C. Cooper concluded that the features which promoted the well known oxidative instability of PAN P were also effective in causing high nitric oxide removal activity. PAN P however became inactive under dynamic conditions, and

did not promote any reaction with carbon monoxide or

hydrogen.

1.2.4 CATALYTIC REDUCTION OF NITRIC OXIDE

In the last decade a great deal of research has been carried out in order to assess catalysts which promote the reduction of nitric oxide. Logically the reducing agents used for this reduction are those which are already present in exhaust emissions, for example carbon monoxide, hydrocarbons and hydrogen.

Thermodynamic data for the reduction of nitric oxide by carbon monoxide and hydrogen is given in Table 4 on page 27. The large negative heats of formation and free energies indicate that potentially such reductions are very good, provided of course that the proper conditions exist and that a thermodynamic barrier is not obtained in any reaction intermediate stage.

Despite the thermodynamic feasibility of such reactions the reduction of nitric oxide is not as simple as it would first seem. The ability of the catalyst to be selective to the reaction in question is one of the major problems. The catalyst may promote a series of competitive reactions in an exhaust atmosphere producing undesirable products or act to poison the catalyst. Besides this catalyst poisons such as lead- lead alkyls are already present in exhaust emissions. Together, these problems effectively reduce the catalyst efficiency and life. A summary of the competitive desired and undesired reactions are listed in Table 5 on page 27. Some of the reactions listed in the Table 5 will be discussed later.

1.2.5 CATALYTIC REDUCTION OF NITRIC OXIDE BY CARBON MONOXIDE

Catalyst surveys of Taylor[35](1959), Sourirajan and Blumenthal[34] (1961), Roth and Doerr[37](1961) and Ayen and Ng Yu-Sim [38] (1966)

have demonstrated that the removal of nitric oxide present in low concentrations by reduction with carbon monoxide and/or hydrogen can be achieved by catalysts such as zinc-copper chromite, iron-oxide, iron-chromite, barium promoted copperchromite, chromium promoted·iron oxide and copper oxide-silica. A comparison similar to that made by Boreskov[21] (section 1.2.3) has been made by Shelef et al.[39]. Over transition metal catalysts, such as those described above, the carbon monoxide - nitric oxide reaction rates were compared to the carbon monoxide - oxygen reaction rates. These authors observed that for 50% removal of carbon monoxide most catalysts with the exception of iron oxide and supported chromia showed that the carbon monoxide - oxygen reaction was considerably faster. They also noted that with the exception of the position of iron oxide the relative catalyst sequence in the carbon monoxide-oxygen reaction followed a well established series of the oxides with respect to oxidation-reduction catalytic reactions. On the other hand, the sequence for the carbon monoxide - nitric oxide reaction followed $Fe_2O_3 > Cu\,Cr_2O_4 > Cu_2O > Cr_2O_3 > NiO > Pt > Co_3O_4 > Al_2O_3$ (5% Silica) $MnO > V_2O5$ which is altogether different from the oxidation - reduction catalytic series. From this result it was suggested that the limiting stage of the oxidation mechanism with the participation of nitric oxide differs from that with the participation of oxygen.

In the majority of cases the search for a catalyst which will effectively promote the reduction of nitric oxide by carbon monoxide has been carried out under a stoichiometric excess of the reducing agent. These conditions effectively maintain the surface of a

metal – metal oxide catalyst in a relatively low oxidation state.

The work of Roth and Doerr[37] points out the importance of the

oxidation state of the catalyst since this will have a profound

effect on the chemisorption behaviour of nitric oxide.   When the

reaction conditions are reversed, that is, a reaction which takes

place under a stoichiometric excess of nitric oxide besides the

products carbon dioxide and nitrogen, nitrous oxide is formed.[40,41]

The formation of nitrous oxide was described by Baker and

Doerr[40] as involving the partial reduction of nitric oxide by

carbon monoxide for example:–

$$2NO + CO = N_2O + CO_2 \qquad \Delta H f^o_{298} \quad - \quad 382.2 \text{ kJ mol}^{-1}$$

$$N_2O + CO = N_2 + CO_2 \qquad \Delta H f^o_{298} \quad - \quad 364.5 \text{ kJ mol}^{-1}$$

overall reaction

$$2NO + 2CO = N_2 + 2CO_2 \qquad \Delta H f^o_{298} \quad - \quad 746.6 \text{ kJ mol}^{-1}$$
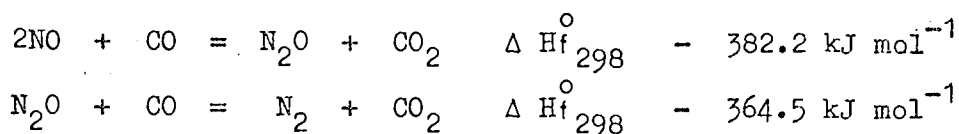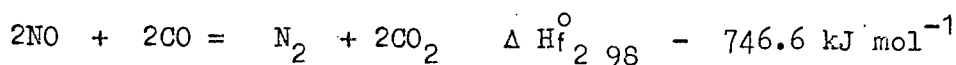
Thermodynamically these reactions are still feasible (data taken

from Table 4) although the negative heats of formation are app-

roximately one half that described for the overall reaction.

The formation of nitrous oxide was shown to take place on

a wide assortment of catalysts by Shelef and Otto[41].   Iron

oxide, copper oxide, nickel oxide, platinum and oxides of chrom-

ium and cobalt were among some of the catalysts tested.   These

authors noted that the formation of nitrous oxide not only de-

pended upon reactant stoichiometry but also upon reaction tem-

perature.   In all cases tested nitrous oxide formation passed

through a peak with temperature rise.   For an iron oxide cat-

alyst this peak occured at 200^oC, above 350^oC no nitrous oxide

was measured.   Similarities between the temperature - nitrous
oxide curves and catalyst efficiency   for the reduction of nitric
oxide by carbon monoxide were also noted.   In general, the greater
the temperature range the catalyst was less effective in the
formation of carbon dioxide.   In conclusion it was suggested[41,19]
that nitrous oxide behaves as a true gas intermediate, in the
sequence of reactions described above.

Relatively little is known about the mechanism of reaction
between nitric oxide and carbon monoxide.   The mechanism will
obviously depend upon the catalyst and the reaction conditions
used.   Ayen and Ng[38] and Force and Ayen[42] have reported that the
kinetics of the reaction carried out in the presence of copper chro-
mite can be described by a rate expression derived from a single
mechanism which assumes that the rate limiting step is the reaction
between adsorbed carbon monoxide and nitric oxide.   The equation
which describes this mechanism was derived from Langmuir - Hinshelwood
kinetic theory[22], estimates of the constants involved were obtained
by linear and non-linear least squares analysis[43].

$$ r = \frac{k \; b_{NO} \; P_{NO} \; b_{CO} \; P_{CO}}{(1 \; + \; b_{NO}P_{NO} \; + \; b_{CO}P_{CO})^2} $$

where P = pressure of reactant

b = adsorption constants

k = surface reaction rate constant.

Shelef and Kummer[19] have criticized this mechanism because
it fails to explain the formation of nitrous oxide, and because a
dual site mechanism was proposed for this catalytic system.   These

authors were of the opinion that the mechanism may be regarded as the redox type involving the alternate reduction and oxidation of the catalyst surface, i.e the reduced surface of supported chromia or copper chromite reacting with nitric oxide to produce nitrous oxide and/or nitrogen. Shelef, Otto and Gandhi[39] were of the same opinion, nitric oxide serving to re-oxidize the surface, this step was assumed to be the rate limiting one. Since the overall redox mechanism is associated with the scission of the surface-oxygen bond the decreasing reactivity sequence of the transition metal oxides to this reaction (mentioned earlier in this section) was stated as further evidence for this rate limiting step. This sequence correlates well with increasing oxygen - surface bond strengths[21].

London and Bell[44,45] using simultaneous infrared and kinetic studies have described a more detailed mechanism for the reaction over a copper oxide catalyst. This mechanism consists of nine elementary steps and includes the participation of nitrous oxide. The principal assumptions being that nitric oxide dissociates upon adsorption, that nitrous oxide acts as an intermediate to the formation of nitrogen, and that carbon monoxide maintains the catalyst surface in a reduced state as well as competing for sites needed for the dissociation of nitric oxide. The expression which describes nitric oxide consumption, resulted from these nine elementary steps:-

1 $\quad Cu + NO \rightleftharpoons Cu - NO$

2 $\quad Cu - NO + Cu^+ \longrightarrow Cu - N + Cu^{2+} O^-$

3 $\quad Cu - N + NO \longrightarrow Cu + N_2O$

4      $Cu^+ + CO \rightleftharpoons Cu^+ CO$

5      $Cu + N_2O \rightleftharpoons Cu - ONN$

6      $Cu - CNN \rightarrow Cu^+ O^- + N_2$

7      $Cu^{2+}O^- + CO \rightarrow Cu^+ + CO_2$

8      $Cu^+ O^- + CO \rightarrow Cu + CO_2$

9      $CuN + CO \rightleftharpoons Cu^+ NCO^-$
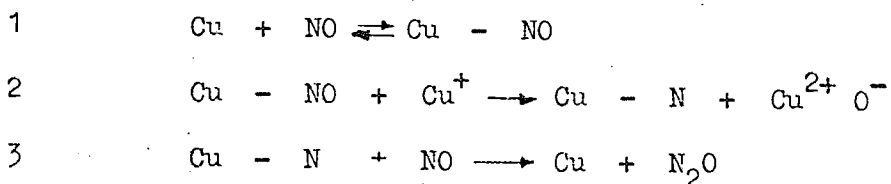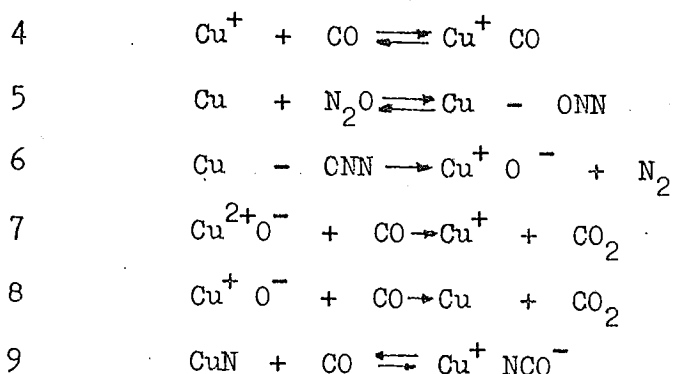
proposed reaction rate expression

$$- r_{NO} = \frac{2b \, b_2 \, C_{NO}}{(1 + b_2 \, C_{NO} + b_3 \, C_{N_2O})(1 + b_4 \, C_{CO})}$$

where b, b_2, b_3 and b_4 are constants.

Evidence for the dissociation of nitric oxide was gained by the identification of a surface isocyanate species equation 9.

Unland[46,47,48] has also identified the formation of surface isocyanate species during the reduction of nitric oxide by an excess of carbon monoxide on platinum, palladium, rhodium and ruthenium - alumina catalysts. Of all the noble metal catalysts ruthenium was found to give the weakest isocyanate spectrum. The discovery of the presence of a surface isocyanate has led to the postulation of new mechanistic pathways for the nitric oxide - carbon monoxide reaction. Unland[46] has proposed for example that the isocyanate acts as a true reaction intermediate and offered the following plausible pathway

$$NO \xrightarrow[\text{>300}^\circ C]{Pt/Al_2O_3} N_{ads} + O_{ads}$$

$$N_{ads} + CO \longrightarrow NCO_{ads}$$

$$O_{ads} + CO \longrightarrow CO_2$$

$$NCO_{ads} + NO \longrightarrow N_2 + CO_2$$

$$2NO + 2CO \longrightarrow N_2 + 2CO_2 \quad \text{Total reaction}$$
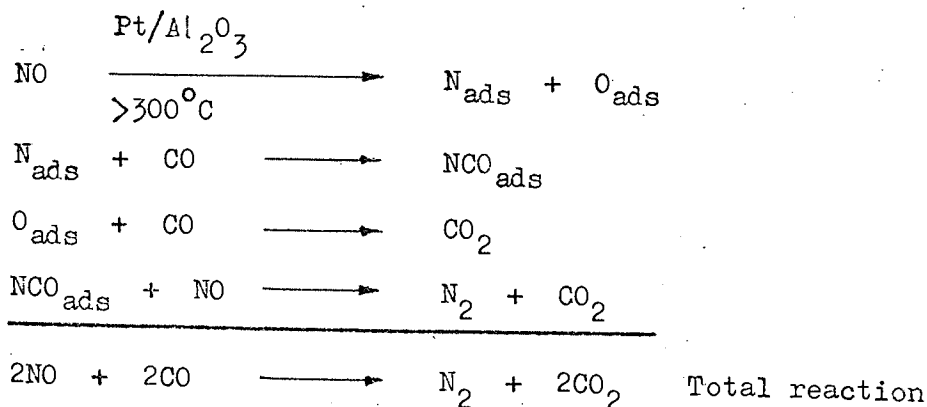
This mechanism is compatible with that of London and Bell[45], each requires the dissociation of nitric oxide as a prerequisite to isocyanate formation. It is still not clear if this occurs through direct dissociation of nitric oxide on the surface or during the formation of a reaction intermediate involving carbon monoxide.

1.2.6 CATALYTIC REDUCTION OF NITROUS OXIDE BY CARBON MONOXIDE

Nitrous oxide formation during the nitric oxide-carbon monoxide catalyzed reaction has been described as a reaction intermediate[41,45] and occurs as a result of the partial reduction of nitric oxide (section 1.2.5). Because of this it is necessary to consider separately the reduction of nitrous oxide by carbon monoxide represented by the equation

$$N_2O + CO = CO_2 + N_2 \quad - \Delta H f_{298} \quad - 364 \text{ k J mol}^{-1}$$

A limited amount of information is available on the catalyzed reduction of nitrous oxide. Bawn (1935)[49] studied this reaction in a quartz vessel at $550^{\circ}C$, and established that the reaction proceeded by a dual surface mechanism having a rate law of $\frac{dCO_2}{dt} = k \frac{[N_2O]}{[CO]}$, carbon monoxide being strongly adsorbed on quartz. Diluent inert gases and nitric oxide did not appreciably affect the reaction rate but carbon dioxide was found to be auto-catalytic. The explosive limits of the reaction were also established, the minimum explosive limit for a 1:1 reactant ratio being 106 kNm^{-2} at $590^{\circ}C$. Since Bawn's work the reaction has also been found to occur catalytically on charcoal[50,51] zinc oxide[52], and chromium promoted iron oxide[53]. Tanaka and Blyholder[52] have suggested different reaction mechanisms for the photochemical and the catalytic reaction over zinc oxide. The slow steps of the thermal

catalytic reaction was described as the reaction between weakly adsorbed carbon monoxide and an intermediate O^- species while under illumination the slow step was thought to be reaction between N_2O^- and CO^- sites produced by illumination. Interestingly, the catalytic slow step is similar to that described by Shelef et al.[39] (section 1.2.5) a redox process. The reaction rate laws obtained[52] are reflected in the following suggested mechanisms:-

thermocatalytic rate $\quad r = k\ PCO\ PN_2O^0$

photocatalytic rate $\quad r = k\ PCO^{0.4}\ PN_2O^{0.4}$

More recently Leach and Peters[53] selected a chromium promoted iron oxide catalyst for a kinetic study into the nitrous oxide – carbon monoxide reaction. This catalyst was selected because it showed high activity for the nitric oxide – carbon monoxide reaction and promoted nitrous oxide formation as an intermediate. A number of rate expressions were evaluated using the Langmuir –Hinshelwood approach[22] and the power rate model suggested by Weller[54]. A dual surface reaction was again proposed, which fitted an empirical power rate model derived on the basis of carbon monoxide adsorbed on a Lewis acid site and nitrous oxide adsorbed on a Lewis base site. The reactant was found to be retarded in the presence of carbon dioxide.

1.2.7 CATALYTIC REDUCTION OF NITRIC OXIDE BY HYDROGEN, AMMONIA AND HYDROCARBONS

The two main sources of hydrogen from exhaust emission interactions arise from 1) hydrogen formation by the water gas shift reaction:-

$$CO + H_2O \rightleftharpoons CO_2 + H_2$$

and 2) hydrogen formation from hydrocarbons, and from steam reforming of hydrocarbons.

$$C_n H_{(2n+2)} + 2n\ H_2O \rightleftharpoons nCO_2 + (3n+1)\ H_2$$
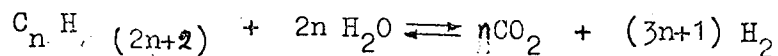
In the reaction between nitric oxide and hydrogen three different products can be formed depending upon reactant stoichiometry, 1) the formation of ammonia 2) the formation of nitrogen and 3) the formation of nitrous oxide: in each case water is the other product

$$NO + \tfrac{5}{2}\ H_2 \rightleftharpoons H_2O + NH_3$$

$$NO + H_2 \rightleftharpoons H_2O + \tfrac{1}{2}N_2$$

$$2NO + H_2 \rightleftharpoons H_2O + N_2O$$
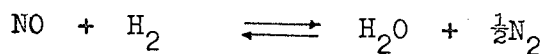
Early observations on the reduction of nitric oxide by hydrogen are given in a review in Gmelen's Handbuck[55]. Recently, Kokes[56] showed that for a large excess of hydrogen ammonia is almost the sole product of this reduction, (over platinium). Ammonia formation has been noted by a number of workers[57,58] when sampling gases from a dual bed catalyst exhaust test systems. Shelef and Gandhi[57] have considered a number of base and noble metal catalysts for the removal of nitric oxide. For each group of catalysts the formation of ammonia increased and subsequently decreased with increasing temperature. In the presence of carbon monoxide ammonia formation decreased for palladium and platinium catalysts but increased for a ruthenium catalyst. This result was confirmed by Taylor and Klimish[59] in a comparison of noble metal catalysts platinium, palladium and ruthenium for reaction mixtures containing nitric oxide, hydrogen and carbon monoxide.

For reaction mixtures containing nitric oxide and hydrogen a

relatively low ammonia yield was noted[59] for the ruthenium cata-lyst in comparison with palladium and platinum catalysts. This result was attributed to the relatively strong chemisorption prop-erty of nitric oxide on ruthenium and the relative affinity of ruthenium to promote nitrogen formation rather than ammonia[57]. Ayen and Peters[60] suggested the mechanism and the rate controlling step for the formation of ammonia, was the reaction between diss-ociated reactant molecules. Other workers[59] have also proposed the dissociation mechanism whereby a single N-surface site is formed, thus facilitating the reaction between hydrogen to form ammonia.

One other mechanism for the formation of ammonia has been des-cribed by Unland[46-48]. In this case it was proposed that ammonia can be formed by the hydrolysis of surface isocyanate species, for example,

$$- (NCO) + 2H_2O \longrightarrow NH_3 + CO_2 + (OH).$$
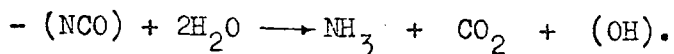
The formation of the isocyanate was described in section 1.2.5.

It is interesting to note the formation of nitrous oxide becomes apparent in the reaction mixtures containing a stoichiometric excess of nitric oxide[61]. These conditions are similar to those which were required to produce amounts of nitrous oxide in the reduction of nitric oxide by carbon monoxide, section 1.2.5. In the reduction of nitric oxide by carbon monoxide, nitrous oxide has been described as a reaction intermediate, it is not unreasonable to suppose that if this is the case, then nitrous oxide could be a reaction intermediate in the reduction of nitric oxide by hydrogen under these conditions. In either case the reaction mechanisms are likely to be very similar if not identical.

The reduction of nitric oxide by ammonia[61,62,63] is allied to the reduction of nitric oxide by hydrogen since it could be classed as a secondary or intermediate reaction in the overall mechanism. Again, there seems to be two different reaction processes depending upon reactant stoichiometry, this is illustrated by the following equations:-

$$4NH_3 + 6NO = 5N_2 + 6H_2O$$

$$2NH_3 + 8NO = 5N_2O + 3H_2O$$
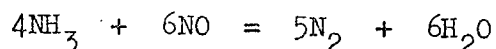
In general catalysts which are active to the reduction of nitric oxide by ammonia are active for the above reactions. Shelef et al.[63] have observed that in the lower temperature range two surface steps governing the nitric oxide-ammonia reaction are an important path in the "defixation" of nitrogen (i.e. formation of nitrogen or nitrous oxide) in the reduction of nitric oxide by hydrogen. Nitrogen was described as being formed predominantly from the interaction of one molecule of ammonia and one molecule of nitric oxide, while nitrous oxide in contrast is formed mainly by the interaction of a pair of nitric oxide molecules.

The formation of ammonia, and its intermediacy as a basis for catalyst selection for nitric oxide reduction has recently been suggested by Klimisch and Taylor[64]. These authors used dual functional catalysts to promote the formation of ammonia and its subsequent decomposition. For example palladium and platinium catalysts are known to produce ammonia in large amounts under the above reaction conditions, whilst nickel catalysts actively decompose ammonia. By catalyst combination a major

path to the formation of elemental nitrogen with ammonia as an
intermediate was suggested

$$NO \longrightarrow NH_3 \longrightarrow N_2$$
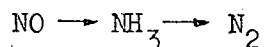
Ruthenium posseses the unusual quality in that it performs both
functions effectively under certain conditions.

Apart from the catalytic reduction of nitric oxide by carbon
monoxide, hydrogen and ammonia the feasibility of the reaction
with hydrocarbons has also been investigated.[58,65] Once again
the reaction products are governed by reactant stoichiometry.
Using methane as an example, catalytic reactions can occur by the
following:—

$$CH_4 + 4NO = 2N_2 + 2H_2O + CO_2$$

$$5CH_4 + 8NO + 2H_2O = 5CO_2 + 8NH_3$$
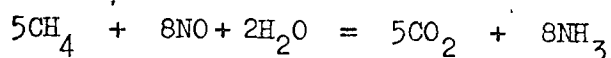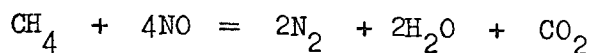
Ammonia formation in the reduction of nitric oxide with sat-
urated hydrocarbons is minimal over a variety of catalysts in the
absence of water vapour (copper, nickel, ruthenium). In reactions
between olefins, ammonia formation begins at much higher temperature
than the nitric oxide hydrogen reaction[66] but it has a narrow temp-
erature range because of the thermodynamic instability of ammonia
at this temperature.

Shelef and Gandhi[66] are of the opinion that ammonia formation
from hydrocarbons in the presence of steam can be disregarded,
the reaction being very much slower than the competitive nitric
oxide hydrogen reaction (hydrogen being generated from the water gas
shift reaction).

1.2.8 CATALYST SELECTIVITY

The question of catalyst selectivity has been mentioned

briefly in section 1.2.4. A summary of the competitive reactions which may occur in an exhaust atmosphere is given in Table 5. The water gas reaction, ammonia formation and methanation reactions are among the major reactions which compete with the reduction of nitric oxide by carbon monoxide. The choice of catalysts now becomes one of relative selectivity towards the reaction in question. Iron catalysts for example promote the water gas reaction in preference to the nitric oxide - carbon monoxide reaction. Iron, nickel and ruthenium catalysts show selectivity for the methanation reaction whereas platinium palladium and iridium are comparatively inert[67]. Ammonia production, in the reaction between nitric oxide and hydrogen increases for the catalysts ruthenium, platinium and palladium[59].

The question of dual functional catalysts has been considered[64,66]. These catalysts generally contain ruthenium, which exhibits high activity for the nitric oxide - carbon monoxide reaction as well as promoting the decomposition of ammonia. Unfortunately, this catalyst exhibits two very different activities depending upon its oxidation state[68]. For example, it promotes the water gas reaction in its oxidized state, but not in the reduced state.

The choice of catalysts for use in an afterburner system not only depends upon selectivity but also upon durability, poison resistance, mechanical properties and thermal stability[8].

1.3 REASON FOR WORK

The previous sections have indicated that reactions of nitric oxide are numerous and more complex that would at first

seem.

Kinetic studies of the reduction and decomposition of nitric oxide have generally been carried out over base metal – oxide catalysts in the presence of diluent gases under dynamic experimental conditions. Diluent gases[31,49] can and do effect catalyst activity and thus have a direct influence upon the resultant kinetic and mechanistic predictions. The mechanisms proposed based on kinetic data have not been substantiated by independent evidence, although the redox approach to some of the reactions is useful in explaining the competitive reactions of nitric oxide and oxygen with reducing agents.

Other studies have been directed towards finding catalysts which promote the reduction of nitric oxide in an exhaust atmosphere. Obviously, there is a need for a study into the reduction of nitric oxide under fundamental reaction conditions, for example in a static system without diluent gases.

A number of catalysts have been described which promote the reduction of nitric oxide. Nitrous oxide, ammonia and surface isocyanate have been described as reaction intermediates, depending upon the reducing agent. The formation of these intermediates seem to be interrelated mechanistically since they depend for their formation upon 1) the degree of affinity of nitric oxide toward the catalyst 2) upon a specific temperature range and 3) upon the amount of reducing agent present in a reaction mixture. The choice of catalyst for this investigation was not only governed by the ability of the catalyst to promote the reduction of nitric oxide but upon the chemical properties of the reactants towards the catalysts.

Palladium and ruthenium were chosen as catalysts since they represent opposing ends of a "reactivity series". Nitric oxide is strongly adsorbed on ruthenium but not on palladium, in contrast carbon monoxide is relatively more strongly adsorbed on palladium but not on ruthenium. In reaction mixtures containing nitric oxide, carbon monoxide, and hydrogen, ruthenium, platinium, and palladium catalysts produce ammonia and nitrous oxide in increasing amounts respectively[59], they also produce an increasing quantity of isocyanate species[48]. The above properties should be reflected in the rate laws which govern the reduction of nitric oxide over palladium and ruthenium catalysts.

Alumina was chosen as a support for these catalysts because it is inert to the reduction of nitric oxide, below $500^{\circ}C$, and it has a high surface area.

Unland[46] has suggested that the surface isocyanate acts as an intermediate in the reduction of nitric oxide by an excess of carbon monoxide over a platinum catalyst. Unlands'[46,47.48] observations and assignments have not been independently substantiated and related to a kinetic study. For this reason an infrared surface study of this reaction over a palladium catalyst was initiated.

FIGURE 1
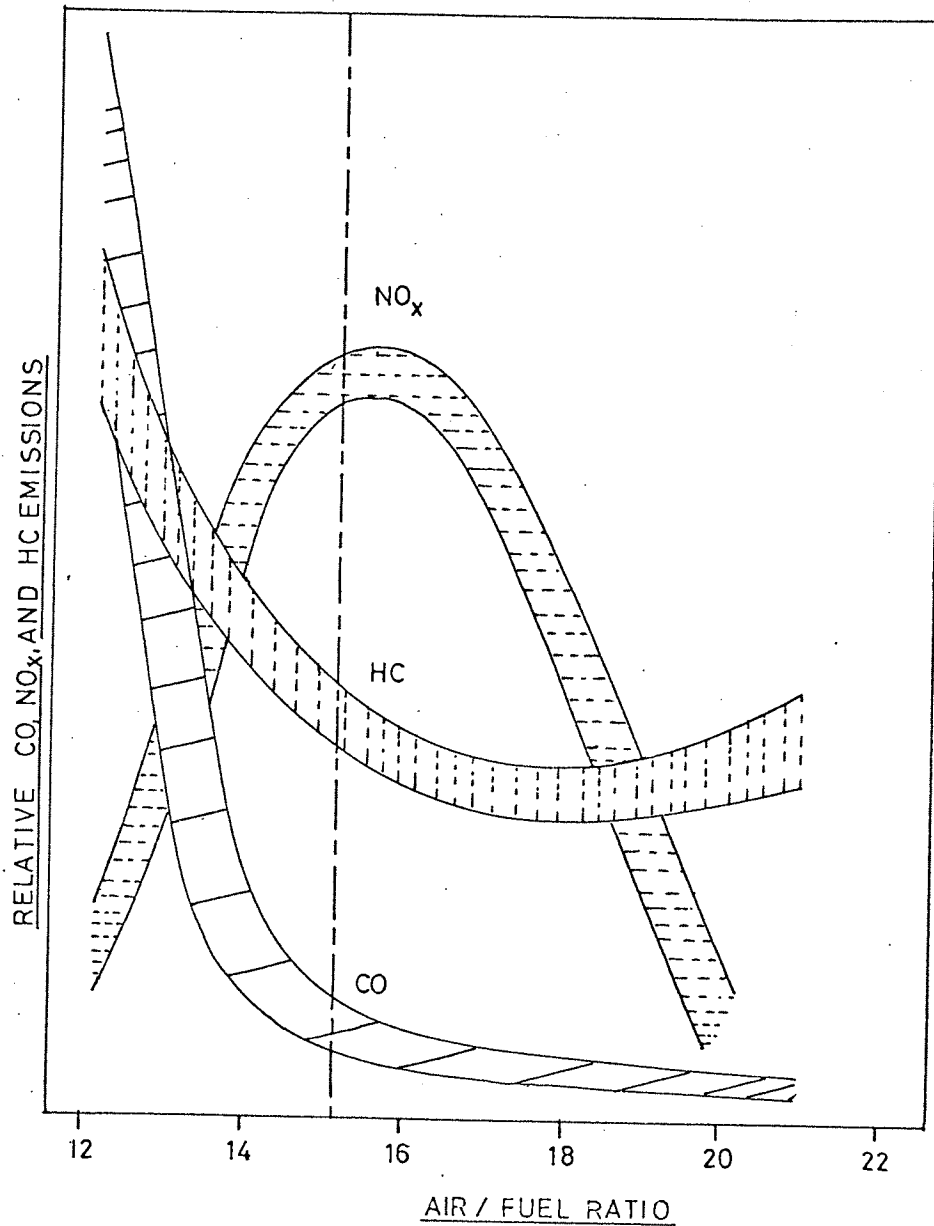
EFFECT OF AIR/FUEL RATIO ON EMISSIONS.[5]
THE RELATIVE CO, NO$_x$, AND HC EMISSIONS
ARE NOT TO SCALE

TABLE 1

Federal Motor Vehicle emission standards, g/mile[2]

SUBSTANCE	1971	1972	1973	1974	1975	1976
HC	4.1	3.0	3.0	0.41	0.41	0.41
CO	34.0	28.0	28.0	3.4	3.4	3.4
NO_x	–	–	3.1	3.1	3.1	0.4

TABLE 2

Showing some of the Physical and Thermodynamic Properties of Nitric Oxide[9]

Molecular Properties	Thermodynamic Properties
Bond energy 631.8 kJmol^{-1}	melting point 109.49° K
Bond length 0.115 nm	boiling point 121.36° K
1st ionization potential 9.5v	$\Delta H f^{\circ}_{298K}$ + 89.9 kJ mol^{-1}
Dipole moment 0.16 Debye	$\Delta G f^{\circ}_{298K}$ + 86.4 kJ mol^{-1}

TABLE 3

Showing different rate laws obtained for the decomposition of Nitric Oxide on Platinum

Surface	Temp. Range $^{\circ}$C	Pressure Range $k\,Nm^{-2}$	Rate Law	Activation Energy kJ mol^{-1}	Ref.
Pt	882 – 1403	13.3–66.6	$r = k \dfrac{[NO]}{[O_2]}$	585	25
Pt	1210	26.8–63.8	$r = k \dfrac{[NO]^2}{[O_2]}$	102.9–112.5	26
Pt	860 – 1060	–	$r = \dfrac{k[NO]}{1+b[O_2]}$	92.0–104.6	27

TABLE 4

Listing Thermodynamic data for the reduction of Nitric Oxide by
Hydrogen and Carbon Monoxide.

* calculated.

Ref	Reaction	$kJmol^{-1}$ 298°K			623°K		
		ΔHf	ΔE^{o}	ΔG^{o}	ΔHf^{o}	ΔE^{o}	ΔG^{o}
35	$2NO+2CO=N_2+2CO_2$	−746.67	−685.19	−687.67	−748.4	−743.6	−750.3
*	$2NO+CO=N_2O+CO_2$	−382.2	−384.4	−326.91	−383.88	−389.1	−387.61
*	$N_2O+CO=CO_2+N_2$	−364.51	−364.51	−360.7	−364.87	−364.7	−364.87
36	$NO+H_2=H_2O+\frac{1}{2}N_2$	−332	−	−316	−	−	−
36	$NO+^{5/}2H_2=H_2O+NH_3$	−378	−	−324			

TABLE 5

Oxidation and reduction reactions with Catalysts in the presence
of Exhaust Gases

D = Desired reaction   UD Undesired reaction   UD* as UD but desired if
large amounts of ammonia
are produced.

REACTION	SELECTIVITY
$NO + CO = \frac{1}{2}N_2 + CO_2$	D
$2NO + CO = N_2O + CO_2$	D
$N_2O + CO = N_2 + CO_2$	D
$NO + ^{5/}2H_2 = H_2O + NH_3$	UD
$NO + H_2 = H_2O + \frac{1}{2}N_2$	D
$CO + H_2O = CO_2 + H_2$	D
$CH_4 + 4NO = 2N_2 + 2H_2O + CO_2$	D
$5CH_4 + 8NO + 2H_2O = 5CO_2 + 8NH_3$	UD
$4NH_3 + 6NO = 5N_2 + 6H_2O$	UD*
$2NH_3 + 8NO = 5N_2O + 3H_2O$	UD*
$2NH_3 + 3N_2O = 4N_2 + 3H_2O$	UD*

CHAPTER 2

EXPERIMENTAL

Studies into the reduction and decomposition of nitric oxide were carried out in a static system with no added diluent gases. The reaction rates were measured as either the appearance or disappearance of product or reactant respectively by mass spectrometry. Butler[69] has used a similar technique for a study into the kinetics of the catalytic decomposition of ethanol over alumina.

2.0   APPARATUS FOR MONITORING REACTION KINETICS: General Desription

The apparatus consists of an A.E.I. MS.10 mass spectrometer coupled to a thermostatically controlled reaction vessel through a 4F grade Metrosil leak.   The reaction vessel is connected to a preheat chamber and a mixing chamber, all of which could be evacuated by a mercury diffusion pump and rotary backing pump: each pump has the usual cold trap facilities.

The Figure 2 page 44   (1:10 scale) represents a diagram of the apparatus described above.   The apparatus in the Figure 2 can be divided into three main sections, a description of these sections follows.

2.01. MASS SPECTROMETER: Specifications and Operating Conditions

The mass spectrometer an A.E.I. MS.10 operated on the single focusing principle had   a mass range of 2 to 200.   Operational sample pressures in the mass spectrometer were of the order of $4 \times 10^{-4} \ Nm^{-2}$.   A needle valve which was bolted on to the analyser tube of the spectrometer enabled the mass spectrometer to be isolated from the leak sampling and reaction vessel systems.   Table 6 lists the operating voltages used, and the specification of the main components (page 51).

2.02. LEAK PROBE

In order to monitor the reactions continuously in the reaction vessel a leak system was used which effectively reduced the gas pressure in the reaction vessel (pressures around 5.3 kNm^{-2}) to the low pressure required for efficient running of the mass spectrometer, around 4.0×10^{-4} Nm^{-2}.

The Figure 3 page 45 is a scale diagram of the leak probe. The leak probe was made up from a B24/29 Quickfit male ground glass joint with a borosilicate 1/16" I.D. glass capillary tube attached through its centre. At the probe end of the leak a 1/4" length of 1/16" dia. 4F grade Metrosil was fused into the capillary tube; this length was found by trial to be the most efficient for the reduction of gas pressure from the reaction vessel to the mass spectrometer. At the opposite end of the capillary and glass joint was attached a Jencons Lynx-Seal metal-glass joint. The stainless steel 1/4" metal tube attached to the glass was connected to a coiled length (30cm) of 1mm bore stainless steel tube, which in turn was connected to the needle valve on the analyser tube of the spectrometer. Vacuum tight joints were made by Hoke Gyrolok adaptors.

The leak probe attached to the flexible coiled stainless steel tube could easily be manoeuvred into position; a vacuum tight seal was obtained when the probe was inserted into the B24 female joint on the reaction vessel.

2.03. REACTION VESSEL AND GAS MIXING SYSTEMS

The third section of the apparatus was made from borosilicate glass and consists of a reaction vessel, pre-heat and gas mixing chambers. Each of these chambers could be isolated by taps A,B,

and H, Figure 2. The volume of these chambers were determined to be 450cc, 257cc and 86.3cc respectively.

The reaction vessel, provided with a central thermocouple well was completely enclosed by an electrical furnace. The temperature of the furnace was controlled by an Ether Transitrol, the thermocouple (chromel alumel) of which was positioned in the well of the reaction vessel directly above the catalyst bed.

The pre-heat chamber was also enclosed by a furnace, the temperature of which was controlled by a variac transformer and thermocouple/potentiometer meter.

The gas mixing chamber consists of a single length 45cm, 1.8cm bore glass tubing. Attached to the tube are two mercury manometers, two gas reservoir bulbs, and a single outlet for an infrared cell; all of which could be individually isolated by ground glass taps C,D,E,F,G, Figure 2. The manometers consisted of 1) a Griffin and George 100mm Hg manometer and 2) a calibrated length of graduated tubing for which 1 unit $=$ 1.165 mm Hg. The second manometer measured gas pressures of up to 420 mm Hg $(56k\ Nm^{-2})$. The gas inlet is controlled by tap H.

The whole system is attached through a three way tap (A) to a vacuum line. Vacuum was obtained from a mercury diffusion pump and a rotary backing pump; each pump having the usual cold trap facilities. Pressures in the system were measured by an Edwards high vacuum gauge through a 65B-2 gauge head and were of the order of 0.13 Nm^{-2}.

A gas inlet system was connected at tap H to the mixing chamber. This system ensured that when tap H was partially opened a positive pressure of reactant gas was always obtained. Each gas was provided with a separate cold trap.

2.1 PREPARATION OF CATALYSTS

One of the most common methods employed for the preparation of supported metal catalysts is by impregnation of a support with an aqueous solution of a metal salt. After drying the salt is reduced in flowing hydrogen at elevated temperatures. This technique was adopted for the preparation of the catalysts used for this work.

2.1.1. PREPARATION OF THE SUPPORT γ-ALUMINA

The support γ-aluminium oxide 8/16 mesh (Fisons) contained sulphur impurities which can act to poison the catalyst. The sulphur was removed as hydrogen sulphide.

In an oven ($\sim$60g) of γ-alumina was heated to 450°C, hydrogen was passed through the oven at 40 ml/min until hydrogen sulphide was no longer detected in the gas effluent stream. The sample was then allowed to cool slowly to room temperature. The oven temperature was controlled by a variac transformer and temperature/ potentiometer meter.

2.1.2 IMPREGNATION OF 0.5% WEIGHT PALLADIUM ON THE SUPPORT

Palladium chloride 0.33 g (B.D.H. Chemicals) containing 60% palladium was dissolved in 250 ml distilled water on a hot plate. The pretreated support γ-alumina 39.7 g was then added to the solution, and the water evaporated off slowly to ensure even impregnation. After drying at 120°C the catalyst was calcined in air over night at 450°C, then reduced in a stream of hydrogen at 40ml/min for 4 hours at 450°C. The catalyst was then allowed to cool to room temperature in a hydrogen atmosphere before bottling.

2.1.3 IMPREGNATION OF A 0.5% WEIGHT RUTHENIUM ON THE SUPPORT

Using the method described in the previous section the catalyst was prepared by adding 20g of pretreated γ-alumina to a solution of ruthenium III chloride (0.257g). The ruthenium chloride was obtained from B.D.H. chemicals and contained 39% ruthenium.

2.2 ANALYSIS OF THE CATALYST CONTENT

To test the efficiency of the impregnation procedure an analysis of the catalyst content was made. The palladium catalyst was chosen for this experiment.

One of the most common methods for the determination of palladium is by gravimetric analysis of a suitable palladium complex, for example palladium 1:2 cyclohexanedione dioxime.[70] This method is used for solutions containing 5-30mg of palladium. The presence of alumina however complicates the gravimetric analysis.

The method adopted for analyses of palladium utilized the measurement of the energy of emitted X-rays. Using a scanning electron microscope coupled to an energy dispersive X-ray analyser, (Kevex Corporation of America), standards containing known amounts of palladium were examined. Characteristic X-ray energies of the elements present, for example palladium L_α, L_{β_1}, 2.838 and 2.990kev respectively, were collected and displayed as a series of peaks on a T.V. monitor.

For a constant counting time the area under the palladium peak is proportional to the concentration of palladium in the sample; (provided the background radiation is first subtracted). This area was measured electronically and expressed as an integral of the total number of counts in the channels under the peak. The number of

channels under the peak could be preselected, 1 channel representing 10 e.v. For standardization nine channels were selected to count the standards and the samples. The background count under these channels was subtracted electronically.

Under identical experimental conditions the area under the palladium L_{α_1} peak was determined for a series of standards and samples. The palladium content of the samples could then be determined from a calibration graph of the standards against counts per unit time.

The advantage of using the Kevex system is that unlike x-ray wavelength analysis[71] the whole spectrum is collected and analysed instantaneously for elements $Z > 11$ to $Z98$. Provided conditions are standardized the spectrum can be analysed quantitatively using a series of known standards.

2.2.1 METHOD: PREPARATION OF CATALYST STANDARDS, AND ELECTRON MICROSCOPE SAMPLES

A series of standards containing 1%, 0.8%, 0.5%, 0.3% and 0.2% by weight palladium to 1g. alumina were prepared using the impregnation technique described in section 2.1.2, with one exception. After the water had been evaporated off the impregnated alumina and residue (if any) was ground in a mortar. Washings from the beaker were also added to the powder, which was then redried and ground. This procedure ensured that any palladium residue was mixed homogeneously in the powder before hydrogenation. The five standards together with two powdered catalyst samples were reduced as described in section 2.1.2.

From each standard and sample a disc of 1cm x $\frac{1}{2}$mm was made by compressing 70-100 mg of the powder at 10 tons/sq.inch in an infra-

red KBr die. Making a note of the sample number and position a $2mm^2$ portion from each disc was mounted (using clear Bostik), on a electron microscope sample stub, 1 cm dia. To ensure a conducting path for the electrons the stub and samples were coated with vapour deposited carbon, sprayed for 8 sec.

2.2.2 OPERATING CONDITIONS OF ELECTRON MICROSCOPE AND KEVEX

Table 7 on page 52 lists the operating conditions used for the electron microscope and energy dispersive x-ray analyser, (Kevex). To ensure standardization the operating conditions were kept constant for each determination. Each sample was counted for 500 sec. over a relatively large sample surface area 4×10^{-8} cm^2, to ensure that a good statistical count was obtained.

Figure 4 on page 46 represents a spectrum obtained for the 1% w/w $Pd-Al_2O_3$ standard. The Figure shows the integrated area under the palladium $L\alpha_1$ peak which was counted.

2.2.3 RESULTS

Figure 5 page 47 is the calibration graph obtained from a plot of the standards against counts per 500 sec. A line of best fit gave a standard deviation of 63 counts which represents 0.04% Pd. The catalyst samples gave counts of 1303 and 1305 respectively, representing a palladium content of 0.49 ± 0.04 by weight to alumina.

The efficiency of the impregnation was calculated to be $> 98\%$, well within experimental limits. This method relies on the fact that the samples must have a homogeneous distribution of palladium, and that they must be prepared and counted under standard conditions.

2.3 DETERMINATION OF THE SURFACE AREA OF THE CATALYSTS

In order that reaction rates could be expressed in terms of

rate per unit surface area, the surface area of the palladium and ruthenium - alumina catalysts were determined. The nitrogen adsorption apparatus used was a modified version of the classical B.E.T. apparatus[72]. Cooper[34] developed this apparatus for the determination of surface areas of polymer catalysts.

The apparatus (1:25 scale) in Figure 6 page 48 was made out of boro-silicate glass. The volumes of the four graduated bulbs, the sample holder S and the dead space are listed in Table 8 page 52 . The apparatus was connected at point E to a vacuum line which consisted of a mercury diffusion pump and rotary backing pump; each pump having the usual cold trap facilities. The vacuum in the system was measured by an Edward's high vacuum pirani gauge.

2.3.1 METHOD

With tap F open to atmosphere and a vacuum up to tap A, taps A and D were adjusted so that a difference in mercury levels of 30 cm was reached in the narrow bore manometer.

The three way tap F was turned to allow successive flushes of nitrogen and vacuum, (tap B being open to vacuum) whilst tap C was opened until the mercury level reached the top of the first graduated bulb. Then, with the preweighed sample in place, tap B was opened, tap F closed, and the sample holder S immersed in an oven. The sample was then evacuated to a pressure of less than 0.13 Nm^{-2} at $250^{\circ}C$ for one hour.

Following evacuation tap B was closed and the oven removed from around the sample. When the sample had cooled to room temperature the vessel S was immersed in a flask of liquid nitrogen. After a period of five minutes to ensure the sample had reached $-196^{\circ}C$,

tap F was opened so that nitrogen at a pressure of one atmosphere, filled the dead space on the right hand side of the apparatus. Bulb 1 was emptied of mercury and tap F turned to isolate the apparatus from the outside nitrogen reservoir. After a period of two minutes for adsorption on the sample to reach equilibrium, bulb 1 was refilled with mercury. The pressure difference between the two columns of mercury in the narrow bore tubes was measured. The whole process starting from the introduction of nitrogen was repeated so that a range of pressure readings, corresponding to adsorbed gas volume, were recorded.

These values were listed under headings VB and ΔP respectively. Where VB represents the volume of nitrogen gas taken from the graduated bulbs, and ΔP the difference in mercury levels. A further value $\langle V_2$ was obtained from a calibration graph of $\langle V_2$ versus ΔP. This represented the calibrated total dead space volume of nitrogen for the pressures indicated under the conditions of adsorption.

This information together with the values of the weight and volume of the catalyst was fed into a Fortran 1904 series computer using the Algol 60 language. The full programme (EBS0601 Cooper) is given on page 53 . The Table 9 on page 54 represents a typical surface area determination values of 0.5% w/w ruthenium alumina catalyst sample.

The volume of nitrogen adsorbed $cm^3 g^{-1}$ verses the pressure increment P/P_o was plotted for a series of runs for each catalyst and is represented by Figure 7 page 49. Point B values were determined from these curves. The point B is the point where the linear

portion of the graph begins, and was chosen by Brunauer and Emmett[73] as a measure of the volume of gas which would fill the monolayer. Assuming one nitrogen molecule occupies $1.62nm^2$. The surface area of each catalyst was found to be 230 m^2g^{-1} and 158 m^2g^{-1} for the ruthenium and palladium-alumina catalysts respectively.

2.4 MATERIALS

All the gases were of lecture bottle quality and were obtained from British Oxygen limited. The following represents the specifications of each gas:-

GAS	% PURITY
Nitric oxide	99
Nitrous oxide	99.998
Nitrogen	99.999
Carbon monoxide	99.95
Carbon dioxide	99.998
Hydrogen	99.999
Oxygen	99.98

Nitric oxide and nitrous oxide were pre-purified by condensing in a storage bulb immersed in liquid nitrogen, pumped for some minutes, then redistilled so that the middle 70% of the distilled gas was used.

2.5 EXPERIMENTAL PROCEDURE FOR MEASURING REACTION RATES

The catalytic reduction of nitric oxide and nitrous oxide by carbon monoxide were the two main reactions studied. In order to monitor these reactions the mass spectrometer was tuned to a unique ion of one of the products or reactants. From the Table

10 on page 55 , which lists the cracking patterns of the reactants and products, it is apparent that the cracking patterns of some of the gases have similar mass to charge ratios. These ions, for example the molecular ions of carbon monoxide and nitrogen have similar mass to charge ratios and cannot be separated by this instrument. In effect they are the same. Fortunately, carbon dioxide has a unique doubly charged parent ion m/e 22. The mass spectrometer was tuned to this peak when monitoring carbon dioxide.

Figure 2 on page 44 should be consulted in conjunction with the following description.

A known weight of catalyst in a small silica boat was positioned in the reaction vessel directly above the thermocouple well. With the leak probe in position the system was evacuated to 0.13 Nm^{-2} and the oven temperatures set to 450°C or to the reaction temperature, whichever temperature was the highest. A period of one hour was allowed for the system to reach equilibrium, the oven temperatures were then adjusted to reaction temperature.

With taps B,C,D,E closed and a positive pressure of reactant gas (either nitric oxide or nitrous oxide) up to tap H, tap H was partially opened to allow gas to pass from the inlet system to the mixing chamber. At equilibrium tap H was closed. With the reservoir bulb 2 immersed in liquid nitrogen tap E was opened to allow the reactant gas to solidify. Tap E was then closed and the inlet procedure repeated several times to ensure that sufficient reactant gas for the experiment was contained in bulb 2.

The mixing chamber was evacuated, with tap A positioned to isolate the reaction vessel. Tap B was closed and the first 20%

of gas in the reservoir allowed to distil into the mixing chamber. The mixing chamber was evacuated, and tap E opened to allow the reservoir to be evacuated. After a period of a few minutes tap E was closed.

The system was opened to the mass spectrometer through the needle valve J. The mass spectrometer had previously been tuned to record the appearance or disappearance of product or reactant respectively. With tap B closed the reactant gas in bulb 2 was allowed to distil into the mixing chamber. At the required pressure tap E was closed. The second reactant gas (usually carbon monoxide) was introduced carefully through tap H. Each gas was measured manometrically. The gas mixture was allowed to enter the preheat chamber, for thermal equilibration, and then allowed into the reaction vessel. The total pressure due to the reactants was recorded, the reaction vessel isolated, and the chart recorder started.

At the end of the reaction the system was evacuated for a period of ten minutes before repeating the procedure. Before starting a series of reactions it was usual to carry out at least three preliminary runs using equal amounts of reactants, to ensure the results were reproducible.

2.6 ANALYSIS OF MS10 REACTION TRACES

Experimental curves of types 1 and 2 represented in Figure 8 on page 50 were obtained when the rate of appearance or disappearance of product or reactant were monitored respectively. In a reaction in which the disappearance of a reactant was monitored it can be seen from Figure 8 curve type 2 that the initial portion

of the curve has been extrapolated to t=0.   The validity of this
extrapolation was tested by introducing the reactants into the
reaction vessel under identical experimental conditions but for
the absence of the catalyst.   The blank run recorded the maximum
positive ion current of the reactant in question and thus the
extrapolation point t=0.   This experiment was carried out in
every case when monitoring the disappearance of a reactant.

For each individual curve the positive ion currents were
read off at convenient time intervals.   The positive ion current
is proportional to the pressure of gas monitored.   Thus knowing
the total pressure and the ratio of reactant gases the positive
ion current can be expressed in terms of pressure.

For type 1 curves to ensure the reaction had reached comp-
letion,   the product gas was introduced into the system under
identical experimental conditions.   The pressure of the product
gas corresponded to the pressure calculated from the stoichiometry
of the reactants.   For 100% reaction the blank positive ion current
should equal that taken from the curve.

A standard procedure was adopted for the determination of
the initial rate from these curves.   The experimental points
were fed into a Micro 16s computer programmed for a polynomial fit
to six coefficients of the equation.

$$t = \sum_{i=0}^{i=5} a_i x_i$$

Where x is the pressure of product at time t.   The computer out-
put listed (a) the six coefficients, (b) the calculated pressures

of product, (c) the rate of formation of the product, (d) the napierian logarithm of the rate of formation of the product, (e) the napierian logarithm of the unreacted reactant which was the reactant present in the least concentration initially. The computed pressures fitted the experimental data to within a standard deviation of $\pm$ 0.06 (an average of 22 plots).

The Table 11 on page 56 represents a typical data output (1mm Hg $\equiv$ 133.3 Nm^{-2}). The full programme in Mathchat 5030 language is given on page 57.

2.6.1 METHOD ADOPTED FOR ANALYSIS OF REACTION KINETICS

A large number of preliminary experiments were carried out in order to examine the limits of the apparatus. These limits set the boundaries for the kinetic analysis. For each reaction studied a further series of preliminary experiments were carried out in order to establish the weight of catalyst required to give reasonable reaction times, within a working temperature, usually between 200° - 500°C. The results of these experiments were analysed using a number of methods of kinetic analysis,[22, 43,54] before a standard method was chosen. The following procedure represents the standard method adopted for the determination of the reaction mechanisms.

A basic kinetic expression was written down for the reaction, for example

$$\text{Rate} = k \, P_A^{\alpha} \, P_B^{\beta} \qquad \qquad (1)$$

where k represents the reaction rate constant, P_A and P_B represent the pressure of reactants A and B, with the exponent values of α and β representing the orders of reaction with respect to reactant. The exponents α and β were determined

by the differential method suggested by Van't Hoff.[22] This was

achieved by designing a series of experiments to show the effect

of the initial concentration of reactants on the initial rate.

Firstly, one reactant was held constant whilst the other was varied

to the pressure limits of the apparatus (see chapter 3). Secondly,

the experiment was repeated but this time the other reactant was

held constant. The data obtained from this series of experiments

was processed by computer to give the initial rate, using the curve

fitting programme described in the previous section. For each

reactant the slope of a double logarithm plot of initial rates

against pressure of reactants represented the exponent value; from

the equation

$$Lnr = lnk + \alpha lnP_A + \beta ln P_B \tag{2}$$

The results were also analysed where appropriate by considering

a single run and measuring the slopes at various times, correspond-

ing to a number of values of reactant pressures. These data were

listed in the computer feed out together with the initial rate

data, for an example of this see page 56. The slope of a

double logarithm plot of these functions gave the value of the

exponents with respect to time according to the equation

$$ln \frac{d \text{ product}}{dt} = lnk + \alpha lnP_A + \beta lnP_B \tag{3}$$

This method is unambiguous when reactant pressures are equal

or when one of the reactants is present in a large excess. For

equal pressures of reactants the slope will equal $\alpha + \beta$, the

overall order with respect to time.

Once the exponent values had been assessed the empirical rate

equation was tested by substituting the results into the integrated rate form of the law and plotting the function against time. This plot should of course be linear. Finally, the empirical rate law was used in a search for a possible mechanism which gave after suitable simplification the rate law found empirically. This search was conducted on the assumptions of classical ideal kinetics, for example Langmuir-Hinshelwood kinetic theory[22].

FIGURE 2

APPARATUS FOR MONITORING REACTION KINETICS

45

FIGURE 3

LEAK PROBE

4F GRADE METROSIL PLUG

GROUND GLASS SEAL B24

METAL-GLASS SEAL

HOKE GYROLOK ADAPTORS

TO MS10

FIGURE 4

FIGURE REPRESENTING AN X-RAY SPECTRUM
OF A 1% w/w Pd-Al$_2$O$_3$ SAMPLE

Pd. Lα_1 2838 kev
Lβ_1 2·990

E XPANSION x 50

Al. kα_1 (Al$_2$O$_3$)

x 10^3 counts

x 10^3 eV
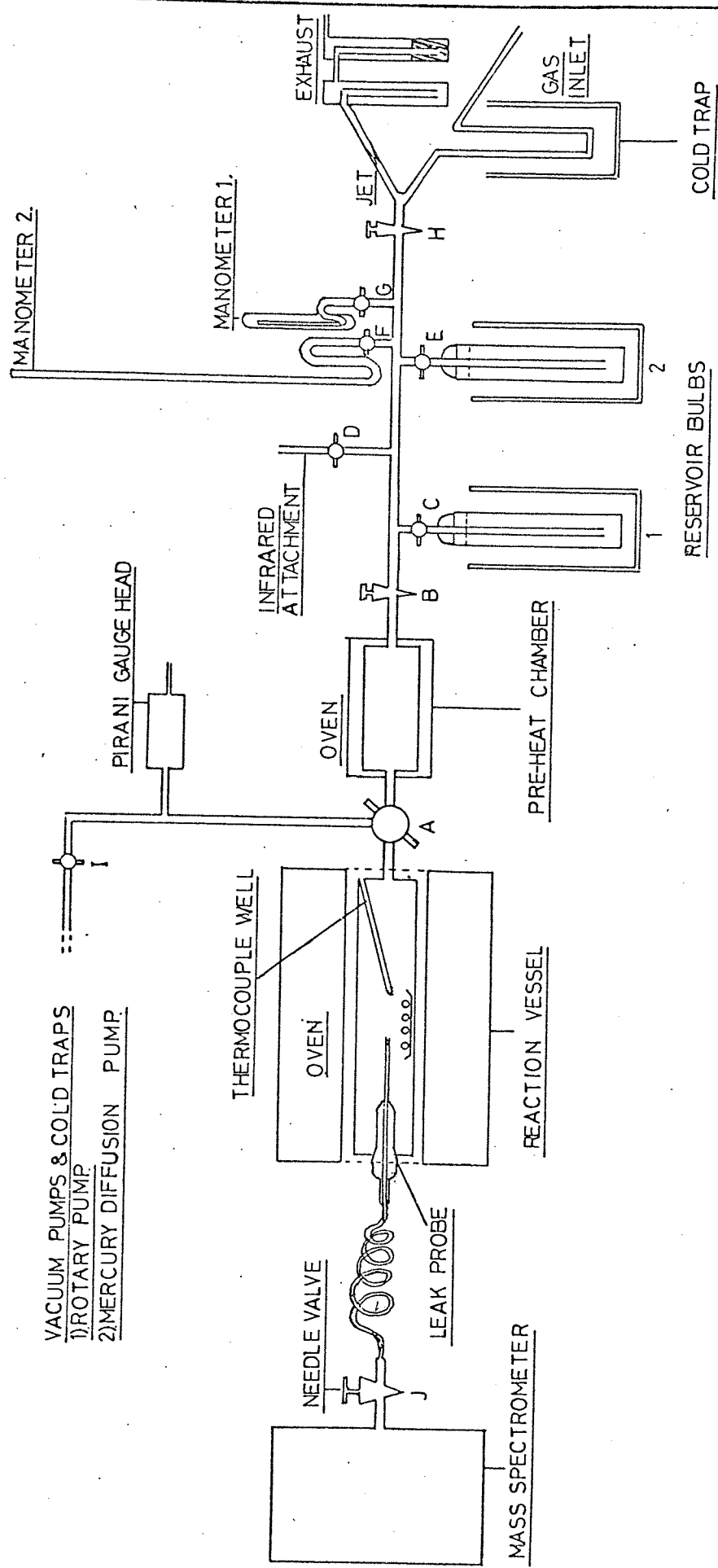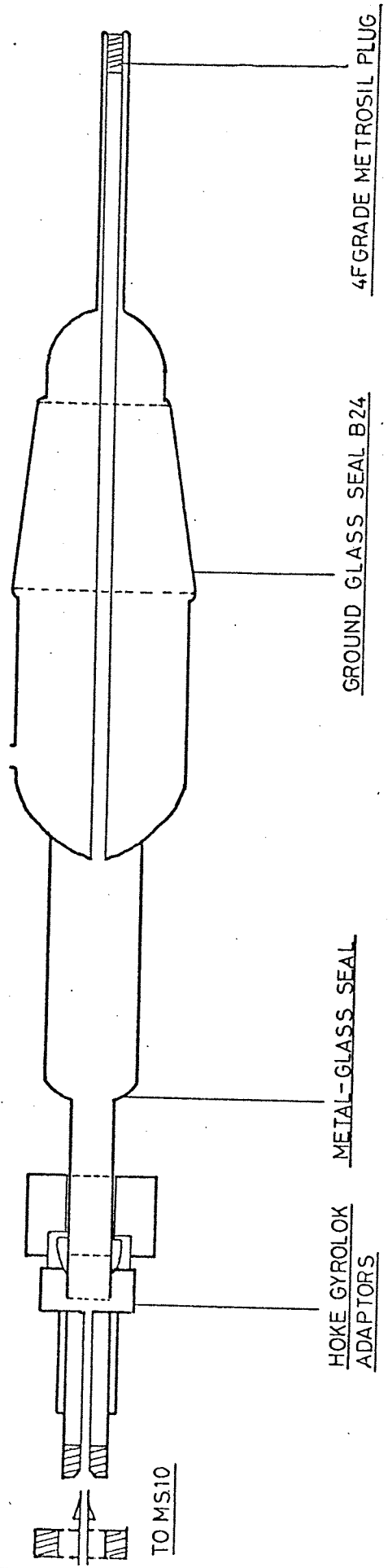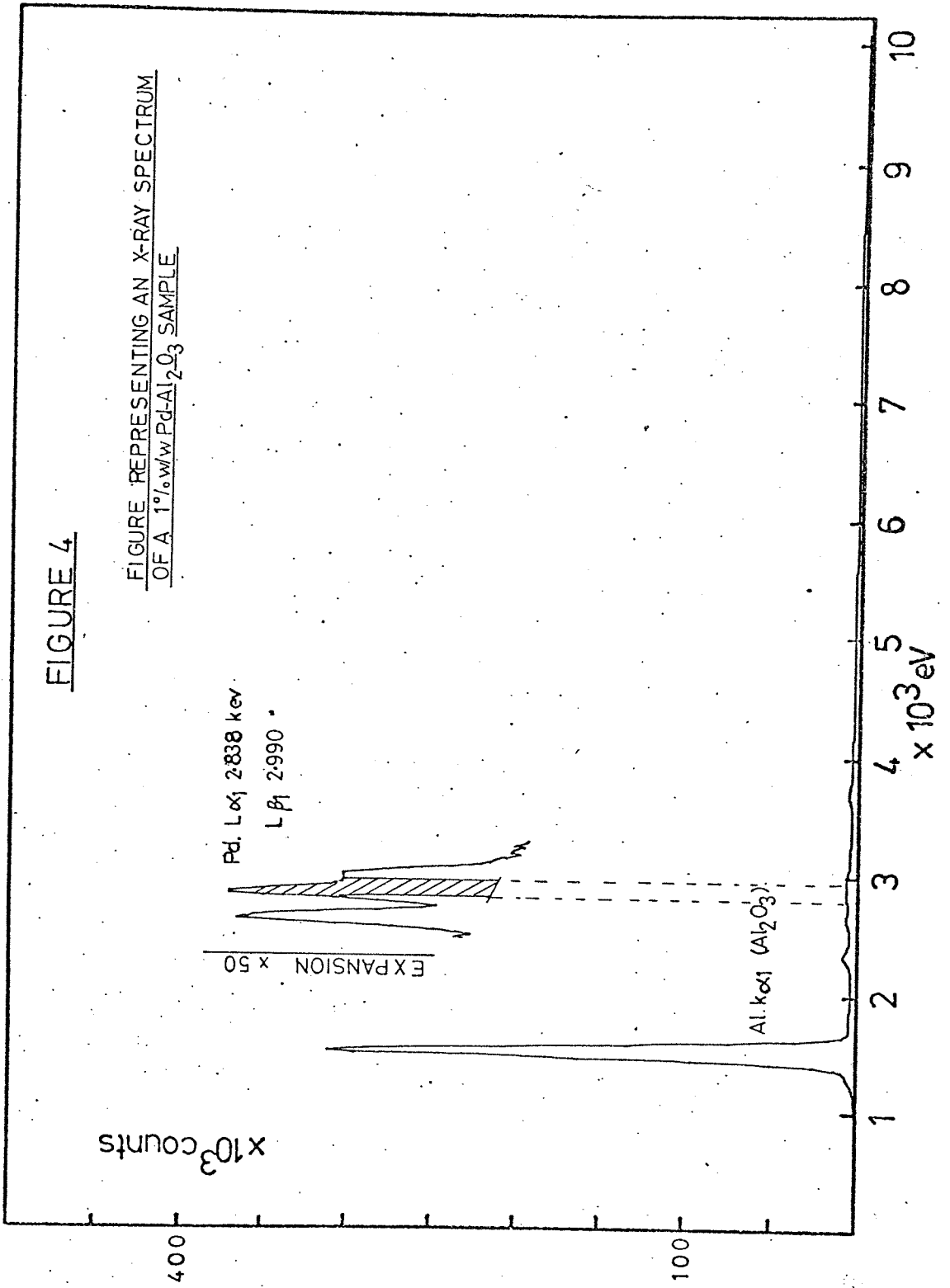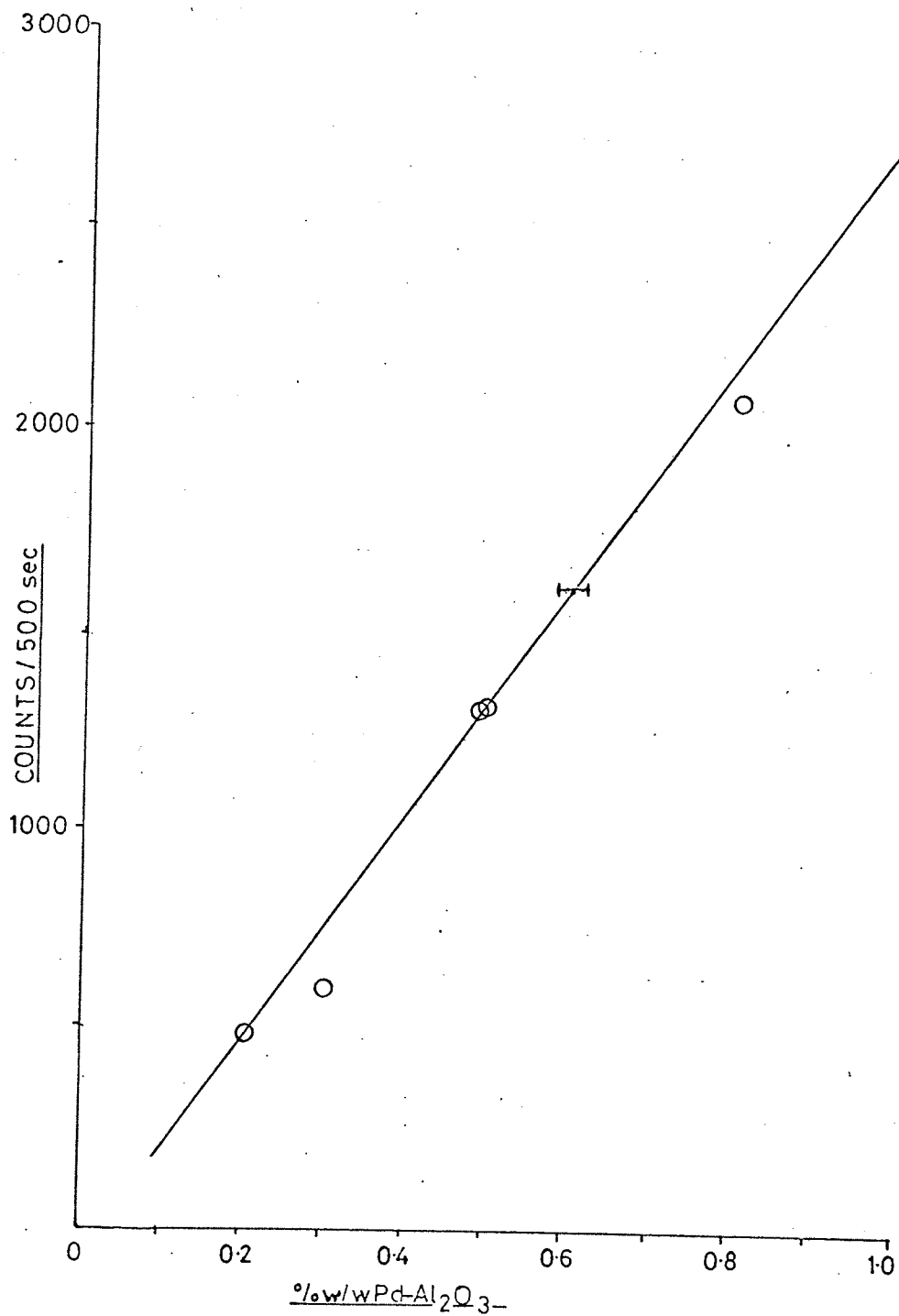
FIGURE 5

CALIBRATION GRAPH OF ALUMINA SUPPORTED PALLADIUM

FIGURE 6
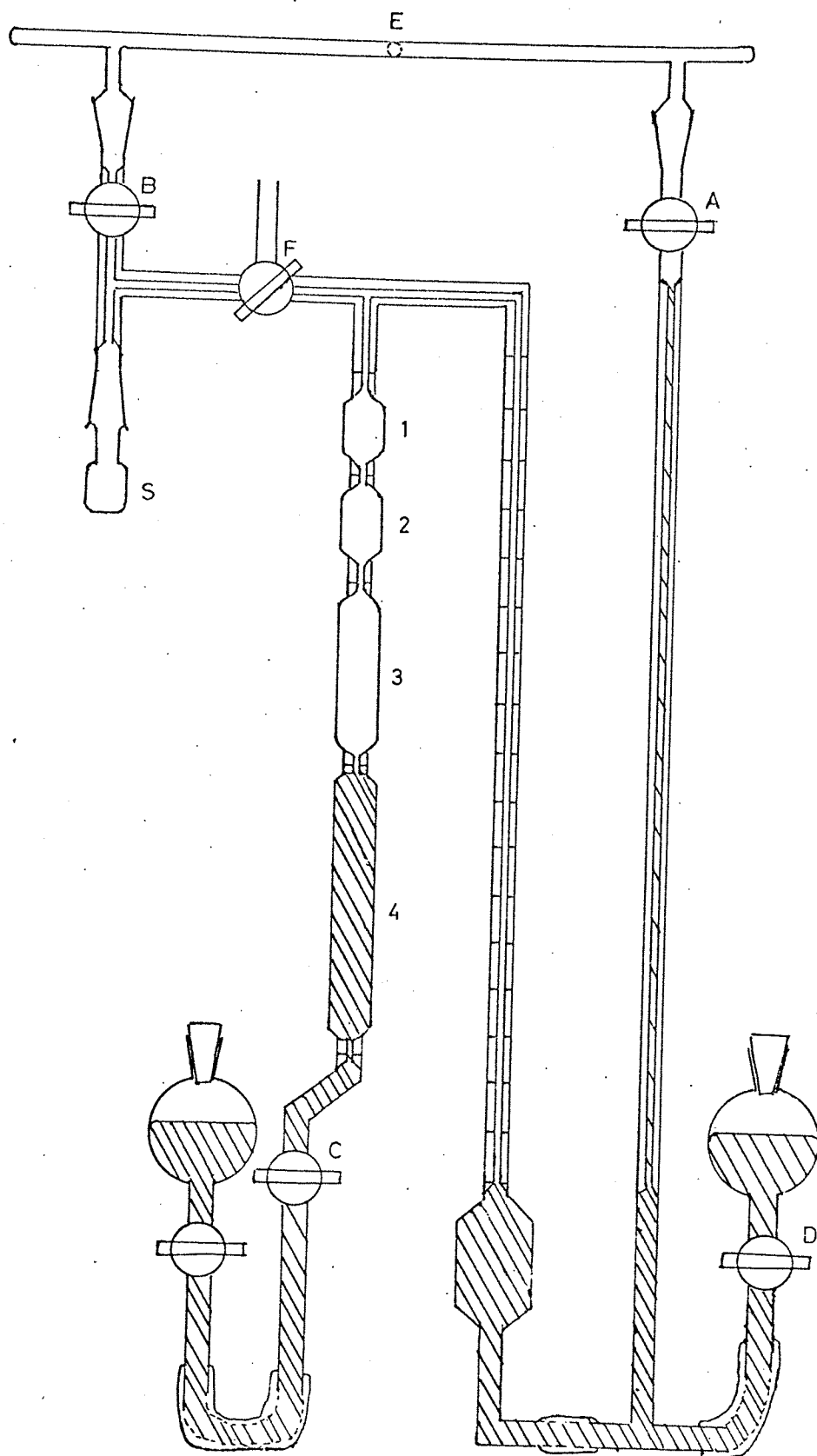
NITROGEN ADSORPTION APPARATUS   D. COOPER [34]

FIGURE 7
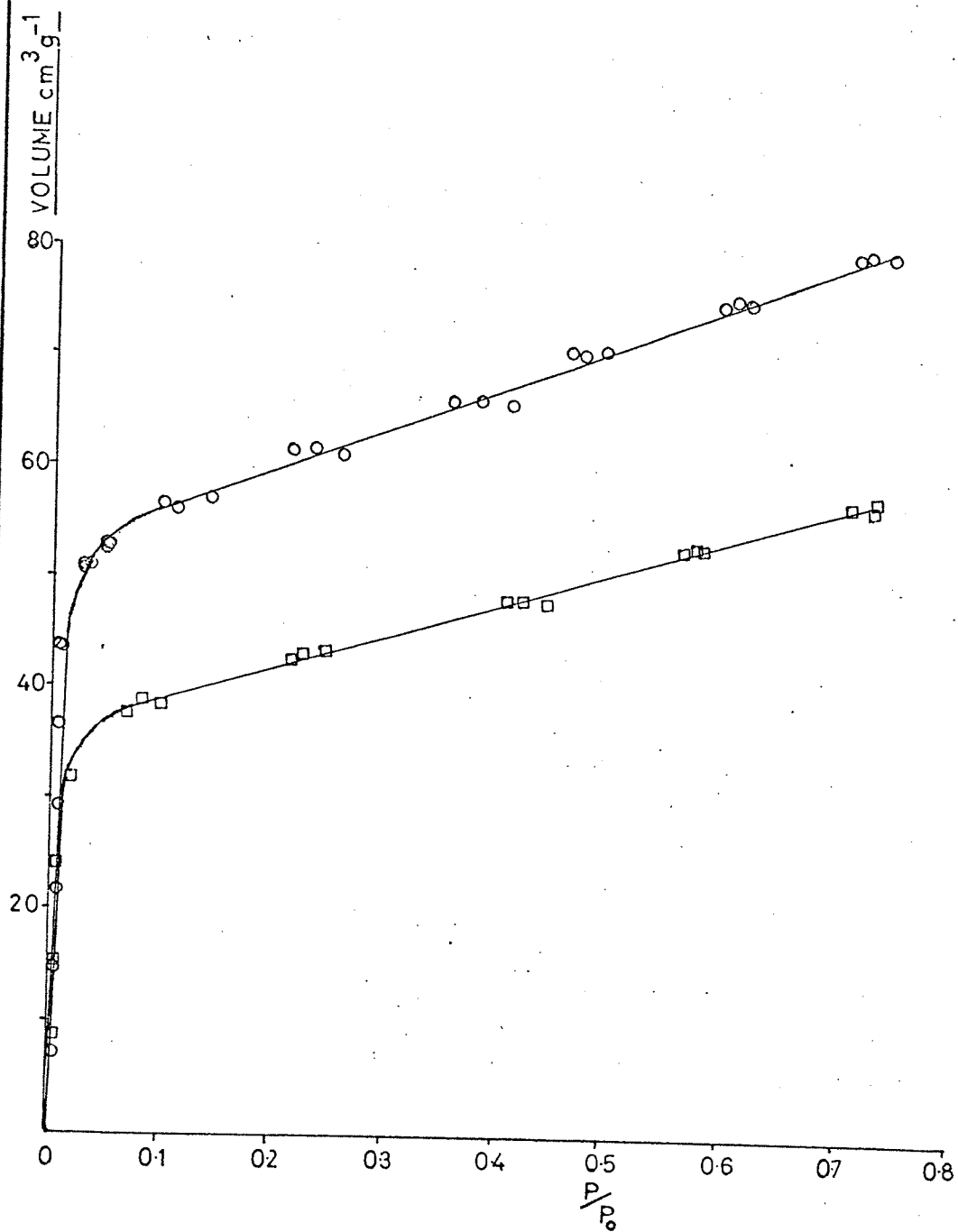
NITROGEN ADSORPTION CURVES FOR: o, 0.5% w/w Ru-Al_2O_3

: □, 0.5% w/w Pd-Al_2O_3

FIGURE 8

TYPE 1

POSITIVE ION CURRENT (PRODUCT)

0   MIN.   10
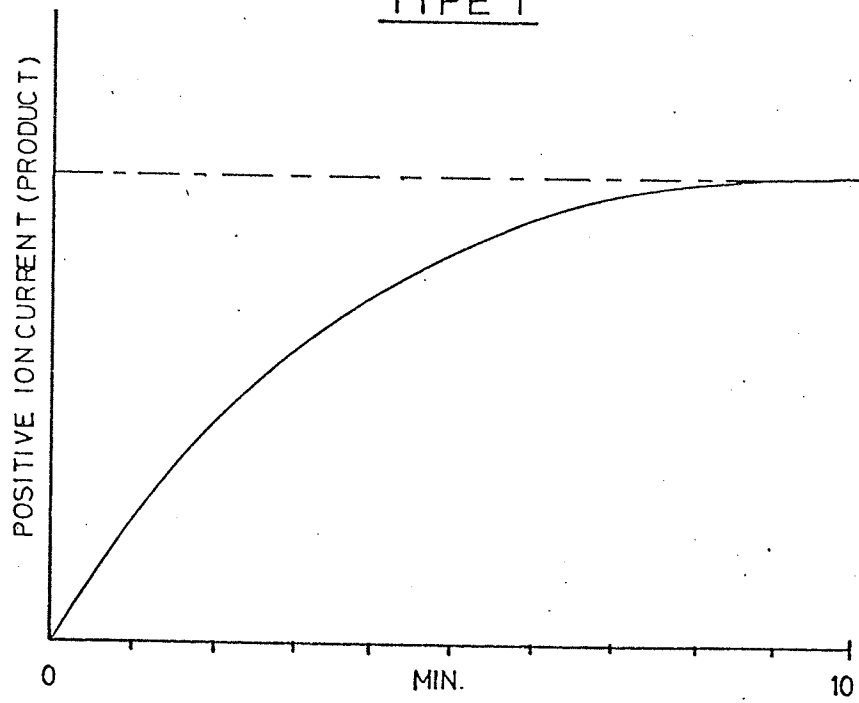
TYPICAL REACTION TRACES FROM THE M.S.10. RECORDER

TYPE 2

POSITIVE ION CURRENT (REACTANT)

BLANK (NO CATALYST)

0   MIN.   10
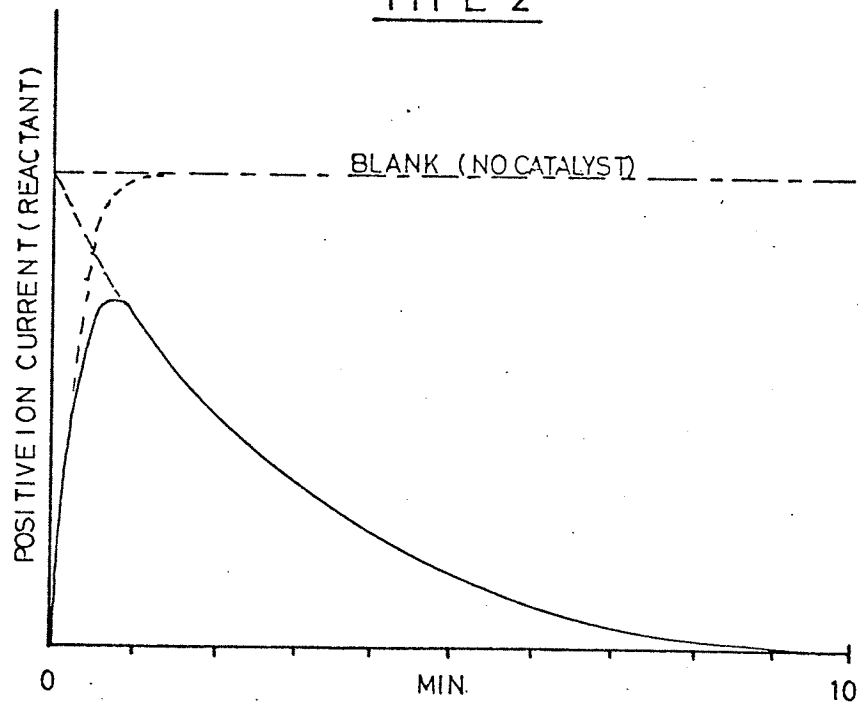
TABLE 6

LISTS THE OPERATING VOLTAGES AND SPECIFICATION OF THE MAIN COMPONENTS

OF THE MS 10.

Mass Spectrometer Operating conditions and Specifications

ELECTRON-ACCELERATING VOLTAGE   + 70 VOLTS   (FILAMENT TO CAGE)

FILAMENT VOLTAGE + 1.6 VOLTS A.C.   RHENIUM WIRE 0.178mm dia. 0.5 OHMS

ELECTRON TRAP POTENTIAL + 35 VOLTS   (CAGE TO TRAP)

TRAP CURRENT   50 μA

ION REPELLER VOLTAGE + 1 VOLT   (CAGE TO ION REPELLER)

PRE-AMPLIFIER ELECTROMETER TYPE ME 1403

AMPLIFIER D.C TYPE, SENSITIVITY RANGE 1000/1 IN SEVEN RANGES

INPUT CURRENTS BETWEEN 10^{-10} AND 10^{-13} AMPS

VACUUM GAUGES: METROVAC VH5 PENNING GAUGE 133.3 to 0.133 Nm^{-2}

METROVAC VC9 IONIZATION GAUGE CONTROL UNIT

RANGE 0.13 - 6.6 x 10^{-6} Nm^{-2}

RECORDER A.E.I POTENTIOMETRIC RECORDER 10mV,10 inch wide chart

RESPONSE TIME 1 SEC FOR FULL SCALE DEFLECTION

DIFFUSION PUMP METROVAC 033 OIL DIFFUSION PUMP DRY-ICE COOLED

ROTARY PUMP   METROVAC GDRI

TABLE 7

Listing the operating conditions of electron microscope and Kevex

EXCITATION POTENTIAL OF SCANNING ELECTRON MICROSCOPE	20 k.v.
BEAM CURRENT	150 μ amps
FILAMENT CURRENT	2.5 amps
SPECIMEN CURRENT	FIXED FOR ALL SAMPLES AS ALL THE SAMPLES WERE MOUNTED ON THE SAME STUB
VACUUM	2.6×10^{-3} Nm^{-2}
NO. OF CHANNELS COUNTED UNDER PALLADIUM Lα_1 2.838 kev	9
SAMPLE AREA COUNTED	4×10^{-8} cm^2
COUNTING TIME	500 sec.

TABLE 8

Listing bulb and dead space volumes measured at 20°C

V_1	1.74 cm^3	Total volume on left-hand side of tap T 4.05 cm^3
V_2	2.58 cm^3	Total volume on right-hand side of tap T 1.35 cm^3
V_3	5.55 cm^3	Total volume on right-hand side of tap T plus
V_4	11.25 cm^3	Mercury at highest graduation 0.63 cm^3
S	2.51 cm^3	

PROGRAMME USED TO CALCULATE THE VOLUME OF $N_2(cm^3 g^1)$
AND THE PRESSURE INCREMENT P/P_o 34.

STATEMENT NO.

```
0      'BEGIN'
1      'REAL''ARRAY'
1      VV2,
1      ANS,P,VB,V2,PN[1:100];
2      'REAL'
2      VC,W;
3      'INTEGER'
3      L,
3      J,K,
3      I,M;
4      K:=READ;
5      'FOR' J:=1 'STEP' 1 'UNTIL' K 'DO'
5      'BEGIN'
6      L:=READ;
7      M:=READ;
8      VC:=READ;
9      W:=READ;
10     'FOR' I:=1 'STEP' 1 'UNTIL' M 'DO'
10     'BEGIN'
11     VB[I]:=READ;
12     P[I]:=READ;
13     V2[I]:=READ;
14     'END';
15     ANS[1]:=(0.045*(30-P[1])+VB[1]-V2[1]-VC)/W;
16     'FOR' I:=2 'STEP' 1 'UNTIL' M 'DO'
16     'BEGIN'
17     VV2[I]:=V2[I]-V2[I-1];
18     ANS[I]:=ANS[I-1]+(0.045*(30-P[I])+VB[I]-
19     'END';                          -VV[I])/W;
20     'FOR' I:=1 'STEP' 1 'UNTIL' M 'DO'
20     PN[I]:=P[I]/30;
21     PAPERTHROW;
22     NEWLINE(10);
23     SPACE(30);
24     WRITETEXT('('TABLE')');
25     PRINT(L,4,0);
26     WRITETEXT('('%OF%VOLUME(CM3/G)%FOR%PRESSURE%-
27     NEWLINE(10); -INCREMENT(P/P_o)')');
28     SPACE(40);
29     WRITETEXT('('VOLUME')');
30     SPACE(13);
31     WRITETEXT('('PRESSURE%INCREMENT')');
32     NEWLINE(4);
33     'FOR' I:=1 'STEP' 1 'UNTIL' M 'DO'
33     'BEGIN'
34     SPACE(36);
35     PRINT(ANS[I],3,6);
36     SPACE(10);
37     PRINT(PN[I],3,6);
38     NEWLINE(2);
39     'END';
40     'END';
41     'END'
```

EXECUTION STARTED

TABLE 9

Represents typical data obtained from a surface area determination

RUN NO.5

Weight of catalyst (w) = 0.4168g

Volume of catalyst (ve) = 0.0983 cm^3

VB	ΔP	ξV_2	COMPUTER READ OUT	
			VOLUME $cm^3 g^{-1}$	PRESSURE INCREMENT P/P_o
1.74	0.1	0.025	7.107	0.003
1.74	0.1	0.025	14.509	0.003
1.74	0.1	0.025	21.912	0.003
1.74	0.1	0.025	29.315	0.003
1.74	0.1	0.025	36.718	0.003
1.74	0.5	0.10	43.898	0.016
1.74	1.3	0.335	50.607	0.043
1.74	5.1	1.21	55.371	0.173
1.74	7.8	1.635	60.922	0.260
1.74	12.4	2.372	65.229	0.413
1.74	14.8	2.735	70.174	0.493
1.74	18.8	3.145	74.574	0.6266
1.74	22.2	3.478	78.792	0.7400

TABLE 10

Listing the cracking patterns of the reactants and products of the two main reactants

Mass to charge ratio	Relative Intensity				
	CO	N_2	NO	N_2O	CO_2
12	4.7				2.46
13	0.05				
14	0.75	5.18	7.48	12.9	
15			2.41	0.1	
16	1.67		1.45	5.0	6.24
22					1.78
28	100.0	100.0		10.8	6.55
29	1.16	0.73		0.1	0.06
30	0.22		100.0	31.1	0.01
31			0.38	0.1	0.01
32			0.21		
44				100.0	100.0
45				0.7	1.16
46				0.2	0.41

TABLE 11

A SAMPLE OUTPUT FROM THE CURVE FITTING/INITIAL RATE/TIME COURSE/PROGRAMME

:6,:17,:38,
COEFFICIENTS ARE

-0.26402635808E+0000
0.17785051208E+0000
-0.37066706108E+0001
0.40500089308E+0000
-0.23001056608E-0001
0.53366385548E-0003

LOG(INF-X), YCALC, DX/DT, AND LOG(DX/DT),

0.35331025008E+0001	0.39507836368E+0001	0.15965856608E+0002	0.27704528308E+0001
0.34134093048E+0001	0.77305195508E+0001	0.14826408008E+0002	0.26600083318E+0001
0.32778909208E+0001	0.11110894048E+0002	0.12976890958E+0002	0.25470890008E+0001
0.31458749038E+0001	0.14126615808E+0002	0.11375927008E+0002	0.24314492408E+0001
0.30040475608E+0001	0.10109255108E+0002	0.89568014008E+0001	0.21994132008E+0000
0.26588600008E+0001	0.23156417448E+0002	0.69700095008E+0001	0.12498237938E+0001
0.24423347038E+0001	0.26939606608E+0002	0.53847800018E+0001	0.16935765008E+0001
0.22470724008E+0001	0.28596075408E+0002	0.41107280038E+0001	0.14157871408E+0001
0.20666869308E+0001	0.30308918008E+0002	0.31343137408E+0001	0.11494109048E+0001
0.18106288338E+0001	0.31763409008E+0002	0.23892789748E+0001	0.86899719608E+0000
0.14327007338E+0001	0.33618471118E+0002	0.14184341008E+0001	0.34955350408E+0000
0.11030095008E+0001	0.34757709048E+0002	0.24007897148E+0000	-0.61002414008E-0001
0.57041046108E+0000	0.35507470098E+0002	0.72778440008E+0000	-0.31775044008E+0000
0.10436003008E+0000	0.36834617008E+0002	0.69174600038E+0000	-0.47503348008E+0000
-0.35667406108E+0000	0.37309548008E+0002	0.52880144118E+0000	-0.63714227008E+0000
		0.41917813008E+0000	-0.86945393238E+0000

PROGRAMME USED FOR CURVE FITTING/ INITIAL RATE DETERMINATIONS/
AND TIME COURSE PLOTS.

```
  1ASK N,M,W; FOR I=1,1,N; SET L(I)=0; FOR J=1,1,N;-
  2SET L(0)=0                                    ;SET R(I,J)=0.
  3FOR J=1,1,M; ASK(0) T,X; SET P(1)=1; DO 30/124
 13FOR I=2,1,N; SET Z=N+1-I; SET X=Z+1; DO 125/136
 18TYPE !,"COEFFICIENTS ARE",!
 19FOR I=1,1,N; SET X=0 ; SET Z=I-1; DO 30/37
 25TYPE !,"LOG(INF-X) XCALC DX/DT AND LOG(DX/DT)",!
 27FOR I=1,1,M; ASK(0) T,X; SET P(1)=1; SET J=2; DO 490/550
 28QUIT
 30SET J=-1
 32SET J=J+1; IF (J-Z),33,33,35
 33SET X=X+L(J)*R(I,J)
 34GO 32
 35CONTINUE
 36SET L(I)=(L(I)-X)/R(I,I)
 37TYPE %,!,L(I)
 80SET I=1
 85SET I=I+1; IF (I-N),90,90,100
 90SET A=I-1; SET P(I)=P(A)*T
 95GO 85
100CONTINUE
110SET I=0
112SET I=I+1; IF (I-N),115,115,124
115SET L(I)=L(I)+X*P(I)
118CONTINUE
119SET K=0
120SET K=K+1; IF (K-N),121,121,123
121SET R(I,K)=R(I,K)+P(I)*P(K)
122GO 120
123GO 112
124CONTINUE
125SET J=0
126SET J=J+1;IF (J-Z),127,127,136
127SET L(J)=L(J)*R(X,X)-L(X)*R(J,X)
128CONTINUE
130SET K=0
132SET K=K+1; IF (K-Z),133,133,135
133SET  R(J,K)=R(J,K)*R(X,X)-R(X,K)*R(J,X)
134GO 132
135GO 126
136CONTINUE
490SET Y=L(1)*P(1); SET Z=0
510IF (N-J), 500,520,520
520SET A=J-1; SET P(J)=P(A)*T
525SET Y=Y+L(J)*P(J); SET Z=Z+L(J)*P(A)*(J-1)
535SET J=J+1; GO 510
540SET X=W-X; SET X=FLOG(X); SET A=FLOG(Z)
550TYPE %,!,X,Y,Z,A
```

CHAPTER 3

RESULTS AND DISCUSSIONS

3.0.   REDUCTION OF NITRIC OXIDE BY CARBON MONOXIDE OVER 0.5% w/w

Pd-Al$_2$O$_3$ CATALYST

A number of workers[41,42] have noted the formation of quantities

of nitrous oxide during the catalytic reduction of nitric oxide by

carbon monoxide.   Shelef and Otto[41] have suggested that nitrous

oxide behaves as a true gas intermediate in the reaction sequence:-

$$2\ NO\ +\ CO\ =\ N_2O\ +\ CO_2$$

$$N_2O\ +\ CO\ =\ N_2\ +\ CO_2$$

$$2NO\ +\ 2CO\ =\ N_2\ +\ 2CO_2\quad \text{Total reaction}$$
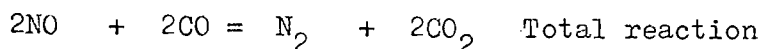
Prior to a kinetic study of the above reactions a number of

experiments were designed to investigate the amounts of nitrous

oxide formed during the reduction of nitric oxide by carbon monoxide.

3.0.1.   NITROUS OXIDE FORMATION DURING THE REDUCTION OF NITRIC OXIDE

BY CARBON MONOXIDE OVER 0.5% w/w Pd-Al$_2$O$_3$

A series of experiments were carried out by mass spectrometry

and infrared analysis in order to establish if the reactants

a) decomposed, b) reacted homogeneously, or c) catalytically on

the support or catalyst at 500°C.   Table 12 on page 81   represents

the results of these experiments.   The table shows that the reduction

of nitric oxide and nitrous oxide by carbon monoxide over palladium

are the only significant reactions.   These reactions reached

completion within eight minutes.   The decomposition of nitric

oxide and nitrous oxide was found to be very slow under these

conditions; this result is consistent with the results of previous

workers.[25,74]

The next series of experiments were designed to investigate the amounts of nitrous oxide formed during the reduction of nitric oxide by carbon monoxide. Reactions containing 1) an excess of nitric oxide 2) an excess of carbon monoxide and 3) equal amounts of reactants were examined at $400^{\circ}C$.

For these experiments the mass spectrometer was calibrated against known pressures of carbon dioxide, mass to charge ratio m/e 22 and 44, nitrous oxide m/e 30 and 44, and nitric oxide m/e 30. The contribution of mass to charge ratios m/e $22/44$ and m/e $30/44$ for carbon dioxide and nitrous oxide respectively were also calculated.

Mass to charge ratios m/e 22, 30 and 44 were monitored throughout the reaction by switching the mass spectrometer to these ratios at convenient time intervals. This method was preferred to a method which monitored the three mass to charge ratios individually in three identical reactions. The positive ion currents due to m/e 22, 30 and 44 were fed into a Micro 16S computer programmed to give an analysis of the pressures of carbon dioxide, nitrous oxide and nitric oxide at time t. The pressures of the reactants and products were calculated from 1) the slope and intercept of a line of best fit obtained from the individual calibrations, 2) the ratios of the contributions of m/e $22/44$, m/e $30/44$ for carbon dioxide and nitrous oxide.

The computer programme used for this analysis is given on page 83.

The results of these experiments are represented graphically, Figures 9, 10, and 11, on pages 73, 74 and 75. In overall oxidizing conditions Figure 9, large amounts of nitrous oxide are produced initially. From the form of this plot it is apparent that reaction occurs between carbon monoxide and nitrous oxide. Stoichiometric reactant pressures and reaction mixtures with excess carbon monoxide produced little if any nitrous oxide, Figures 10 and 11. These observations were found to be general for temperatures up to $500^{\circ}C$. At this temperature the increased rate of reaction between nitrous oxide and carbon monoxide became the limiting factor for the formation of nitrous oxide. The rate of production of carbon dioxide was significantly slower under reducing conditions than under oxidizing conditions.

From the figures 9, 10, and 11 it is apparent that three consecutive reactions take place. These reactions are represented by the following equations

$$NO + CO \xrightarrow{k_1} \tfrac{1}{2}N_2 + CO_2 \qquad - 1$$

$$2NO + CO \xrightarrow{k_2} N_2O + CO_2 \qquad - 2$$

$$N_2O + CO \xrightarrow{k_3} N_2 + CO_2 \qquad - 3$$
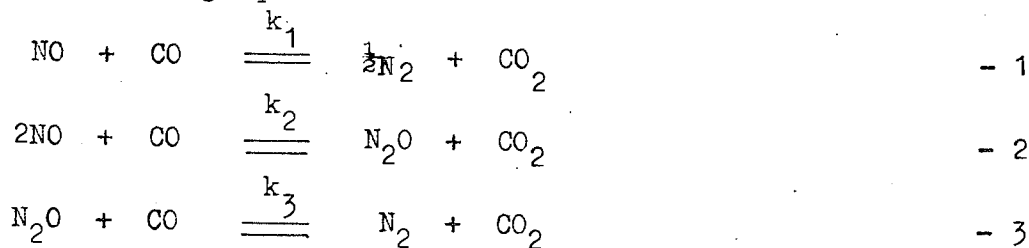
The rate of formation of carbon dioxide is expressed by the empirical rate equation

$$\frac{dP_{CO_2}}{dt} = k_1 P_{NO}^{\alpha} P_{CO}^{\beta} + k_2 P_{NO}^{\gamma} P_{CO}^{\delta} + k_3 P_{N_2O}^{\tau} P_{CO}^{\psi} \qquad - 4$$

where k_1, k_2 and k_3 are the reaction rate constants. P represents the pressure of reactants, with exponent values $\alpha, \beta, \gamma, \delta, \tau$ and ψ

are the orders of reaction with respect to each reactant.
The preferred reactions are, for oxidizing conditions $2 \gg 3 > 1$
and reducing conditions $1 \gg 2$ and 3.   For this reason the
kinetics of the reduction of nitric oxide by carbon monoxide
was studied under reducing condtions.

3.0.2.   A STUDY OF THE KINETICS OF THE REDUCTION OF NITRIC OXIDE

BY CARBON MONOXIDE OVER 0.5% w/w Pd-Al$_2$O$_3$

For reactant mixtures containing 1) equal amounts of reactants
and 2) an excess of carbon monoxide, nitric oxide is predominantly
reduced to nitrogen without the formation of nitrous oxide.

The rate of production of carbon dioxide is expressed by the
empirical rate equation:-

$$\frac{d P_{CO_2}}{dt} = k_1 \, P_{NO}^{\alpha} \, P_{CO}^{\beta} \qquad\qquad - 1$$

The notations used are the same as those in equation 4 section
3.0.1.   The exponents α and β were determined using the standard
method adopted for the determination of reaction mechanisms out-
lined in chapter 2 section 2.6.1.   Figures 12 and 13 on pages
76 , 77 ,   are double logarithm plots of the results obtained from
initial rate experiments.   The order of reaction determined
from the slopes of these plots was found to be 2 and -1 ($\pm$0.05)
for nitric oxide and carbon monoxide, respectively.   The results
were also evaluated by the time course method.   Figure 14 on page
78 is a time course plot obtained from a single run having equal
reactant pressures.   The overall order with respect to time
obtained from the slope of this plot was found to be 1.0.   This
result is consistent with the orders obtained by the initial rate
method since the overall order $= \alpha + \beta$ for equal reactant

pressures.   These results are summarized in Table 13 on page 81.

Equation 1 can now be written in the form of:-

$$\frac{dP_{CO_2}}{dt} = k_1 \, P_{NO}^{2} \, P_{CO}^{-1} \qquad\qquad - \; 2$$

The integrated form of this equation is:

$$\frac{a}{(b-x)} - \frac{a}{b} + \ln\frac{b}{(b-x)} - \frac{b}{(b-x)} + 1 = kt \qquad - \; 3$$

where a and b represent the initial pressures of carbon monoxide and nitric oxide and x the pressure of carbon dioxide at time t. An assessment of the validity of the rate equation was made by substituting the results into equation 3 and plotting the function against time t in the usual manner.   Equation 3 simplifies to a first order relationship when reactant pressures are equal.

The Figure 15 on page 79 represents a sample of the results obtained from a plot of the function for a series of reactions covering the pressure range indicated in Table 13.   Figure 15 shows that straight lines are obtained to at least 60% completion and in some cases to over 80% of the reaction.   It was found that reaction mixtures in the pressure ranges of (1) nitric oxide pressures of 2.0 - 5.0 kNm^{-2}, constant carbon monoxide 5.0 kNm^{-2} and (2) carbon monoxide pressures of 5.0 - 8.0 $k \, Nm^{-2}$, constant nitric oxide 5.0 $k \, Nm^{-2}$, had a reaction rate constant varying between 0.3 $\pm$ 0.1 min^{-1}.   This result together with the linearity of the graphs indicates that the rate law is obeyed between these pressure limits, at $400^{o}C$.

The equation was also found to hold for equal amounts of reactants between a temperature range of 300 - $500^{o}C$.   A line of best fit was obtained from a plot of a first order relation-

ship for each temperature, the slopes and standard deviation of which are summarized in Table 14. Using the data in Table 14 the apparent activation energy of this reaction was determined from an Arrhenius plot to be 91.2 ± 12 kJ mol^{-1}, Figure 16 on page 80 .

Diffusion effects should have a negligible effect on the rate of decomposition, the apparent activation energy and the order of reaction, since the ratio of the rate constants for a diffusion - limited reaction to the maximum rate constant (obtained in this chapter) is of the order $1:10^{-4}$. This value was estimated by the method of Wheeler[22b], assuming Knudsen diffusion and treating the catalyst bed as a single granule with a bulk density of 0.61 g.cm^{-3}, a pore volume of 0.79 cm^3 g^{-1} and a pore radius of 10^{-6} cm^{-1}.

Equation 2 shows that the rate of production of carbon dioxide is inversely proportional to the pressure of carbon monoxide, thus carbon monoxide has an inhibiting effect on the reaction. This negative pressure dependence is indicative of a surface with a relatively high carbon monoxide coverage. This result is consistent with that of Taylor and Klimisch[59] who also observed that the reduction of nitric oxide by carbon monoxide over palladium is inhibited by carbon monoxide.

Carbon monoxide chemisorbed on metal and metal-oxides supported on silica or alumina has been the subject of extensive study. Eichens and co-workers[75] have compared infrared absorption bands obtained from the interaction of carbon monoxide on palladium with the spectra of metal carbonyl compounds. Two

main absorption bands were characterized according to the type

of bonding.   Absorption bands at frequencies below 1900 cm^{-1}

were ascribed to a bridging structure whilst bands above 2000cm^{-1}

were attributed to a linear structure.   The exact position and

intensities of these two bands were found to vary with surface

coverage.   At low surface coverages these authors noted that the

band assigned to the bridged structure predominated whilst the

band attributed to the linear structure grew in intensity at

higher surface coverages.   Desorption experiments revealed that

the molecules responsible for the high frequency bands i.e. line-

arily adsorbed carbon monoxide were less strongly held and could

be removed from the surface by evacuation.

Studies[76] using LEED have also confirmed the presence of

bridged and linear forms of carbon monoxide adsorbed on palladium.

More recently Palazov et al.[77] have identified three main species

of carbon monoxide adsorbed on silica supported palladium.   These

were two linear species, one more firmly bound than the other,

and a bridged species.   These authors found that the linear

species were more tightly bound to the surface than Eischens et

al.[75] results suggested, and concluded that this could have been

due to the sample preparation, or pretreatment since this plays

an important role in the observed spectra.   The following re-

presents a schematic diagram proposed by these authors for a

relatively high surface coverage of carbon monoxide.

$$
\left[\begin{array}{c c} \overset{\displaystyle O}{\underset{\displaystyle C}{\|}} & \overset{\displaystyle O}{\underset{\displaystyle C}{\|}} \\ Pd & Pd \end{array} \right]_{n}
$$
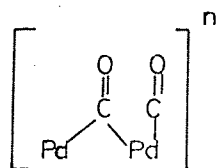
It is still not clear which species reacts with nitric

oxide, but on the basis of the molecularity found by experiment

and the fact that the linear   form predominates for surfaces
with a relatively high surface coverage, it is plausible that
this is the reacting form.

In comparison nitric oxide exhibits a second order pressure
dependence which is indicative of a bimolecular surface reaction.
Infrared studies in this work (chapter 5) indicate that nitric
oxide is relatively weakly adsorbed on palladium.   These results
are in line with those obtained by Dunken and Hobert[78] and
Unland[47].   The fact that nitric oxide does not dissociate
significantly on palladium (up to $500^{\circ}C$; table 12) implies that
the adsorption is predominantly molecular.

Langmuir – Hinshelwood kinetics predicts that the rate of
reaction is proportional to   the fraction of surface covered
by each reactant.   Then a surface reaction between carbon mon-
oxide and nitric oxide can be represented by the following
equation.

$$\frac{dPCO_2}{dt} = k_s \; \Theta_{CO} \; \Theta_{NO} \qquad\qquad - 4$$

where k_s is the reaction rate constant of the surface reaction;
Θ_{CO} and Θ_{NO} the fraction of reactants on the surface are re-
presented by

$$\Theta_{CO} = \frac{b_{CO} \; P_{CO}}{(1 + b_{CO}P_{CO} + b_{NO} \; P_{NO}^{2})} \qquad\qquad - 5$$

$$\theta_{NO} = \frac{b_{NO} \, P_{NO}^2}{(1 + b_{NO} \, P_{NO}^2 + b_{CO}P_{CO})} \qquad - 6$$

where b_{NO} and b_{CO} are adsorption coefficients; combining equations 5 and 6 gives equation 7

$$\frac{dP_{CO_2}}{dt} = \frac{k_s \, b_{CO}P_{CO}b_{NO} \, P_{NO}^2}{(1 + b_{CO}P_{CO} + b_{NO} \, P_{NO}^2)^2} \qquad - 7$$

Equation 7 can be simplified by using the fact that carbon monoxide is relatively strongly adsorbed and exhibits a high surface coverage on palladium. Subsequently nitric oxide has a low surface coverage and is assumed to be relatively weakly adsorbed. Then $b_{CO}P_{CO} \gg 1 + b_{NO} \, P_{NO}^2$ and equation 7 becomes:

$$\frac{dP_{CO_2}}{dt} = \frac{k_s b_{NO} \, P_{NO}^2 b_{CO}P_{CO}}{(b_{CO}P_{CO})^2}$$

$$= \frac{k_s b_{NO} \, P_{NO}^2}{b_{CO} \, P_{CO}} \, , \quad \text{let } \frac{k_s b_{NO}}{b_{CO}} = k$$

$$\text{then} \qquad = \frac{k \, P_{NO}^2}{P_{CO}} \qquad - 8$$

Equation 8 is of the same form as that obtained from the initial rate method, equation 2.

Equation 6 was derived from the assumption that two molecules of nitric oxide occupy one surface site, for example

$$2NO + s \longrightarrow 2NO - s$$
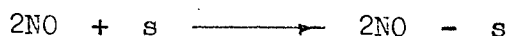
then the rate is $\propto P^2$. For the adsorption process the rate

$= k_a (1 - \Theta) P^2$, and desorption process $= k_d \Theta$. Equating

the rates gives, $\dfrac{\Theta}{1 - \Theta} = \dfrac{ka}{k_d} P^2$, substituting $\dfrac{ka}{k_d} = b$, the

adsorption coefficient; then $\dfrac{\Theta}{1 - \Theta} = bP^2$ and $\Theta = \dfrac{b P^2}{1 + b P^2}$

Cant and Fredrickson[79] have studied this reaction over a

silver catalyst. These authors found that two rate laws could

describe the reaction, 1) $r = kP_{CO} P_{NO}$ and 2) $r = kP_{CO}P_{NO}^2$.

Equation 2 followed from the suggestion of Shelef et al.[39] that

the formation of nitrogen might require pairing of nitric oxide

molecules. The accuracy of Cant and Fredrickson's[79] measurements

was not sufficient to unambiguously distinguish the two rate laws.

There are two feasible explanations for the second order

dependency of nitric oxide.

1) Nitric oxide may form a dimer on a single surface site

eg (NO)(NO). Such structures are known to exist in transition

metal complexes[80]. Peri,[81] Kugler et al.[82,83] and others[78] have

attributed certain infrared absorption bands of nitric oxide

adsorbed on chromia and palladium respectively to the dimer.

2) Nitric oxide may react with a single N - surface site

to form a transient nitrous oxide structure; which reacts with

an adjacent carbon monoxide molecule to give nitrogen and carbon

dioxide. This case effectively requires that two molecules are

adsorbed on a single surface site. The single N - surface site

may be formed through a CO - NO complex, the mechanism of which

will be discussed later.

Of the two explanations the second seems the most probable

since it is unlikely that the dimer will be formed on the surface at high temperatures. A surface mechanism which accounts for the second order pressure dependence of nitric oxide is given by the following scheme.

1).

S(CO) + S(NO) $\longrightarrow$ S(CO$_2$) + S(No)

S + CO$_2$

2). EXCESS CO

S(No) + NO $\longrightarrow$ S(NNO) + S(CO) $\longrightarrow$

S + N$_2$O

S + S + N$_2$ + CO$_2$
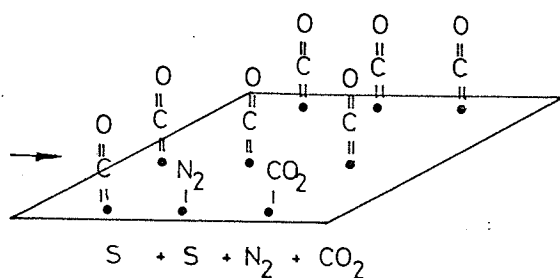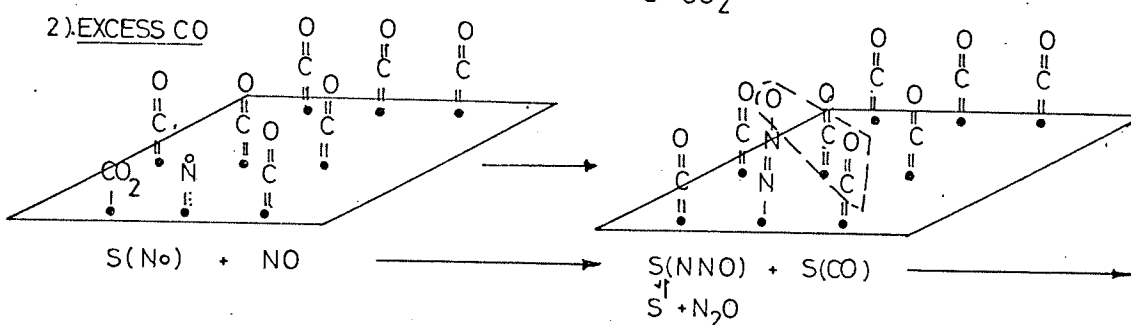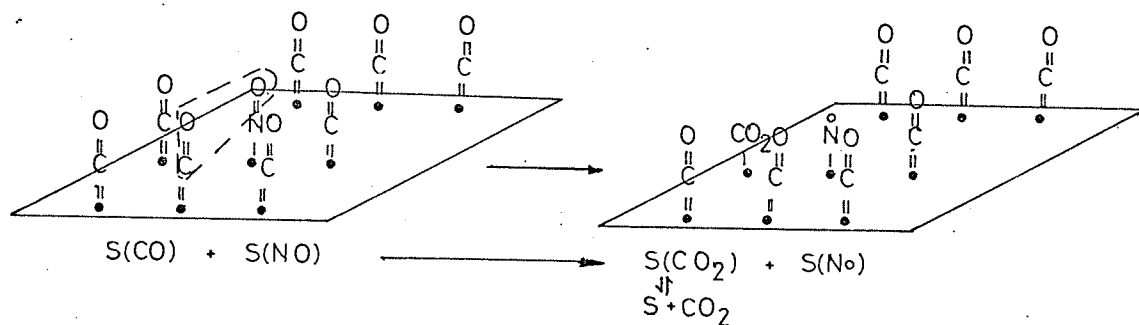
2 ii) ISOCYANATE FORMATION

S(No) + CO $\longrightarrow$ S(NCO)

3). EXCESS NO
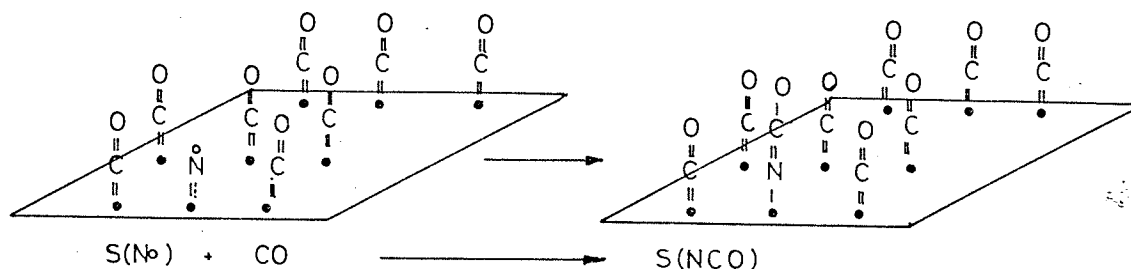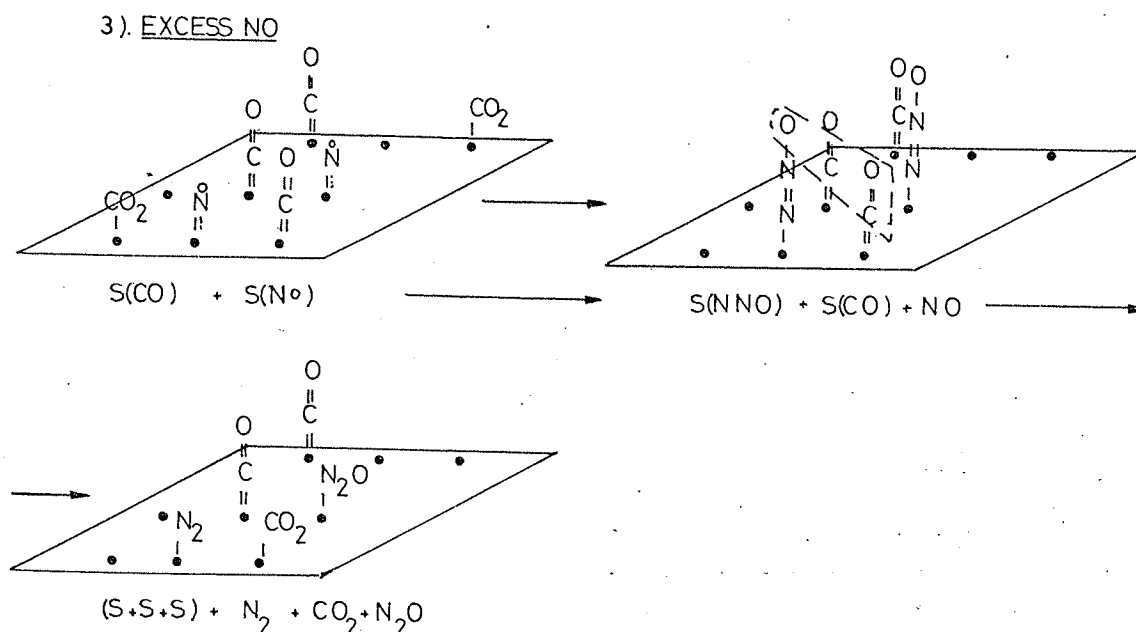
The scheme shows that the reaction may proceed through three seperate stages.

1) This stage is common to stages 2 and 3 and represents the formation of a single N – surface site through CO–NO bimolecular scheme.

2) Stage 2 shows the formation of a transient nitrous oxide structure, which then reacts with an adjacent carbon monoxide molecule to give nitrogen and carbon dioxide.

Reaction 2 requires that even in an excess of carbon mononoxide the nitric oxide in the gas phase quickly adsorbs onto a surface nitrogen atom.

3) Stage 3 shows the formation of nitrogen, carbon dioxide and nitrous oxide. For a reaction mixture containing an excess of nitric oxide the probability of nitrous oxide formation is increased since there is less carbon monoxide on the surface, thus less likelihood of (N_2O)s reacting with adsorbed carbon monoxide.

The production of nitrous oxide and isocyanate are inter-related mechanistically and depend for their formation upon reactant stoichiometry. Stages 2ii and 3 imply that the reactions could proceed by a Rideal - Eley mechanism.

(a) Isocyanate formation

Stage 2ii shows how in the presence of an excess of carbon monoxide a surface isocyanate species may be formed through the interaction of an adsorbed nitrogen atom with carbon monoxide. Infrared studies (chapter 5) have shown that the reaction is still catalyzed in the presence of a surface containing isocyanate species. Furthermore, these species remained unchanged after the reaction, which suggests that they are formed as a bi-product on selected sites rather than acting as intermediates in the reaction.

(b) Nitrous oxide formation

The formation of nitrous oxide during the reduction of an excess of nitric oxide by carbon monoxide has been explained in stage 3.

Nitrous oxide formation has also been observed during the reduction of nitric oxide by hydrogen [61] and ammonia [63] over transition metal catalysts. The common feature of these react-ions is that they require an excess of nitric oxide to form nitrous oxide. Shelef et al.[39,63] have described a mechanism whereby the formation of nitrous oxide requires the interaction of two adjacent surface nitric oxide molecules. The explanation offered in this work of a rapid two stage process occurring at one site would also statistically account for the results of

Shelef et al..

Nitrous oxide is more likely to be formed by the method described above than by the interaction of two adjacent or dimeric nitric oxide molecules since in the latter case there is no obvious interrelationship between the formation of nitrous oxide and isocyanate. To illustrate this point a comparison has been made with an analogous system which occurs in transition metal complexes. Bhaduri, Johnson and co-workers[84] have reported the production of carbon dioxide and nitrous oxide from the reaction of carbon monoxide with $[Ir\ P_2\ (NO)_2\ ][PF_6]$*; this forms $[IrP_2\ (CO)_3][PF_6]$ which in turn reacts with nitric oxide to generate the dinitrosyl, a continuous redox process. The mechanism which is based on the formation of $M - (N_2\ O_2)$ or $M\ (NO^+)\ (NO^-)$ as intermediates agrees with that of Haymore and Ibers[85] and is represented by the following reaction scheme[80]
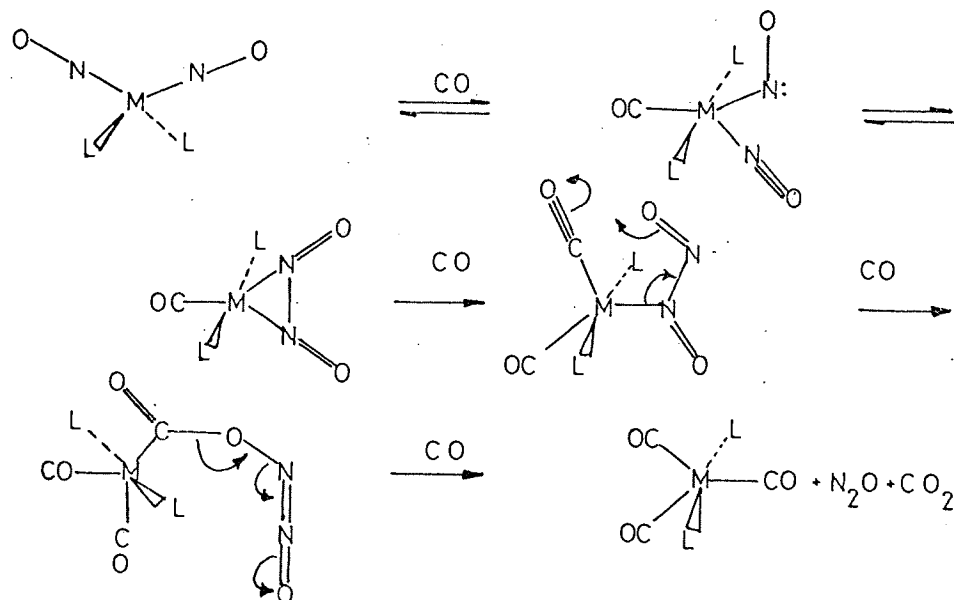

This scheme does not include the formation of an isolated nitrogen

* P ≡ triphenylphosphine.

atom, thus in an excess of carbon monoxide isocyanate is not formed.

In summary the mechanism proposed for the reduction of nitric oxide by carbon monoxide is consistent with:

(a)   the chemisorption properties of each reactant

(b)   the formation of nitrous oxide (in an excess of nitric oxide)

(c)   the formation of surface isocyanate species (in an excess of carbon monoxide)

(d)   the rate law which has been found by experiment.

FIGURE 9
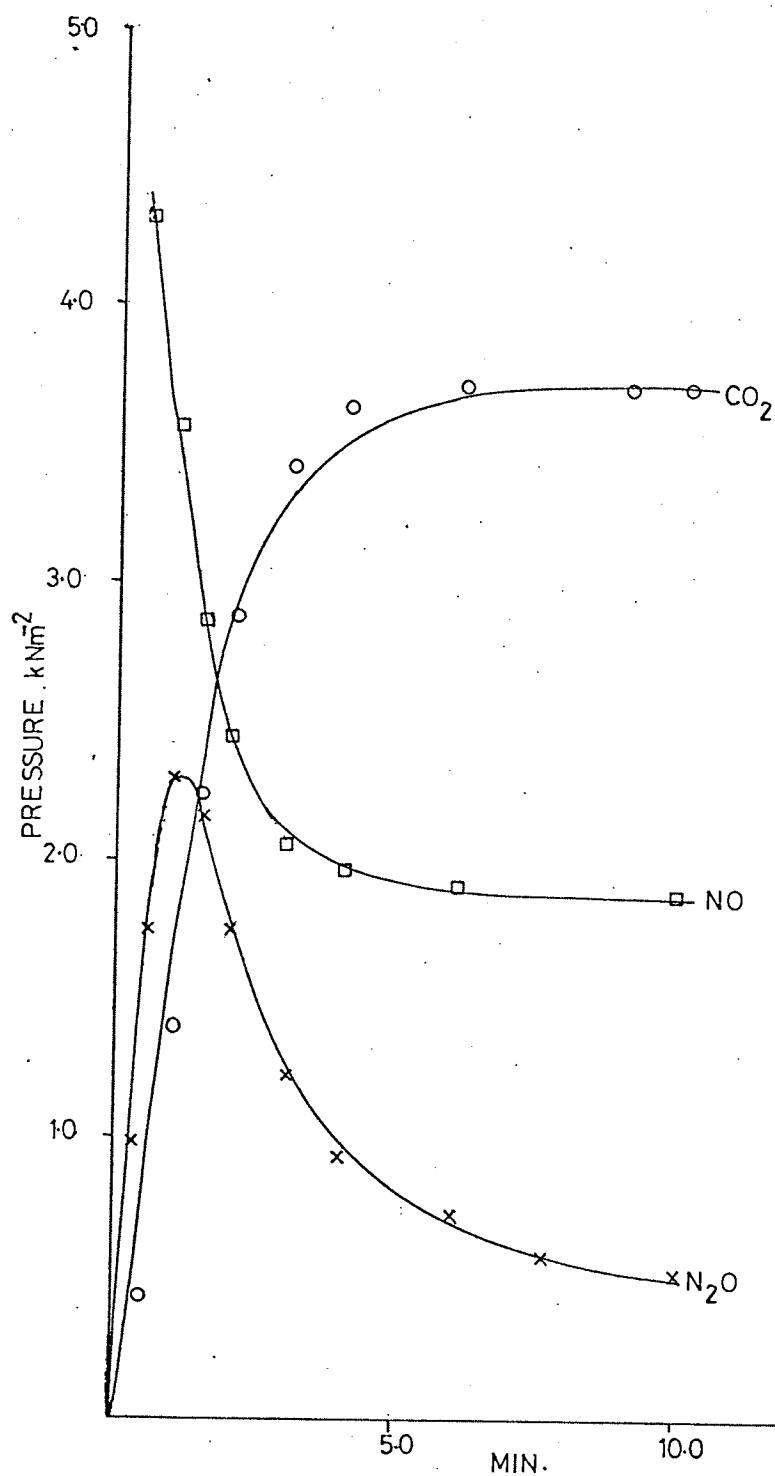
COMPOSITION/ TIME PLOT :- FOR THE REDUCTION OF $6.1 kNm^{-2}$
NO BY $3.7 kNm^{-2}$ CO OVER $0.5\%w/w Pd-Al_2O_3$ ($0.13g$) ; $400°C$.

FIGURE 10
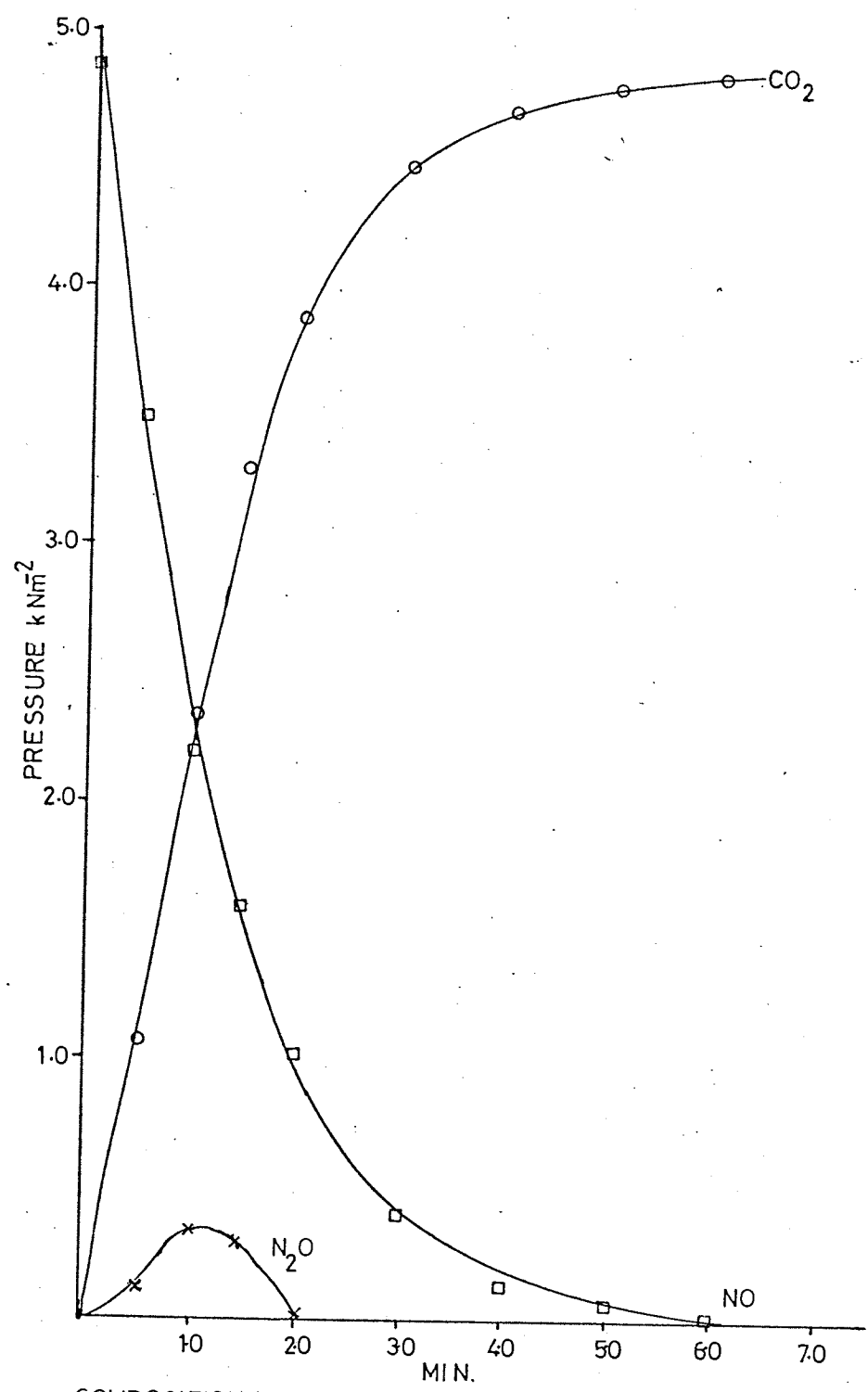
COMPOSITION / TIME PLOT :- FOR THE REDUCTION OF 4.8kNm⁻²
NO BY 4.8 kNm⁻² CO OVER 0.5%w/wPd−Al₂O₃,(0.13g); 400°C.

FIGURE 11
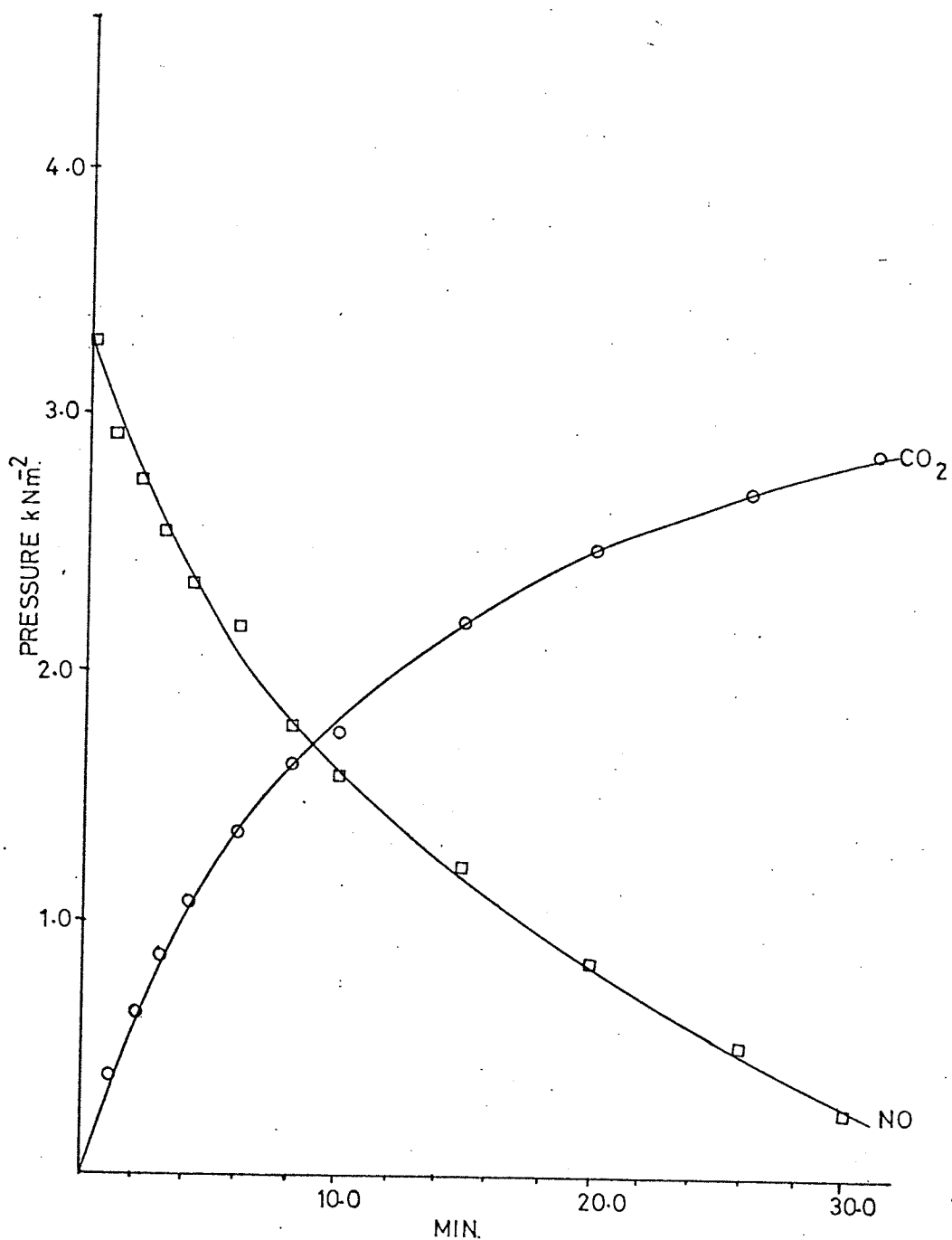
COMPOSITION/ TIME PLOT:- FOR THE REDUCTION OF 38kNm^{-2} NO BY 6.5kNm^{-2} CO OVER 0.5% w/w $Pd-Al_2O_3$ (0.13g); $400°C$.

FIGURE 12

PLOT OF Log INITIAL RATE AGAINST Log INITIAL
PRESSURE OF NO, FOR THE REDUCTION OF
NO BY CO OVER 0.5% w/w Pd-Al_2O_3, (0.21 g).
AT 400°C; CONSTANT CO 5.1 k Nm^{-2}.
SLOPE=2(± 0.05)

$Log_{10} P_{NO}$
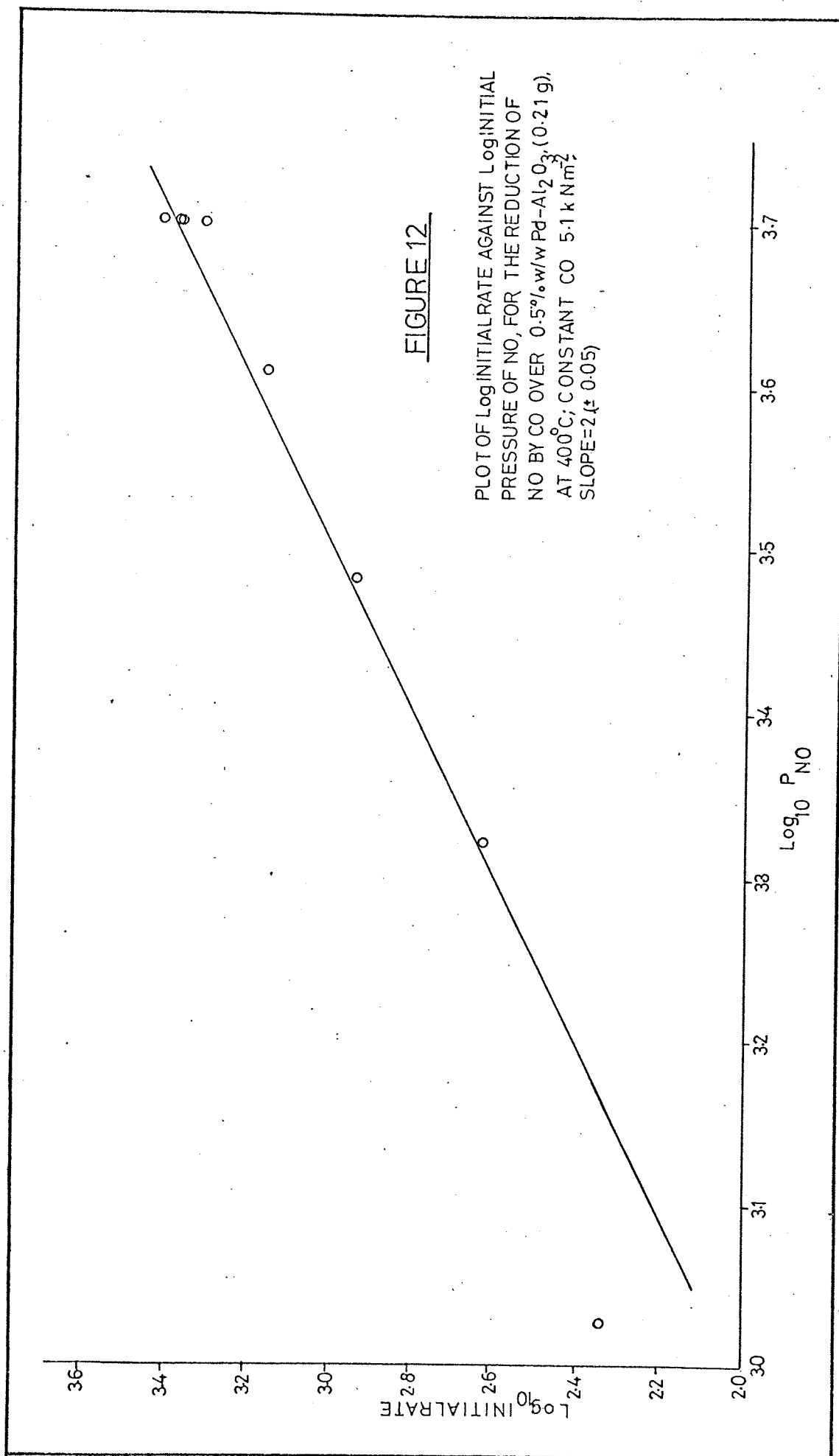
Log_{10} INITIAL RATE

FIGURE 13

PLOT Log INITIAL RATE AGAINST Log INITIAL
PRESSURE OF CO, FOR THE REDUCTION OF NO
BY CO OVER 0.5%w/w Pd-Al$_2$O$_3$, (0.21g) ; AT
400°C; CONSTANT NO 5.1 kNm^{-2}; SLOPE=-1.
(±0.05)

FIGURE 14

PLOT OF Ln RATE AGAINST Ln UNREACTED CO
FOR A SINGLE RUN WITH STOICHIOMETRIC
REACTANT PRESSURES (51 k Nm^2) OVER
0.5%w/w Pd-Al$_2$O$_3$, (0.21 g); 400°C.
SLOPE~1.
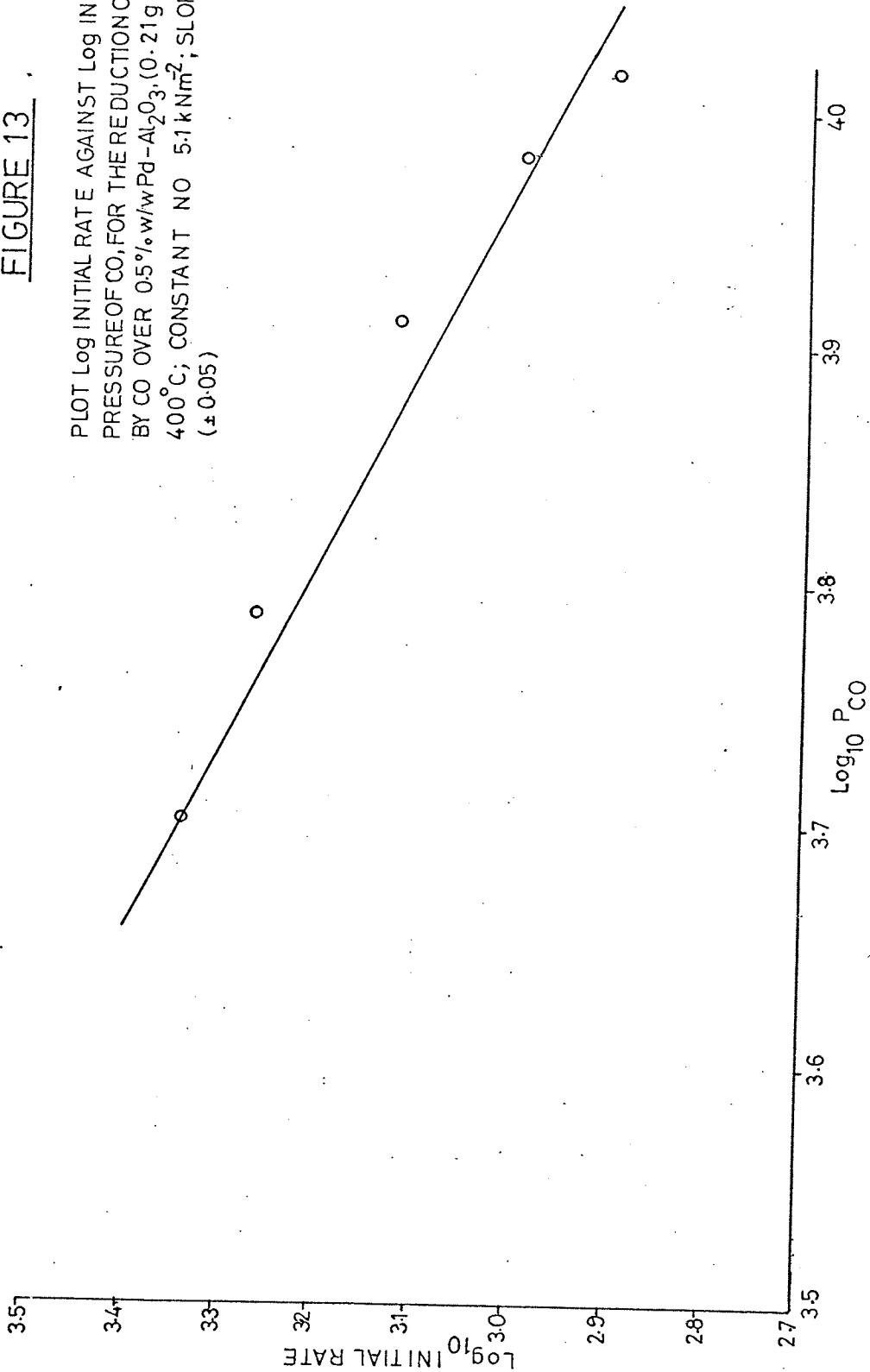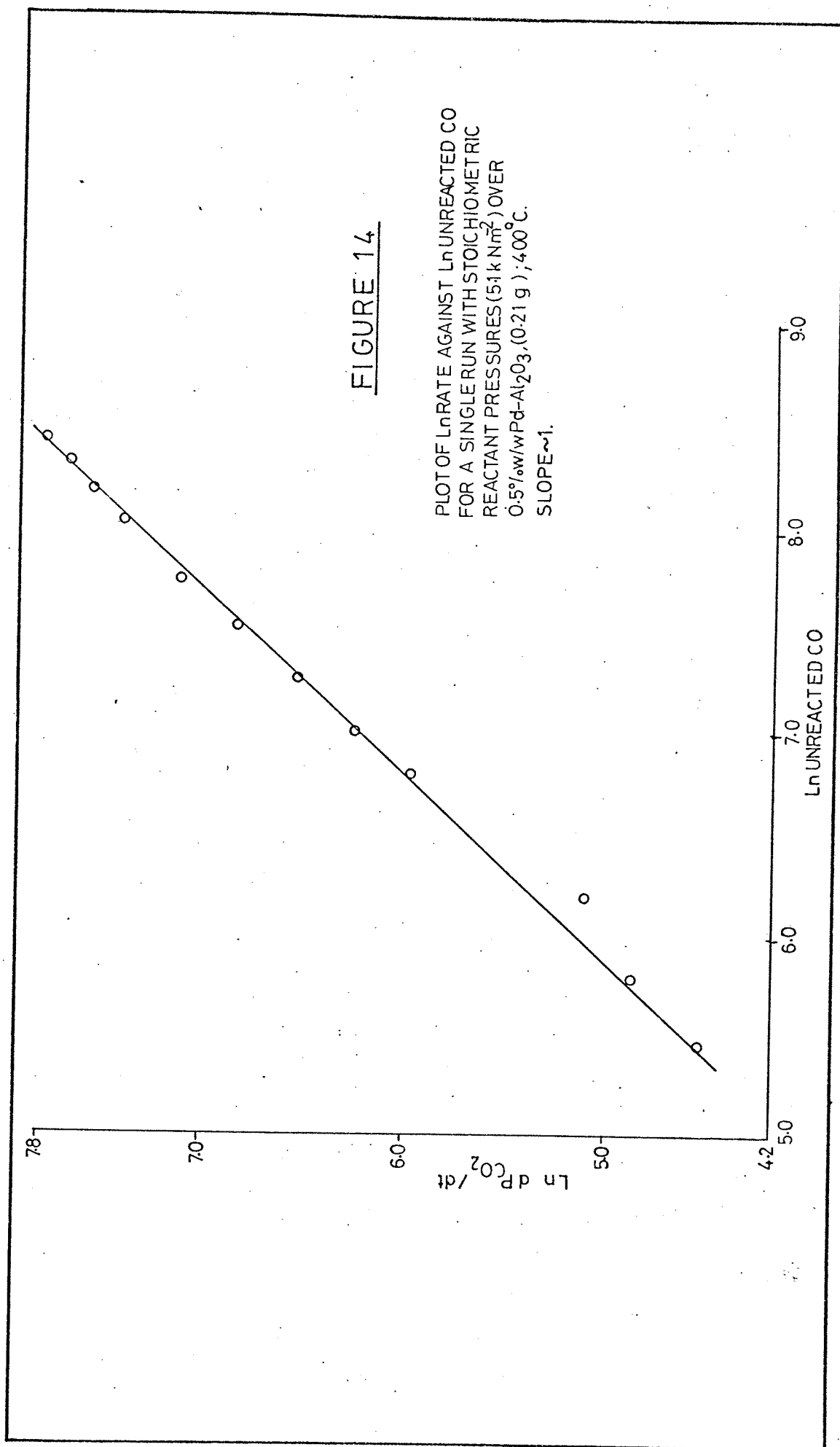
FIGURE 15

PLOT OF THE INTEGRATED RATE LAW $R = k \, P_{NO}^2 / P_{CO}$

COVERING THE PRESSURE RANGE INDICATED IN TABLE 13; 0.5% w/w Pd-Al_2O_3 (0.21g); 400°C.

$a. \equiv P_{NO} = 3.1 \; kNm^{-2}$, $P_{CO} = 5.1 \; kNm^{-2}$.

$b \equiv P_{NO} = 5.1 \; kNm^{-2}$; $P_{CO} = 6.1 \, kNm^{-2}$.

$c. \equiv P_{NO} = P_{CO} = 5.1 \; kNm^{-2}$.
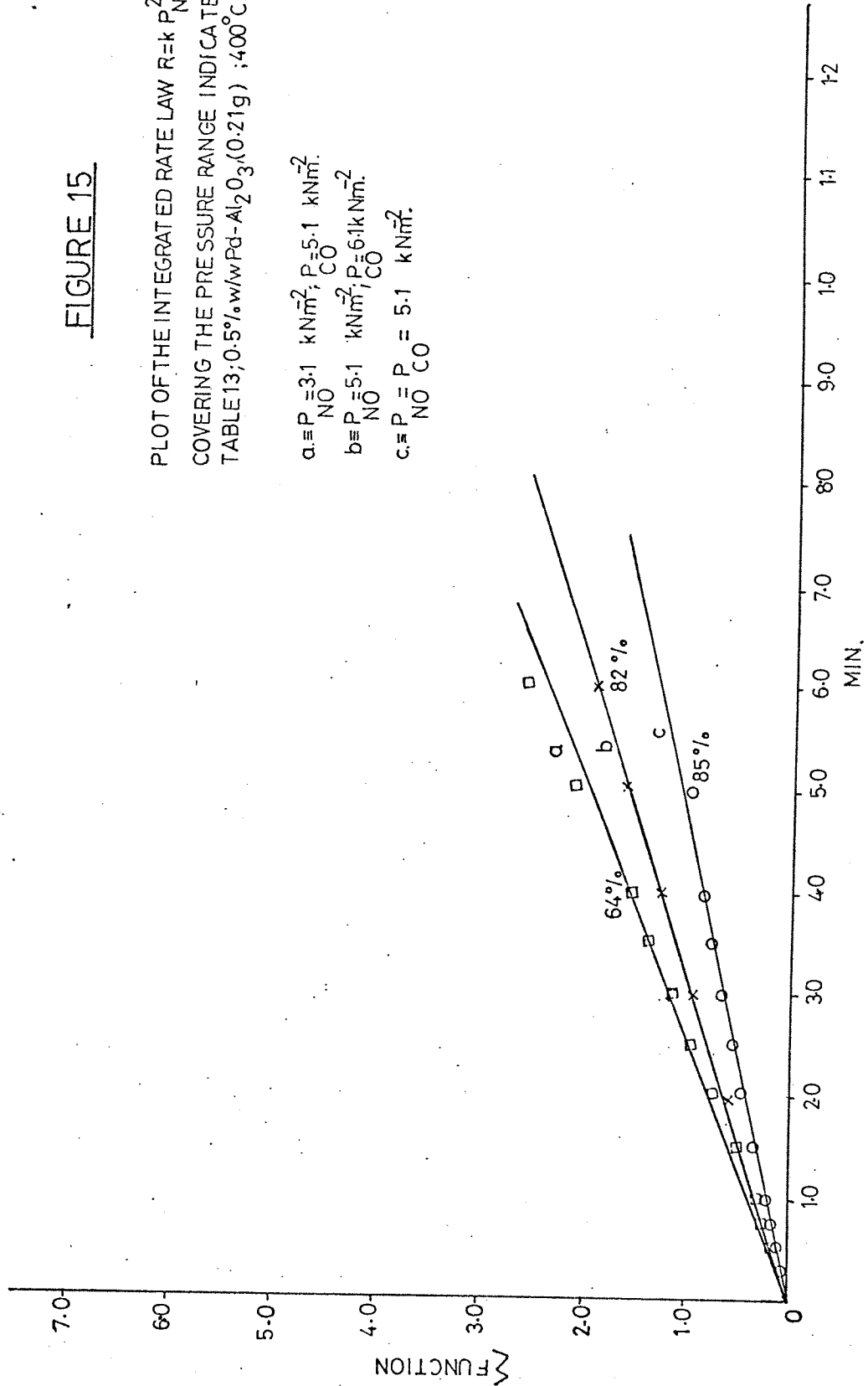
FIGURE 16
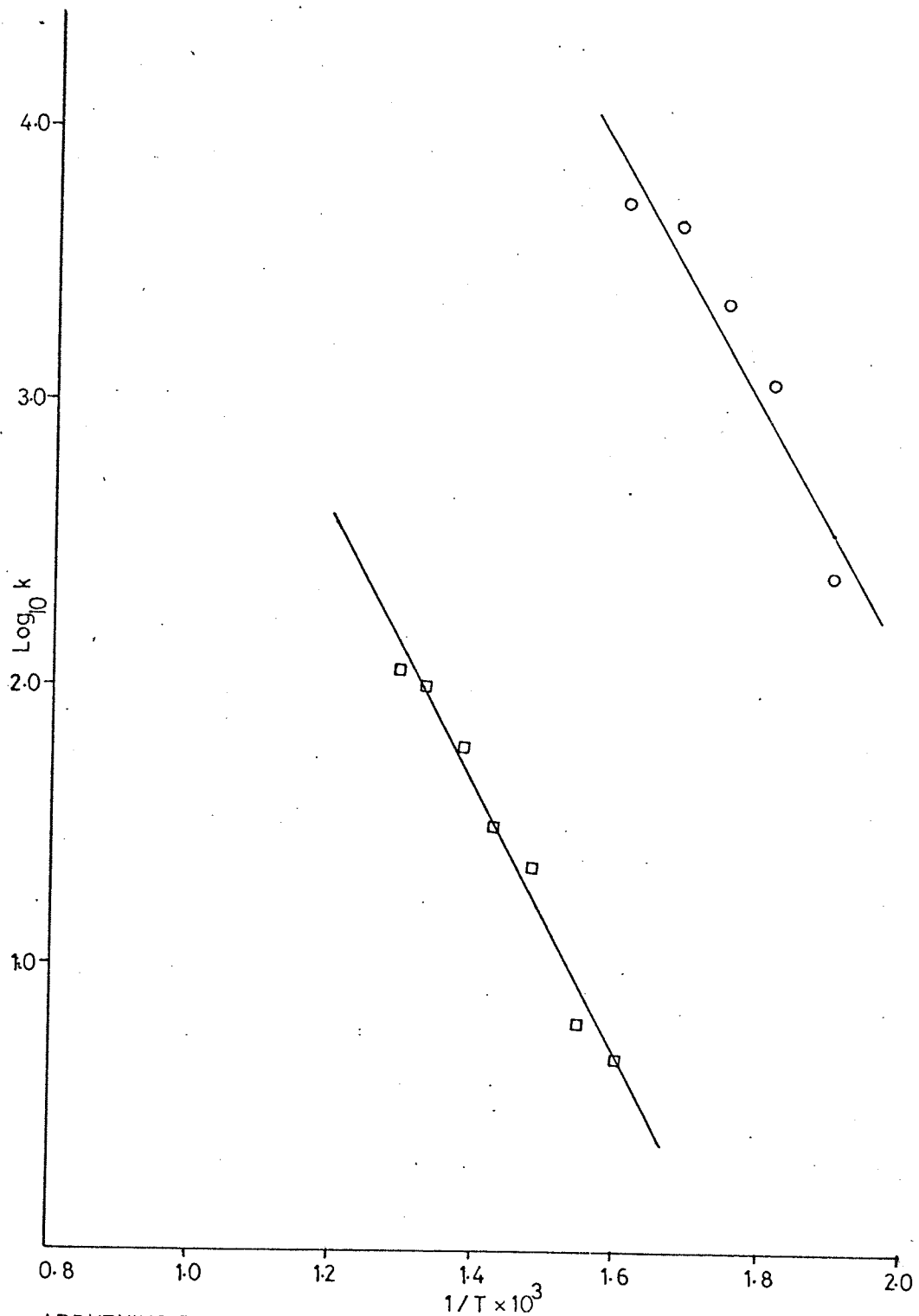
ARRHENIUS PLOTS FOR THE REDUCTION OF NITRIC OXIDE BY CARBON MONOXIDE
OVER : □.0.5°/o w/w Pd–Al_2O_3 ,(FIRST ORDER RELATIONSHIP, DATA GIVEN IN
TABLE 14; $CO = NO = 5.0 kNm^{-2}$.) $2 + Log_{10} k$.

: o.0.5°/o w/w Ru–Al_2O_3, (ZERO ORDER APPROXIMATION, DATA GIVEN IN
TABLE 16; $CO = NO = 4.6 k Nm^{-2}$).

TABLE 12

Listing preferential reactions over Al_2O_3 or 0.5 % w/w $Pd-Al_2O_3$

− no reaction after 10 min.

+· very slow reaction approximately 3-5% in 10 min.

+++ fast reaction, complete in 5-8 min.

TEMP 500°C REACTANTS	CATALYST ABSENT	SUPPORT Al_2O_3 0.1g	0.5% w/w $Pd-Al_2O_3$ 0.1g
NO	−	+	+
CO + NO	−	+	+++
N_2O	−	+	+
CO + N_2O	−	+	+++

TABLE 13

Summarizing the reaction order obtained for the nitric oxide carbon monoxide reaction over 0.5% w/w $Pd-Al_2O_3$ temperature 400°C catalyst weight 0.21g

PRESSURE LIMITS k Nm^{-2}	GAS KEPT CONSTANT k Nm^{-2}	O.W.R.T. NO α ($\pm$ 0.05)	O.W.R.T. CO β ($\pm$ 0.05)	EMPIRICAL RATE FORM RATE = $k_1 P_{NO}^{\alpha} P_{CO}^{\beta}$
CO (5.0-13.3)	NO, (5.0)		− 1.0	
NO (1.0-5.0)	CO, (5.0)	2.0	− 1.0	Rate = $k_1 P_{NO}^{2} P_{CO}^{-1}$

TABLE 14

Summarizing the temperature dependence of the first order reaction
rate constant for equal pressures of nitric oxide and carbon mon-
oxide (5.0k Nm^{-2}) over 0.5% w/w $Pd-Al_2O_3$ (0.219g)between $300^\circ C-500^\circ C$

TEMPERATURE $^\circ C$	k_1 min^{-1}	PERCENT REACTION	SD %
300	0.05066	31	–
350	0.0478	53	7.4
375	0.06206	50	3.0
400	0.2319	78	16.0
425	0.3108	63	5.2
450	0.6766	80	4.6
475	0.9366	94	4.0
500	1.1381	66	2.0

PROGRAMME (IN MATHCHAT) USED TO CALCULATE THE PRESSURE OF CO_2, N_2O AND NO (in torr for conversion to S.I. units ×133.3) FROM POSITIVE ION CURRENTS m/e 22,44 and 30.

```
4A V;T !
5FOR I=1,1,3; A M(I),C(I);T !!
6FOR R=1,1,N;DO 10/140
7QUIT
10T ,"X=";A X;T ,"Y=";A.Y;T ,"Z=";A Z;T !
40T !," SIGC02  SIGC02 SIGN2044 SIGN2030 SIGN0   PCO2  PV20  PNO ",!
59S A=X*32.3
60S NA=(A-C(1))/M(1)
70S B=Y-4;IF(B),75,80,80
75SET NB=0;GO900
80S VB=(B-C(2))/M(2)
90S J=B*.428
95IF(R),96,96,100
96S P=Z;GO110
100S P=Z-J
110S NP=(P-C(3))/M(3)
140T %6.03,A,B,J,P,NA,NB,NP,!
```

3.1. REDUCTION OF NITRIC OXIDE BY CARBON MONOXIDE OVER 0.5% w/w Ru-Al$_2$O$_3$ CATALYST

Preliminary experiments showed 1) that after fifteen minutes at 350°C the catalytic decomposition of nitric oxide (4.7 k Nm^{-2}) was insignificant compared with its catalytic reduction 2) that for reaction mixtures with an excess of nitric oxide amounts of nitrous oxide were formed. For this reason the kinetics of the reduction of nitric oxide by carbon monoxide were studied under reducing conditions.

A series of experiments similar to those used for the kinetic analysis of the reaction over a palladium catalyst were carried out. The results were analyzed using the standard methods outlined in chapter 2 section 2.6.1.

Figures 17 and 18 on pages 91 and 92 are double logarithm plots of the results obtained from initial rate data. Figure 17 shows a changing order with respect to nitric oxide pressure. This curve was divided by straight lines into two pressure regions A and B. Region A represents a pressure range between 1.0 to 4.7 k Nm^{-2}. Nitric oxide pressures below 1.0 k Nm^{-2} are represented in region B. The order of reaction determined from the slopes of these lines was found to be zero for region A and first order for region B. The effect of carbon monoxide pressure on the initial rate Figure 18, shows in spite of scatter no strong dependence. The order with respect carbon monoxide determined from the slope of a line of best fit was 0.22 $\pm$ 0.12.

Time course plots of reaction mixtures containing 1) stoichiometric reactant pressures, and 2) an excess of carbon monoxide are shown in Figure 19 on page 93. Figure 19 shows that for

a nitric oxide pressure of 0.9 Nm^{-2} (region B) the order with respect to time determined from the slope is 0.7. This result compares with a value of 1.0 obtained from the initial rate figure (region B). For stoichiometric reaction mixtures the slope of the time course plot is around zero for 70% of the reaction. This result implies that the overall order with respect to time is zero.

Reaction conditions and orders obtained from the initial rate method are summarized in Table 15 on page 96. For reaction mixtures up to a 5:1 ratio of carbon monoxide – nitric oxide (region A) a zero and a fractional order obtains for nitric oxide and carbon monoxide. This result implies that even though the reaction has an excess of carbon monoxide nitric oxide is relatively more strongly adsorbed than is carbon monoxide. Only when the reaction mixture exceeds the 5:1 ratio does the order with respect to nitric oxide tend to 1. This is consistent with a decrease in surface coverage by nitric oxide due to a proportionate increase of coverage by carbon monoxide.

The large error associated with the carbon monoxide order 0.22 $\pm$ 0.12 is similar to that obtained by McKee[67] and others[86,87] for the interaction of hydrogen and carbon monoxide over ruthenium. In this case, the order with respect to carbon monoxide was taken to be zero. An explanation for the large deviation may be due to the complex catalytic behaviour of ruthenium which is dependent upon its oxidation state[68]. This makes reproducibility difficult. Voorhoeve and Trimble[88] have shown that ruthenium on alumina

catalysts has at least five states with characteristic conversion patterns in the reduction of nitric oxide with a mixture of carbon monoxide and hydrogen.

There are two interpretations of the order with respect to carbon monoxide. The first is consistent with a bimolecular surface reaction in which an intermediate value of the Langmuir-isotherm applies for carbon monoxide, within this pressure range, such that carbon monoxide is less strongly adsorbed than nitric oxide. Secondly, if the order is taken as zero, it must be assumed that the reactants are adsorbed on two different types of surface site. In these circumstances the order with respect to each reactant will approach zero when the reactant pressures are high and the surface sites are fully covered. Of the two interpretations the first seems the most likely since the two molecules probably compete for the same site[57,66].

Carbon monoxide and nitric oxide are considered to be strongly adsorbed on ruthenium, in particular when its surface is reduced[67,77,89]. The reactants form structures which are comparable to those of the nitrosyls and carbonyls in transition metal complexes. Dinitrosyl structures[80] similar to those described in section 3.0.2 have also been observed. At 275°C, the predominant form of nitric oxide adsorption on ruthenium is molecular; dissociative adsorption occurs at temperatures above 350°C[90].

The two rate laws described in Table 15 were tested by substituting the results into the appropriate integrated rate expression of these laws and plotting the function with respect to time. For ease of integration the reactant orders were adjusted to the nearest half power. This means that the function approximates

to zero order kinetics for region A, and first order with respect
to nitric oxide for region B.

Figure 20 on page 94 reports the results of a zero order
plot. Figure 20 shows straight lines were obtained in most cases
to over 80% of the reaction. The reaction rate constant varied
between 12 ± 2 k $Nm^{-2}min^{-1}$ for most of the tested cases. This
result together with the linearity of the graphs indicates that
the zero order approximation is obeyed in region A. For region
B, the first order relationship with respect to nitric oxide was
also found to hold Figure 21 page 95.

The activation energy determined from an Arrhenius plot
Figure 16 page 80 was found to be 82.4 ± 15 kJ mol^{-1}. Data
for this plot was obtained from a series of reactions using stoich-
iometric reactant mixtures between $250^{\circ} - 350^{\circ}C$. The results
from a zero order approximation were interpreted in Table 16
page 96. The temperature range was limited to between $250^{\circ}-$
$350^{\circ}C$ because the reaction was very slow at the lower end and
became too fast to monitor above $350^{\circ}C$. Also, it was noted in
preliminary experiments that above $350^{\circ}C$ the catalyst activity
changed.

It has been shown that for the pressure limits outlined in
Table 15 the respective empirical rate equations give an adequate
representation of the reaction. These laws imply that nitric
oxide is more strongly adsorbed on ruthenium than carbon monoxide.
This means that even in an excess of carbon monoxide nitric oxide
proportionately excludes carbon monoxide from the surface. This
result is similar to that of Taylor and Klimisch[59]. These authors

noted that in reaction mixtures containing carbon monoxide and hydrogen ($300^{o}C$) nitric oxide inhibited its own removal; which indicates a strong interaction of nitric oxide with ruthenium. Because of this strong interaction the rate equations do not reflect the molecularity.

Ruthenium has the unique ability to switch between two meta-stable states during the reduction of nitric oxide by hydrogen and carbon monoxide mixtures[67]. These states have been associated with ammonia formation: 1) high NH_3 "reduced" Ru catalyst 2) low NH_3 "oxidized" Ru catalyst. A correlation between state 1 and isocyanate formation has been suggested by Unland[47], in that the isocyanate may act as an intermediate in the formation of ammonia, (through isocyanate hydrolysis). Unland[47] found that isocyanates are formed on freshly prepared ruthenium samples (state 1), but after several cycles the catalyst became inactive to isocyanate formations (state 2).

In state 1 where isocyanates are formed the reaction could follow the surface mechanism that has been described for the palladium catalyst (section 3.0.2.). In state 2, when the catalyst has aged, the reaction is likely to proceed through a scheme which precludes the formation of isolated nitrogen atoms, so that the SN· + CO reaction does not take place. A reaction mechanism such as that of Bhaduri, Johnson and co-workers[84] which was described in section 3.0.2 may be used to illustrate this. Since it is unlikely that the dimer will be formed on the surface at high temperatures the interaction is more likely to occur between two adjacent surface nitric oxide molecules.

If in state 2, nitric oxide is adsorbed on ruthenium in a bent mode[80] this would enhance the interaction of the oxygen atom with the ruthenium-surface and weaken the nitrogen-oxygen bond. In this way the interaction of surface nitric oxide and carbon monoxide molecules will lead to the formation of nitrogen and carbon dioxide, for example

1) Excess CO

a) N_2 + CO_2

b) OS + COS $\rightleftharpoons$ CO_2 + $2 S$

2) Excess NO

$\longrightarrow$ N_2O + CO_2
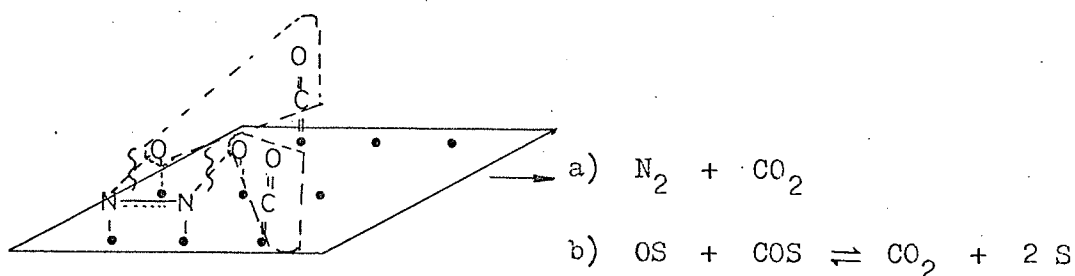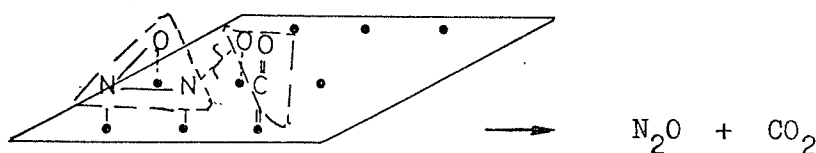
1) The above mechanism shows how in an excess of carbon monoxide nitrogen formation occurs without the formation of an isolated nitrogen atom. This leaves a surface oxygen atom which may react with an adjacent carbon monoxide molecule to give carbon dioxide; (ruthenium exhibits a high activity for this reaction in comparison with other platinum group metals, see also, the experimental evidence described in section 3.3.2).

2) In an excess of nitric oxide the probability of nitrous

oxide formation is increased since there is less carbon monoxide
on the surface.   However, ruthenium is very selective in the
conversion of nitric oxide to molecular nitrogen[57,64] in the
presence of carbon monoxide or hydrogen.   This explains why
nitrous oxide is not formed to any extent in oxidizing conditions,
i.e. the N – pairing probability and selectivity to nitrogen is
greater than that over palladium, thus the probability of nitrous
oxide formation diminished.

The surface mechanisms described for this reaction over
ruthenium in state 1 and state 2 are consistent with the proposals
of Voorhoeve and Trimble[88].   These authors have suggested that
the dual nature of ruthenium catalysts is due to heavy coverage
of the surface with nitrogen in the reduced state and to partial
coverage with oxygen in the oxidized state: i.e. the mechanism
described for the reduction over ruthenium in state 1, gives
nitrogen without the production of atomic oxygen whereas ruthen-
ium in state 2 yields atomic oxygen albeit transient, as well as
nitrogen.

FIGURE 17

PLOT OF Log INITIAL RATE AGAINST Log INITIAL
PRESSURE OF NO, FOR THE REDUCTION OF NO
BY CO OVER 0.5%w/w Ru-Al$_2$O$_3$;(0.5 9g);AT 275°C;
CONSTANT CO 4.6kNm^{-2}.
SLOPE A= 0.04, B=0.8.

FIGURE 18

PLOT OF Log INITIAL RATE AGAINST Log INITIAL PRESSURE
OF CO, FOR THE REDUCTION OF NO BY CO OVER 0.5%
w/w Ru-Al$_2$O$_3$·(0.59g); AT 275°C; CONSTANT NO 4·6kNm^{-2},
SLOPE = 0·2.

Log$_{10}$ P$_{CO}$

Log$_{10}$ INITIAL RATE

FIGURE 19

PLOT OF Ln RATE AGAINST Ln UNREACTED NO
FOR A SINGLE RUN OVER 0.5% w/w Ru-Al_2O_3,
(0.59g), AT 275°C, FOR:-
1) STOICHIOMETRIC REACTANT PRESSURES, 51
kNm^{-2}
2) CO = 51 kNm^{-2}; NO = 933 Nm^{-2}.

FIGURE 20

A ZERO ORDER PLOT FOR THE REDUCTION
OF NO BY CO OVER 0.5% w/w Ru-Al$_2$O$_3$,(0.59g),AT 275°C,
CONSTANT CO 4.6 kNm^{-2}; ⊚ ≡ P$_{NO}$=1.9 kNm^{-2},o≡P$_{NO}$=4.6kNm^{-2}.

FIGURE 21

A FIRST ORDER PLOT FOR THE REDUCTION OF NO BY CO OVER 0.5% w/w Ru-Al$_2$O$_3$, (0.59 g), AT 275°C. CONSTANT CO 4.6 kNm^{-2} : (RATE = k $\tilde{P}^1_{NO}$ $\tilde{P}^0_{CO}$).

o $\equiv$ P$_{NO}$ 933 Nm^{-2} ; □ $\equiv$ P$_{NO}$ 400 Nm^{-2}.
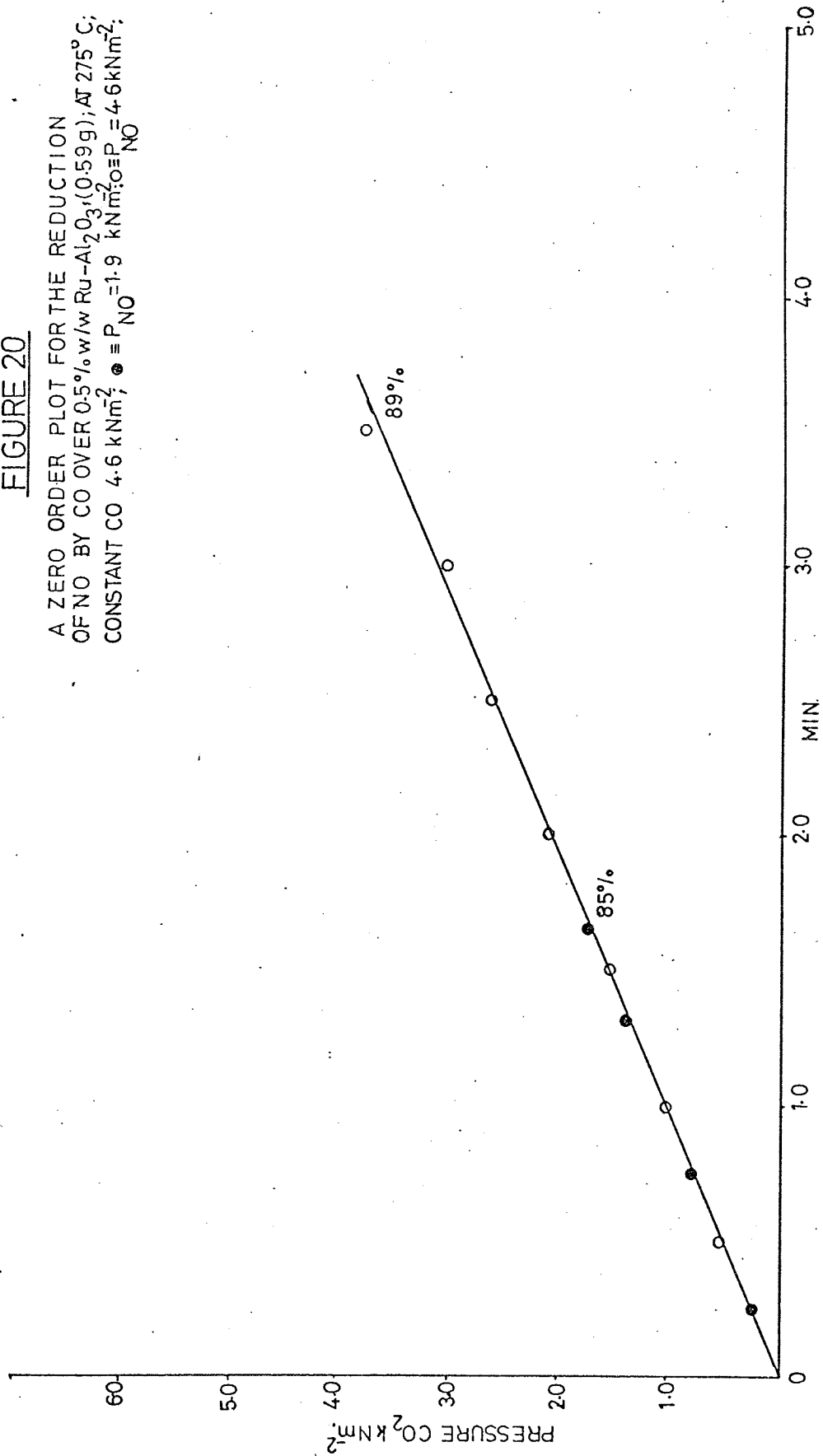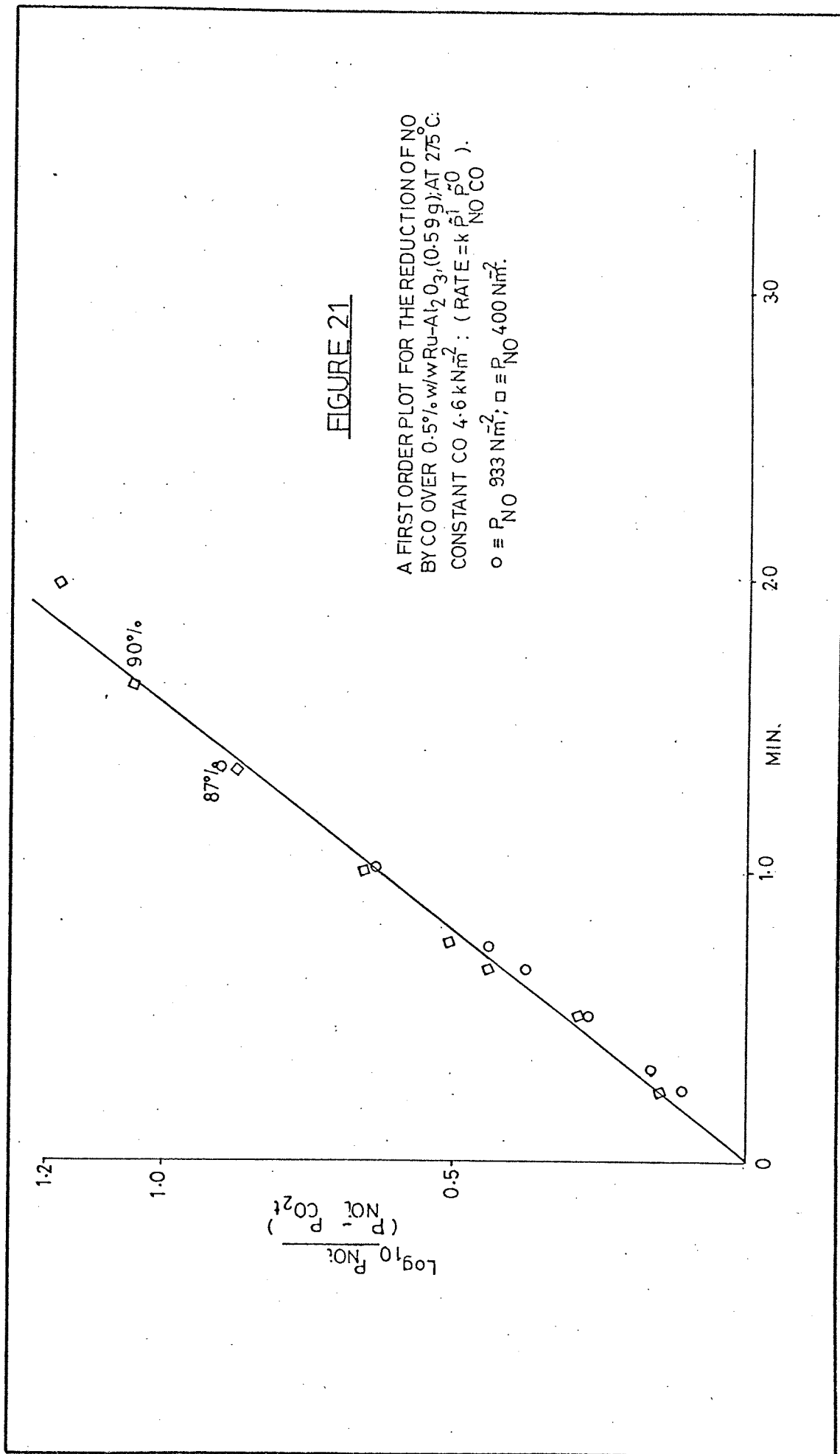
TABLE 15

Summarizing reaction orders obtained for the nitric oxide – carbon

monoxide reaction over 0.5% w/w Ru – Al_2O_3; temperature $275^{\circ}C$;

catalyst weight 0.59g

PRESSURE LIMITS k Nm^{-2}	GAS KEPT CONSTANT k Nm^{-2}	O.W.R.T. NO α	O.W.R.T. CO β $\pm$ 0.12	EMPIRICAL RATE FORM Rate= $kP_{NO}^{\alpha} \cdot P_{CO}^{\beta}$
CO.4.7–13.3	NO.4.7		0.22	
A.NO.4.7– 0.9	CO.4.7	0	0.22	Rate=$k_1 P_{NO}^{0.04} P_{CO}^{0.22}$
B.NO.0.9–0.4	CO.4.7	1	0.22	Rate=$k_2 P_{NO}^{0.8} P_{CO}^{0.22}$

TABLE 16

Summarizing the temperature dependence of the reaction rate constant

for equal pressures of nitric oxide and carbon monoxide (4.7 k Nm^{-2})

over 0.5% w/w Ru–Al_2O_3 (0.59g) between 250° – $350^{\circ}C$

TEMPERATURE $^{\circ}C$	k k Nm^{-1} min^{-1}	Percent reaction	SD %
250	2.572	30	4.0
275	12.076	75	2.7
300	24.803	73	5.0
325	48.336	57	0.4
350	54.53	61	0.7

3.2 REDUCTION CF NITROUS OXIDE BY CARBON MONOXIDE OVER 0.5% w/w

Pd-Al$_2$O$_3$ CATALYST.

Nitrous oxide formation during the nitric oxide – carbon
monoxide catalyzed reaction occurs as a result of the partial
reduction of nitric oxide (section 1.2.5., 1.2.6., and 3.0.1.).
For example in oxidizing conditions the following reactions
occur:

$$2\ NO\ +\ CO\ \overset{k_1}{=}\ N_2O\ +\ CO_2 \qquad -\quad (1)$$

$$N_2O\ +\ CO\ \overset{k_2}{=}\ N_2\ +\ CO_2 \qquad -\quad (2)$$
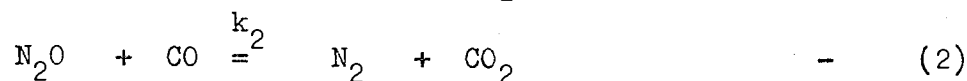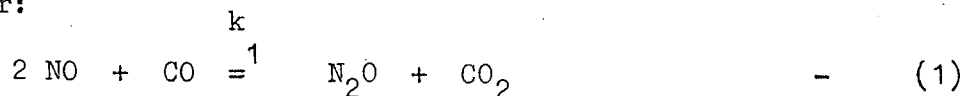
Reaction 2 is important in the reduction of nitric oxide by
carbon monoxide since the reaction rates are in the order of

$r_1 >\ r_2.$

The following represents the results and discussion of a
study of the reaction kinetics of the reduction of nitrous oxide
by carbon monoxide.

Table 12 on page 81   reports that the reduction of nitrous
oxide by carbon monoxide over a 0.5% w/w Pd-Al$_2$O$_3$ catalyst at
500°C is the only significant reaction.

The rate of production of carbon dioxide is expressed by
the empirical rate equation

$$\frac{dP_{CO_2}}{dt}\ =\ k\ P_{N_2O}^{\gamma}\ P_{CO}^{\nu} \qquad -\quad (3)$$

The notations used are the same as those used previously (section
3.0.1 equation 4).   The exponents γ and ν were determined
using the standard method adopted for the determination of react-
ion mechanisms outlined in chapter 2, section 2.6.1.

Figures 22 and 23 on pages 104 and 105   are double logarithm

plots of the results obtained at 470° from initial rate data.
These Figures show a change in order with respect to nitrous
oxide and carbon monoxide depending upon reactant pressures.
Reaction orders were evaluated by a least squares fit of the
data. A similar set of results were obtained for a series of
experiments carried out at $350^{\circ}C$ (Figures not shown). The
orders with respect to carbon monoxide and nitrous oxide are
listed in Table 17, page 117.

Time course plots of reaction mixtures containing 1)
stoichiometric reactant pressures 2) a 1:13 mixture of carbon
monoxide to nitrous oxide and 3) a 1:13 mixture of nitrous oxide
to carbon monoxide are represented by Figures 24, 25 and 26 on
pages 106 , , 107 and 108. Figure 24 reports that for
stoichiometric reactant mixtures the overall order with respect
to time is 1. This result agrees with the orders obtained from
the initial rate method, i.e. the overall order τ + $\mathcal{V}$ =
$(0.47 \pm 0.05 + 0.49 \pm 0.03)$(Table 17, $470^{\circ}c$). The order with
respect to time for carbon monoxide and nitrous oxide reported
in Figures 25 and 26 also agree with those listed in Table 17.
For example, for the reaction mixture with a large excess of
carbon monoxide the order with respect to nitrous oxide was found
to be around 1.0, while a value of 0.88 ± 0.06 was obtained from
the initial rate method.

Table 17 reports that the orders with respect to carbon
monoxide and nitrous oxide are fractional. Under mainly reduc-
ing conditions the carbon monoxide order changes from 0.3 to 0.67

($\pm$ 0.07) as the temperature is increased from 350° to 470°C.

This is consistent with a relative decrease of surface coverage by carbon monoxide as the temperature is increased. Similarly in oxidizing conditions an increase in temperature increases the order with respect to carbon monoxide from 0.67 ± 0.07 to 0.95 ± 0.03. The change in temperature influenced the surface coverage by carbon monoxide on an oxidized surface more strongly than on a reduced surface. The same reasoning applies with regard to the order with respect to nitrous oxide in that at the lower temperature under oxidizing conditions the order approaches zero due to an increase in surface coverage.

Table 17 lists the empirical rate laws which apply for the reduction of nitrous oxide by carbon monoxide. The following represents an interpretation of these laws:

(a) Excess carbon monoxide; N_2O: CO ratio $> 1:3$; rate =

$$kP_{CO}^{\frac{1}{2}} P_{N_2O}$$

For a large excess of carbon monoxide it must be assumed that the surface is predominantly covered by carbon monoxide. This means that nitrous oxide has a low surface coverage; (if at all). In these circumstances a Rideal - Eley mechanism is favoured; the rate of production of carbon dioxide is given by

$$\frac{dP_{CO_2}}{dt} = k\Theta_{CO} P_{N_2O} \qquad - 3$$

For a high surface coverage by carbon monoxide the order should approach zero, which is the case. A first order obtains for nitrous oxide which is consistent with this mechanism.

The rate law which describes this case was tested by substituting the results into the integrated rate expression (Table 18 on page 118 and plotting the functions with respect to time in the usual manner. Figure 27 on page 109 reports the results of such a plot. The Figure shows linearity to at least 55% completion for most tested cases.

b) When $N_2O \simeq CO$: rate = $k \, P_{CO}^{\frac{1}{2}} \, P_{N_2O}^{\frac{1}{2}}$

When the reactant mixtures approach stoichiometry the rate law becomes rate = $k \, P_{CO}^{\frac{1}{2}} \, P_{N_2O}^{\frac{1}{2}}$. The rate law implies that nitrous oxide influences carbon monoxide adsorption so that a fractional surface coverage is obtained by both reactants. Nitrous oxide may be dissociatively adsorbed which could account for the half order pressure dependence. In these circumstances a dual site surface reaction is favoured.

Table 18 shows that for equal reactant pressures a first order relationship obtains. A plot of this function (Figure 28 page 110 for a series of reactions carried out between $250^{\circ}C$ and $500^{\circ}C$ shows good linearity. The first order relationship was also found to hold for equal reactant pressures between 0.7 to 4.7 k Nm^{-2}, Figure 29 page 111.

The integrated form of rate = $k \, P_{CO}^{\frac{1}{2}} \, P_{N_2O}^{\frac{1}{2}}$ has been plotted in Figures 30 and 31 on pages 112 and 113. These plots cover the pressure limits outlined in Table 17. The results show that the above equation gives an adequate representation of the reaction up to about 70% completion. Greatest deviation occurred for reactions with an excess of carbon monoxide.

c) Excess nitrous oxide; CO: N_2O ratio $> 1:3$; rate $=k \, P_{CO}^{1}$ $P_{N_2O}^{\frac{1}{2}}$.

For a reaction with a large excess of nitrous oxide the rate law becomes, rate $= k \, P_{CO}^{1} \, P_{N_2O}^{\frac{1}{2}}$. Despite the weak adsorption of nitrous oxide the large amount of nitrous oxide in the gas phase will be reflected by an increased surface coverage of nitrous oxide, which will restrict the sites available for carbon monoxide adsorption. Thus the order with respect to carbon monoxide will approach unity.

Figure 32 on page 114 reports the results of a plot of the appropriate function for a series of reactions in this pressure range. The Figure shows linearity to at least 80% for most tested cases. The curve does not pass through the origin due to an error in the chart recorder.

The apparent activation energy determined from Arrhenius plot Figure 33 page 115 was found to be $65.1 \pm 9 \, k \, J \, mol^{-1}$. Data for this plot was obtained from a series of reactions using stoichiometric reactant pressures between 250° and $500^\circ C$.

The chemisorption of carbon monoxide on palladium was discussed in section 3.0.2. There is general agreement in the literature that nitrous oxide adsorption is both molecular and dissociative depending upon the oxidation state of the surface.[74,91-95] Infrared surface studies of Unland[47] indicate that nitrous oxide is not strongly adsorbed in palladium which agrees with the infrared observations of this work, Chapter 5. The fact that surface

isocyanate species are not observed is evidence supporting the view that dissociation does not take place to any extent

$$2 N_2O \rightleftharpoons 2NO + N_2$$
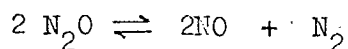
In summary, the interpretation of the rate laws discussed in a, b and c to some extent reflect the chemisorption properties of each reactant. In order to explain the fractional order pressure dependence of nitrous oxide it was proposed that nitrous oxide may modify carbon monoxide adsorption.

Leach and Peters[53] found the reaction to be retarded in the presence of carbon dioxide over a chromium promoted iron oxide catalyst. This possibility was investigated by carrying out a series of experiments in which carbon dioxide had been added initially to stoichiometric reactant pressures. Figure 34 on page 116 represents the results of these experiments. The Figure shows that for a reaction with stoichiometric reactant mixtures (4.6 k Nm^{-2}) 1 k Nm^{-2} of added carbon dioxide has no effect on the first order representation.

3.2.1. A COMPARISON OF THE NITROUS OXIDE AND NITRIC OXIDE REACTION WITH CARBON MONOXIDE OVER 0.5% w/w Pd-Al$_2$O$_3$

For a large excess of carbon monoxide the reduction of nitrous oxide proceeds mainly by a Rideal – Eley mechanism in which nitrous oxide in the gas phase reacts with adsorbed carbon monoxide. When the ratio of carbon monoxide to nitrous oxide falls below 3:1 a Langmuir-Hinshelwood mechanism predominates. It is for this condition that the comparison has been made.

In an excess of carbon monoxide the rate of the two reactions

are given by

$$\text{rate} = k\, P_{NO}^{2}\, P_{CO}^{-1} \qquad : \qquad \text{rate} = k\, P_{N_2O}^{\frac{1}{2} \to 1}\, P_{CO}^{\to \frac{1}{2}}$$

reaction temperature : 623 K : 623 K

Since the reaction temperatures were similar the difference in the rate laws must be attributed to the differing properties of nitric oxide and nitrous oxide. Conceivably, the presence of nitric oxide modifies the surface so that carbon monoxide - surface interactions are stronger than those for the reduction of nitrous oxide. In these circumstances carbon monoxide would inhibit the reduction of nitric oxide to a greater extent than for nitrous oxide.

The reduction of nitric oxide by carbon monoxide is about ten times slower than the corresponding nitrous oxide - carbon monoxide reaction (see Table 21, page 154 section 3.4.). One reason for the difference in activities may be due to the formation of surface isocyanate species[47]. Surface isocyanates form during the reduction of nitric oxide by an excess of carbon monoxide only. Infrared surface studies have shown (chapter 5) that the surface isocyanate species are relatively stable; thus when formed they will reduce the number of sites available for the reduction process.

FIGURE 22

PLOT OF Log INITIAL RATE AGAINST Log INITIAL
PRESSURE OF CO FOR THE REDUCTION OF N_2O
BY CO OVER 0.5%w/w Pd-Al_2O_3, (0.12g); AT 470°C;
CONSTANT N_2O 5.3 kNm^{-2}.

$Log_{10} P_{CO}$

Log_{10} INITIAL RATE

FIGURE 23

PLOT OF Log INITIAL RATE AGAINST Log INITIAL PRESSURE OF N_2O FOR THE REDUCTION OF N_2O BY CO OVER 0.5%w/w Pd-Al_2O_3.(0.12 g);AT 470°C; CONSTANT CO 5.3 kNm^{-2}.

FIGURE 24

PLOT OF Ln RATE AGAINST Ln UNREACTED CO (OR N_2O)
FOR A SINGLE RUN WITH STOICHIOMETRIC REACTANT
PRESSURES (53 kNm^{-2}) OVER 0.5% w/w Pd-Al_2O_3,
(0.12g); AT 470°C; (calculated in torr for conversion
to S.I. units add 4.89)
SLOPE ~ 1

FIGURE 25

PLOT OF Ln RATE AGAINST Ln UNREACTED CO FOR A SINGLE RUN WITH $5.3 \, kNm^{-2} \, N_2O$, $0.4 \, kNm^{-2}$ CO, OVER 0.5% w/w Pd Al_2O_3, $(0.12g)$; AT 470°C; (calculated in torr for conversion to S.I. units add 4.89) INITIAL SLOPE~0.7

FIGURE 26

PLOT OF Ln RATE AGAINST Ln UNREACTED N_2O FOR A SINGLE RUN WITH 53 kNm^{-2} CO, 0.4 kNm^{-2} N_2O, OVER 0.5%w/w Pd Al_2O_3, (0.12g), AT 470°C; (calculated in torr for conversion to S.I. units add 4.89) INITIAL SLOPE ~1

FIGURE 27

PLOT OF THE INTEGRATED RATE LAW $R = k \, P_{CO}^{1/2} \, P_{N_2O}$

WHEN THE PRESSURE OF N_2O TO CO IS $\sim$ 1:3;
CONSTANT CO $4.8\,kNm^{-2}$; $0.5\%\,w/w$ Pd-Al_2O_3; $(0.12\,g)$; $350°C$.

$o = P_{N_2O}\,0.4\,kNm^{-2}$: $x = P_{N_2O}\,1.9\,kNm^{-2}$: $\Box = P_{N_2O}\,2.7\,kNm^{-2}$.

TO $\sim$ 60% REACTION

FIGURE 2 8

FIRST ORDER PLOTS FOR EQUAL PRESSURES OF
N_2O AND CO $(4 \cdot 8 \, kNm^{-2})$, IN A TEMPERATURE
RANGE OF $250° - 500°C$; $0 \cdot 5 \% \, w/w \, Pd \, Al_2O_3, (0 \cdot 12g)$.
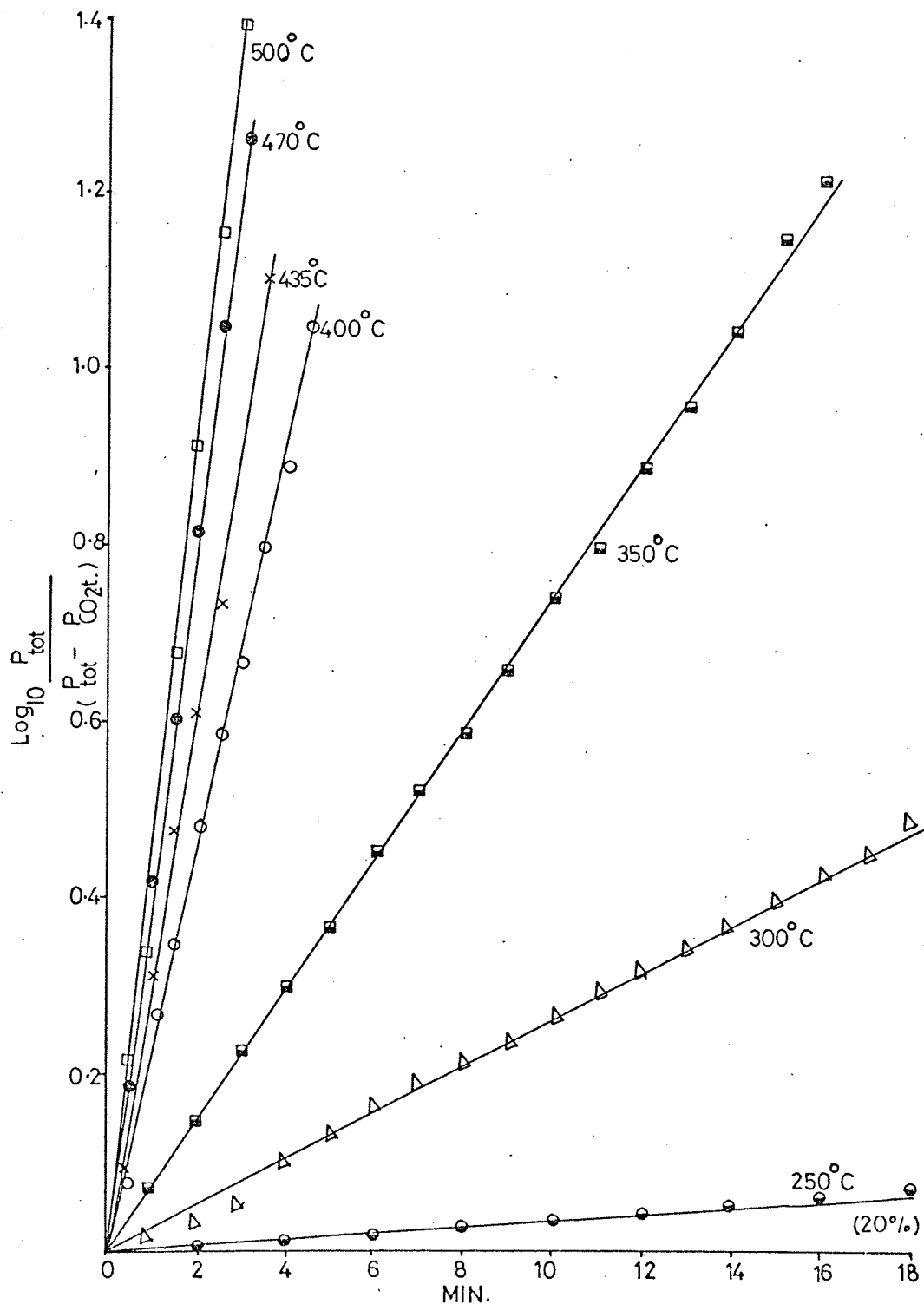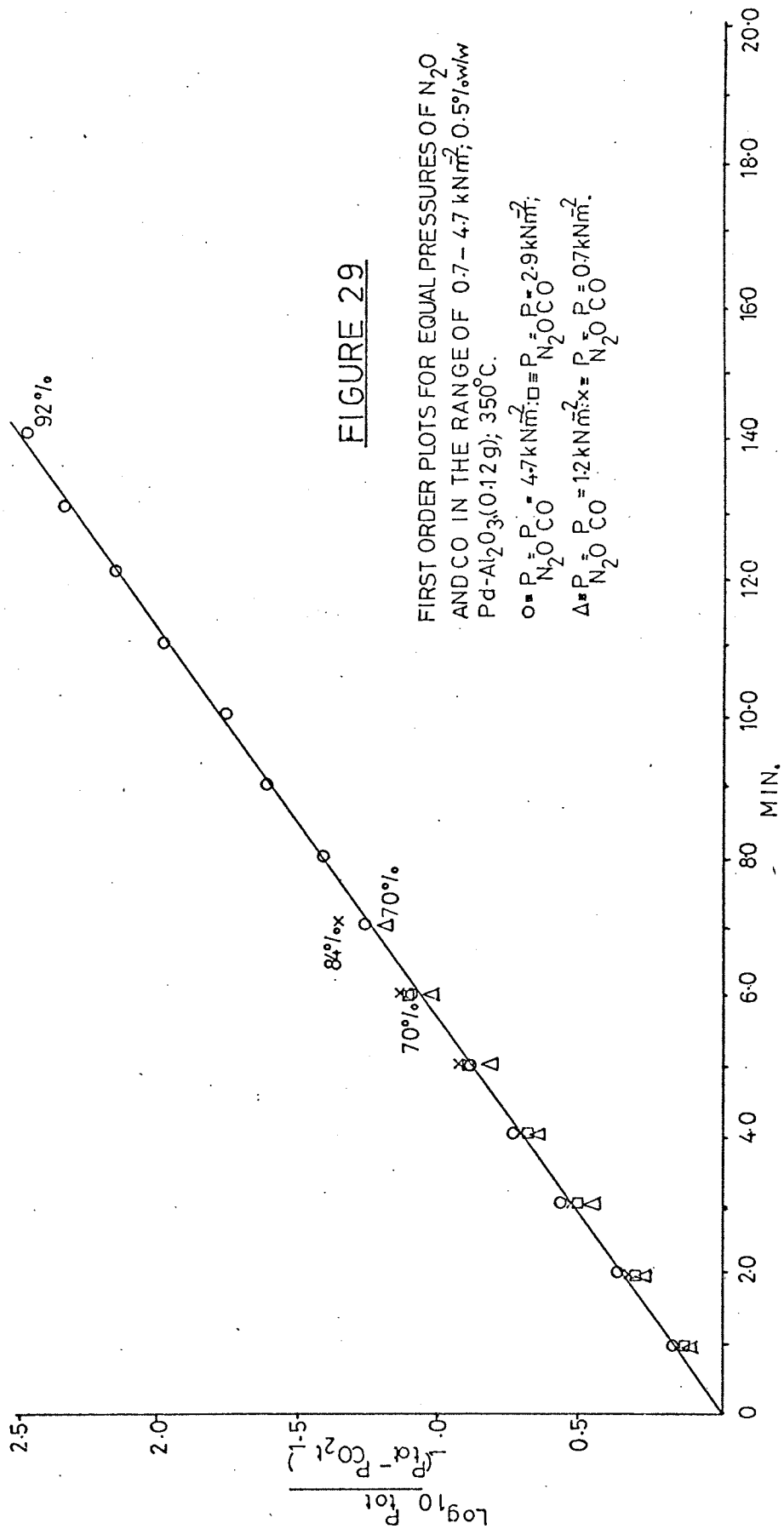
FIGURE 29

FIRST ORDER PLOTS FOR EQUAL PRESSURES OF N_2O AND CO IN THE RANGE OF 0.7 – 4.7 kNm^{-2}; 0.5%w/w Pd-Al_2O_3,(0.12g); 350°C.

o= P_{N_2O}= P_{CO} = 4.7 kNm^{-2}: □= P_{N_2O}= P_{CO}= 2.9 kNm^{-2};

Δ= P_{N_2O}= P_{CO} = 1.2 kNm^{-2}: x= P_{N_2O}= P_{CO} =0.7 kNm^{-2}.
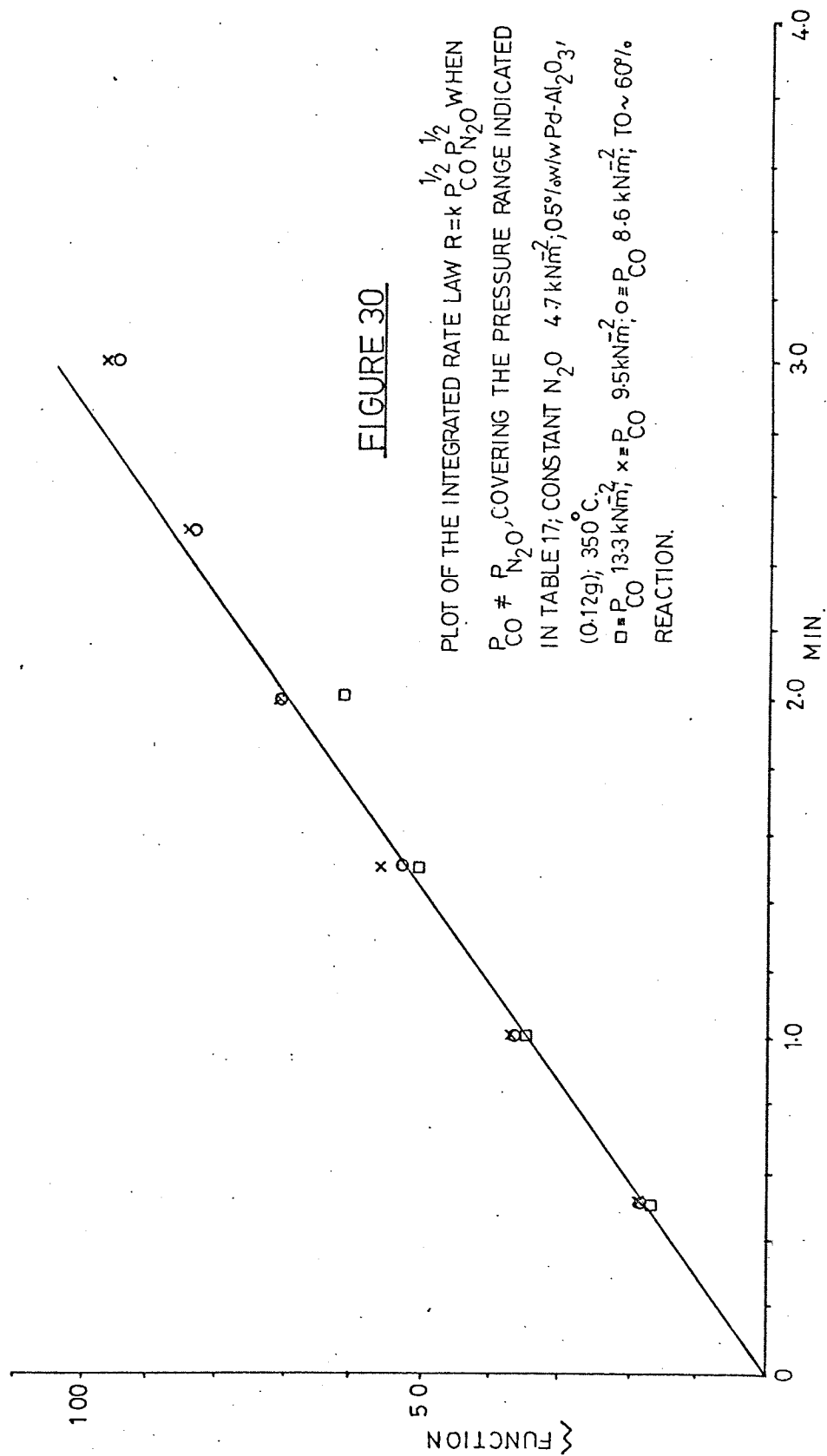
FIGURE 30

PLOT OF THE INTEGRATED RATE LAW $R = k \, P_{CO}^{1/2} \, P_{N_2O}^{1/2}$ WHEN $P_{CO} \neq P_{N_2O}$, COVERING THE PRESSURE RANGE INDICATED IN TABLE 17; CONSTANT N_2O $4.7 \, kNm^{-2}$; $05\%_{o}w/w \, Pd-Al_2O_3$, $(0.12g)$; $350\,^{\circ}C$.

$\square = P_{CO} \, 13.3 \, kNm^{-2}$; $\times = P_{CO} \, 9.5 \, kNm^{-2}$; $o = P_{CO} \, 8.6 \, kNm^{-2}$; TO $\sim 60\%$ REACTION.

113

FIGURE 31

PLOT OF THE INTEGRATED RATE LAW $R = k P_{CO}^{1/2} P_{N_2O}^{1/2}$ WHEN $P_{CO} \neq P_{N_2O}$, COVERING THE PRESSURE RANGE INDICATED IN TABLE 17; CONSTANT P_{CO} 4·7 kNm^{-2}; 0·5% w/w Pd-Al$_2$O$_3$, (0·12 g); 350°C.

$O = P_{N_2O}$ 4·3 kNm^{-2}; $\square = P_{N_2O}$ 8·5 kNm^{-2}; $\times = P_{N_2O}$ 14·6 kNm^{-2}.

FIGURE 32

PLOT OF THE INTEGRATED RATE LAW $R = k P_{CO} \, P_{N_2O}^{1/2}$ WHEN THE PRESSURE

OF CO TO N_2O IS $\rightarrow$ 1:3; CONSTANT N_2O $4.8 kN\,m^{-2}$; $0.5°/o\,w/w$

Pd-Al_2O_3, $(0.12g)$; $350°C$: $\square$ ■ P_{CO} $0.4 kN\,m^{-2}$: $\circ$ = P_{CO} $0.9 kN\,m^{-2}$.

82°/o 83°/o

{ FUNCTION

MIN.

FIGURE 33

ARRHENIUS PLOT OF FIRST ORDER REACTION
RATE CONSTANTS DEDUCED FROM THE DATA
GIVEN IN FIGURE 28.
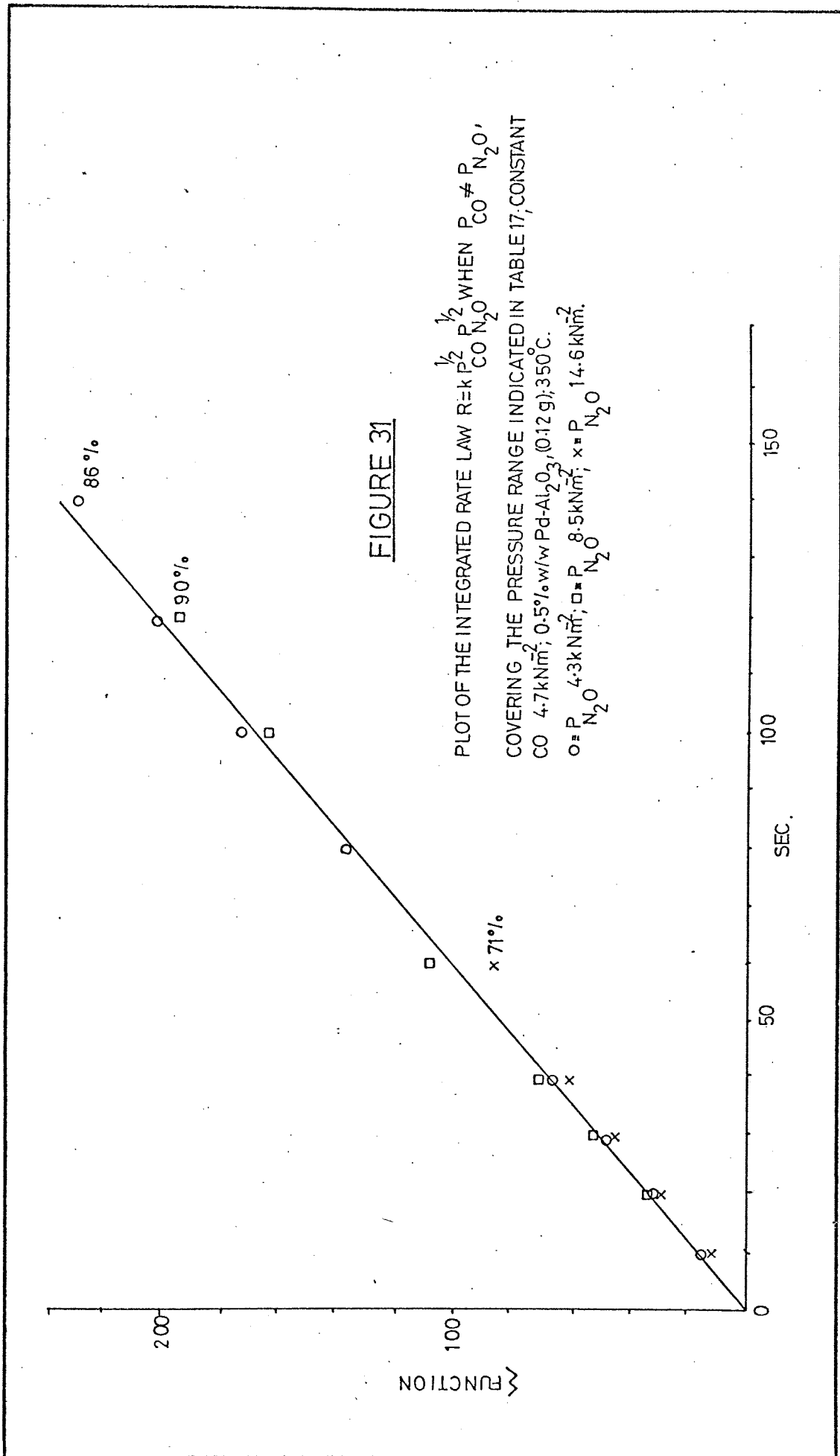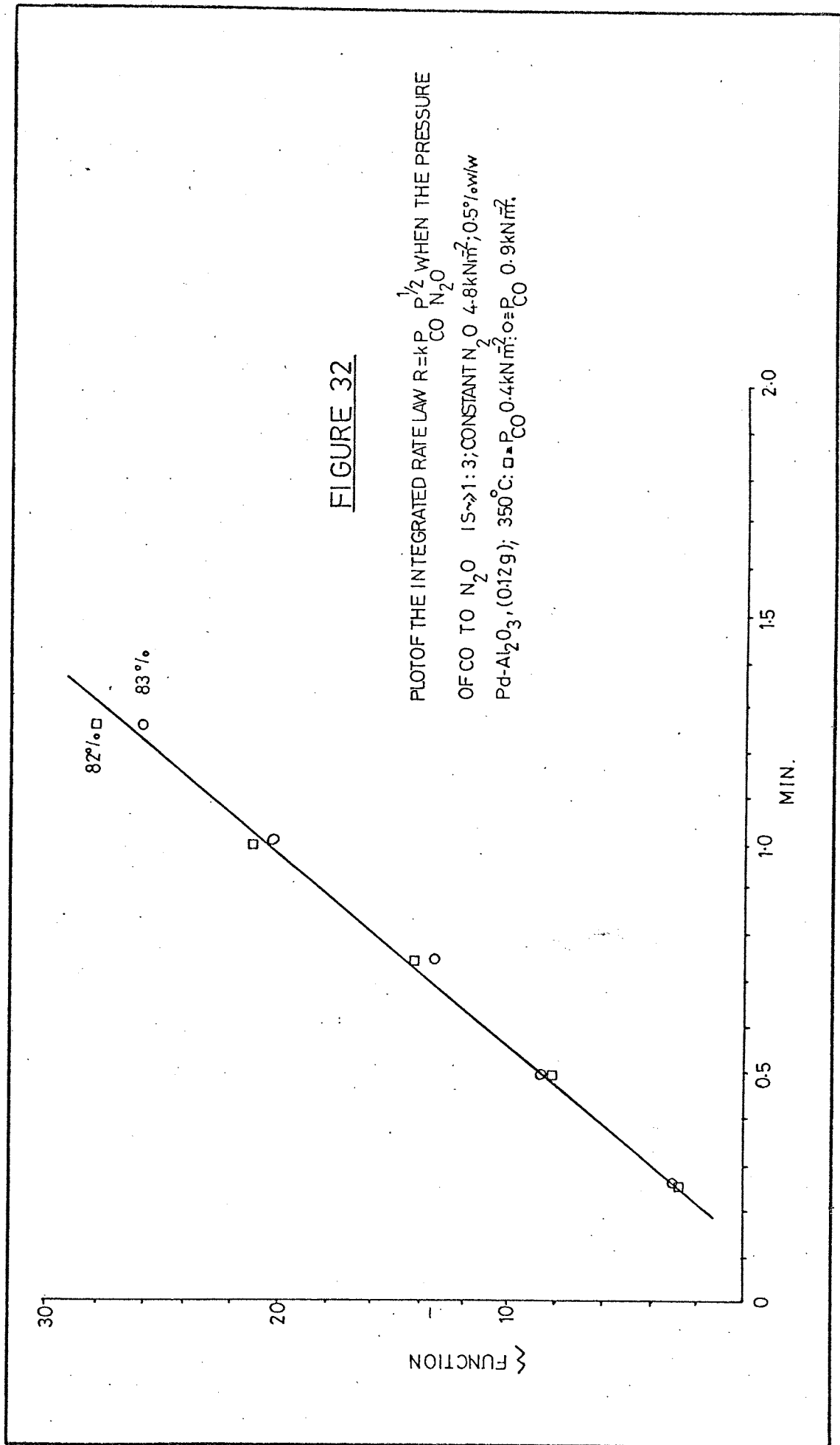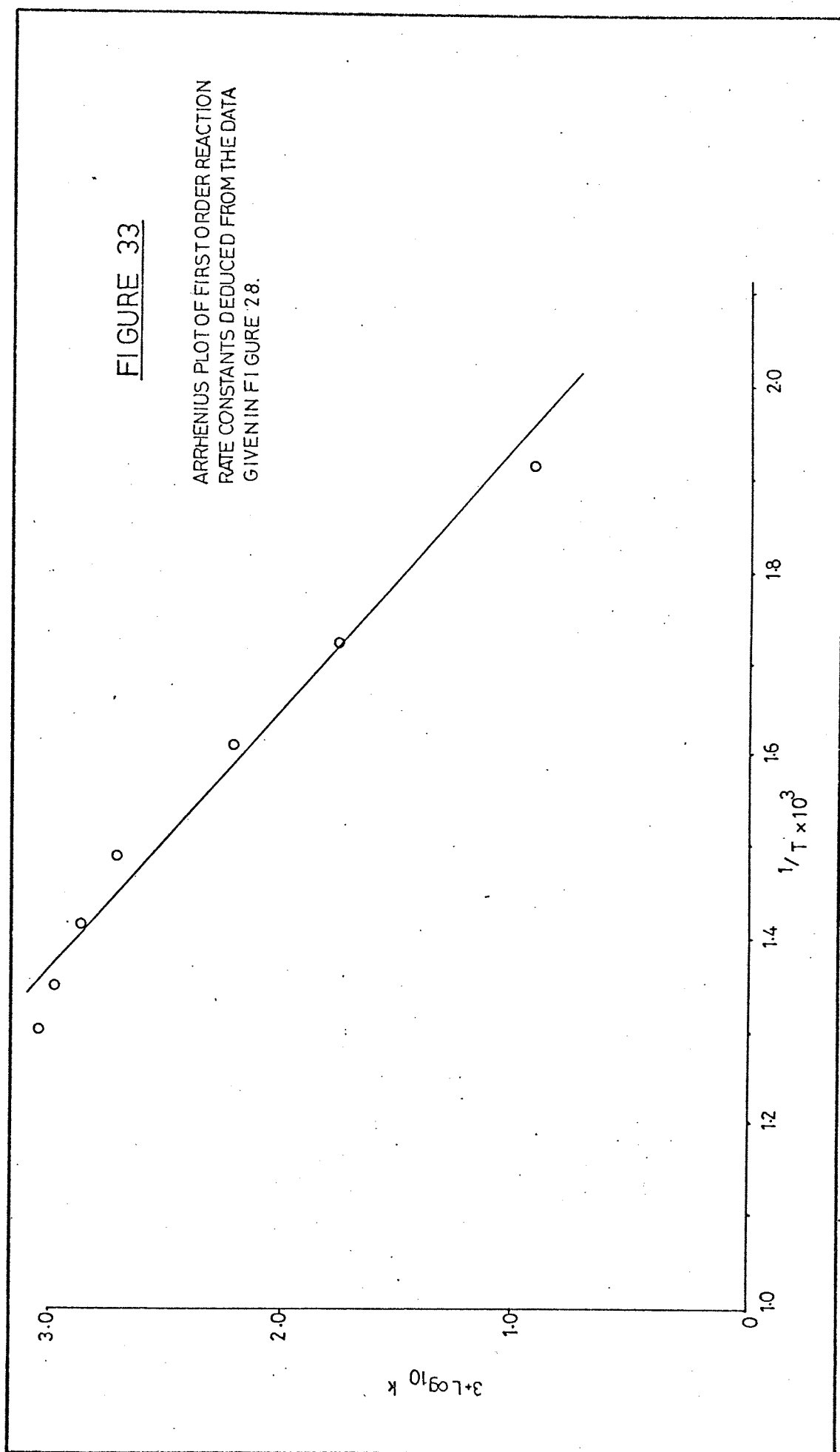
FIGURE 34

FIRST ORDER PLOTS FOR EQUAL PRESSURES OF N_2O AND CO (4.6 kNm^{-2}) WITH AND WITHOUT $1kNm^{-2}CO_2$ ADDED INITIALLY ; 0.5%w/w Pd-Al_2O_3, (0.1g); $350^{\circ}C$. o = STANDARDS ▷ = + CO_2.
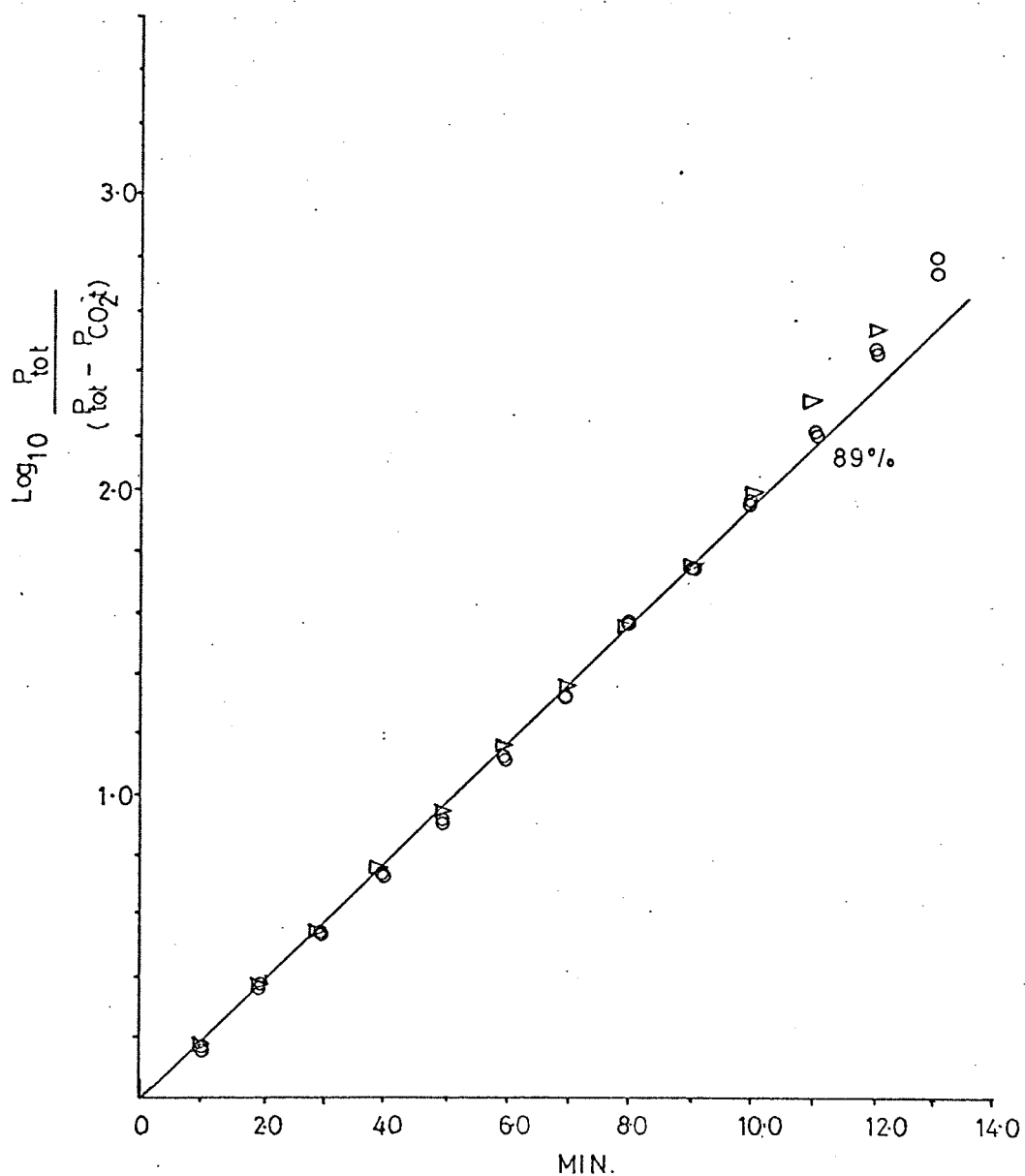
TABLE 17

Table 17.i) A summary of reaction orders evaluated from initial rate data.

CONDITIONS 350°C	PRESSURE LIMITS k Nm^{-2}	GAS HELD CONSTANT	O.W.R.T. γ N$_2$O	O.W.R.T. γ CO
mainly reducing	CO(3.9-13.4)	N$_2$O(4.6)	"	0.3±0.06
oxidizing	CO(0.4-2.9)	N$_2$O(4.6)	"	0.67±0.07
oxidizing	N$_2$O(3.8 13.4)	CO(4.6)	0.3±0.04	"
reducing	N$_2$O(0.4-2.9)	CO(4.6)	1.1±0.07	"
470°C				
mainly reducing	CO(4.3-14.6)	N$_2$O(5.3)	"	0.49±0.03
oxidizing	CO(0.4-3.2)	N$_2$O(5.3)	"	0.95±0.03
oxidizing	N$_2$O(4.3-14.6)	CO(5.3)	0.47±0.05	"
reducing	N$_2$O(0.4-3.2)	CO(5.3)	0.88±0.06	"

Table 17.ii) Proposed empirical rate expressions based on orders obtained from the initial rate method.

CONDITIONS k Nm^{-2}	PROPOSED EMPIRICAL RATE EXPRESSIONS	PLOTS OF THE INTEGRATED FUNCTION FIGURE NO.
$\dfrac{P_{CO}}{P_{N_2O}}$ $\dfrac{4.3 - 14.6}{5.3}$	Rate = k $P_{CO}^{0.27-0.49} P_{N_2O}^{0.3-0.47}$	30
$\dfrac{P_{CO}}{P_{N_2O}}$ $\dfrac{0.4-3.2}{5.3}$	Rate = k $P_{CO}^{0.65-0.95} P_{N_2O}^{0.3-0.47}$	32
$\dfrac{P_{N_2O}}{P_{CO}}$ $\dfrac{0.4-3.2}{5.3}$	Rate = k $P_{CO}^{0.27-0.49} P_{N_2O}^{0.88-1.1}$	27
$\dfrac{P_{N_2O}}{P_{CO}}$ $\dfrac{4.3-14.6}{5.3}$	Rate = k $P_{CO}^{0.27-0.49} P_{N_2O}^{0.3-0.47}$	31
$\dfrac{P_{N_2O}}{P_{CO}}$ = 1	Rate = k $P_{CO}^{0.27-0.49} P_{N_2O}^{0.3-0.47}$	29

EMPIRICAL RATE EQUATION *	RATE EQUATION	INTEGRATED EQUATION	UNITS k
Rate = $k_A P_{CO}^1 P_{N_2O}^{\frac{1}{2}}$	$\frac{dx}{dt} = k(a-x)(b-x)^{\frac{1}{2}}$	$kt = \frac{1}{(b-a)^{\frac{1}{2}}} \ln\left[\frac{(-1)(b-x)^{\frac{1}{2}} - (b-a)^{\frac{1}{2}}}{(a-x)}\right]^2 - C$	$(Nm^{-2})^{-\frac{1}{2}} min^{-1}$
Rate = $k_C P_{CO}^{\frac{1}{2}} P_{N_2O}^1$	$\frac{dx}{dt} = k(a-x)^{\frac{1}{2}}(b-x)$	$kt = \frac{1}{(a-b)^{\frac{1}{2}}} \ln\left[\frac{(-1)(a-x)^{\frac{1}{2}} - (a-b)^{\frac{1}{2}}}{(b-x)}\right]^2 - C$	$(Nm^{-2})^{-\frac{1}{2}} min^{-1}$
Rate = $k_B P_{CO}^{\frac{1}{2}} P_{N_2O}^{\frac{1}{2}}$	$\frac{dx}{dt} = k(a-x)^{\frac{1}{2}}(b-x)^{\frac{1}{2}}$	$kt = \ln\left[\frac{(a-x)^{\frac{1}{2}}(b-x)^{\frac{1}{2}} - (b-x)}{(b-x)}\right]^2 - C$	min^{-1}
when $P_{CO} = P_{N_2O}$	$\frac{dx}{dt} = k(a-x)$	$kt = \ln\frac{a}{(a-x)}$	

TABLE 18

where x = pressure carbon dioxide

a = initial pressure of carbon monoxide

b = " " " nitrous oxide

* for ease of integration the reactant orders were adjusted to the nearest half power.

3.3. REDUCTION OF NITROUS OXIDE BY CARBON MONOXIDE OVER 0.5% w/w Ru-Al$_2$O$_3$

The formation of nitrous oxide occurs when an excess of nitric oxide reacts with carbon monoxide over ruthenium. In these circumstances the reaction of nitrous oxide with carbon monoxide becomes significant.

Preliminary experiments showed that the decomposition of nitrous oxide over ruthenium was significant compared with its catalytic reduction by carbon monoxide. This means consecutive reactions can take place over the catalyst: 1) The decomposition of nitrous oxide 2) the reaction between oxygen and carbon monoxide and 3) the reaction between nitrous oxide and carbon monoxide. These reactions are given by the following

$$N_2O + s \underset{}{\overset{k_1}{\rightleftharpoons}} N_2Os \qquad - 1$$

$$N_2O_s \underset{}{\overset{k_2}{\rightleftharpoons}} N_2g + Os \qquad - 2$$

$$2(Os) \underset{}{\overset{k_3}{\rightleftharpoons}} O_2g + 2s \qquad - 3$$

$$O_2g + s \underset{}{\overset{k_4}{\rightleftharpoons}} O_2s \qquad - 4$$

$$COg + Os \underset{}{\overset{k_5}{\rightleftharpoons}} CO_2g + s \qquad - 5$$

$$COg + s \underset{}{\overset{k_6}{\rightleftharpoons}} COs \qquad - 6$$

$$COs + Os \underset{}{\overset{k_7}{\rightleftharpoons}} CO_2g + s \qquad - 7$$

$$COs + O_2s \underset{}{\overset{k_8}{\rightleftharpoons}} CO_2g + Os \qquad - 8$$

$$\text{or } N_2Os + COs \underset{}{\overset{k_9}{\rightleftharpoons}} CO_2g + N_2g + 2s \qquad - 9$$
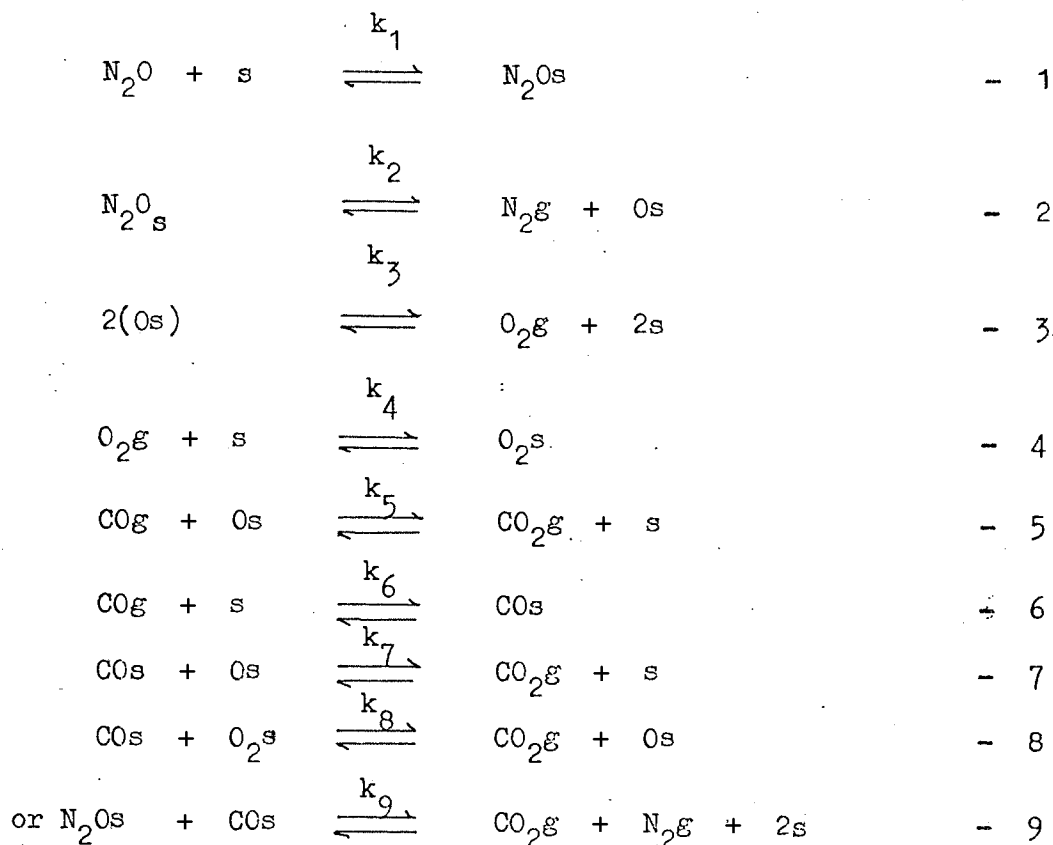
where g and s represent the gas and surface phases.

Prior to a study of the catalytic reaction between nitrous oxide and carbon monoxide an examination of the decomposition of nitrous oxide over ruthenium was carried out in order to establish the reaction kinetics.

3.3.1. DECOMPOSITION OF NITROUS OXIDE OVER 0.5% w/w Ru-Al$_2$O$_3$ CATALYST

As a result of monitoring the molecular ion of nitrous oxide m/e 44, type 2 chart traces were obtained. These were analyzed as described in chapter 2, section 2.6.1. The rate of decomposition of nitrous oxide is expressed by the empirical rate equation:-

$$- \frac{d\, P_{N_2O}}{dt} = k\, P_{N_2O}^{\propto} \qquad - 1$$

The exponent $\propto$ of the equation was determined by the initial rate method. Figure 35 on page 125 represents the results of 1) a plot of the initial rate verses the initial pressure of nitrous oxide, and 2) a double Logarithm plot of the above data. The exponent determined from the slope of the second curve was found to be 0.76$\pm$0.07.

The results were also evaluated by the time course method. Figure 36 page 126 is a time course plot obtained from a single run for an initial nitrous oxide pressure of 5.5 k Nm^{-2}. The plot shows linearity to 65% completion. The slope of this portion which represents the order with respect to time was found to be 0.8. This result is consistent with the order obtained by the initial rate method. After 65% reaction a sharp increase

in the order is noted. The fact that the order with respect
to time in this region is greater than the order with respect
to concentration means that the reaction is inhibited by the
reaction products. The inhibition is most probably due to
the effect of oxygen, a phenomenon which has been previously
observed[93]. The effect of oxygen and added oxygen on the
decomposition of nitrous oxide will be discussed later in this
section.

The experimental results plotted as a first order relation-
ship for the decomposition of nitrous oxide are reported in
Figure 37 on page 127. Figure 37 shows that straight lines
are obtained to at least 80% of the reaction for initial nitrous
oxide pressures between 0.8 - 13.9 k Nm^{-2}. Note also, the rate
constant decreases from 0.8 to 0.5 min^{-1} as the initial pressure
is increased. The first order relationship was also found to
hold between a temperature range of 300 - 500°C, Figure 38 page
128. The apparent activation energy determined from an
Arrhenius plot, Figure 39 page 129 was found to be 42.5$\pm$2 k J
mol^{-1}.

Graphical analysis of the results has verified that the
decomposition of nitrous oxide over ruthenium follows first
order kinetics. The first order rate constant was found to
be pressure-dependent. The pressure dependence is of the form

$$Log\ k_{abs} = k - k_2\ Log\ (P_{N_2O})_{initial} \qquad - 2$$

where the constants k_1 = 0.41 and k_2 = -0.16, with a correlation

coefficient of 0.995. $k_{abs} = \dfrac{k \ V}{60Af}$, where k is the first order

rate constant, $V = 4.5 \times 10^{-4} m^3$, the volume of the system,

$A = 111 \ m^2$, the surface area of the catalyst, and $f = 2.4 \times 10^{-3}$,

the weight fraction of ruthenium on the support. The result

of a plot of logarithm k_{abs} against the logarithm of the initial

pressure of nitrous oxide is shown in Figure 40, page 130.

Figure 40 shows linearity across the pressure range 0.8 - 13.9

$k \ Nm^{-2}$.

Similar relationships to that shown in equation 2 have been

observed by other workers for the decomposition of nitrous oxide.

Read[96] found that equation 2 was obeyed over neodymium

oxide in the pressure range of 0.1 to 13.3 k Nm^{-2}. The constants

k_1 and k_2 were found to be temperature - dependent between 420 -

$600^{\circ}C$. Gay and Tompkins[97] found that an expression of the form

shown in equation 2 was obeyed over nickel oxide in the pressure

range of 6.6 - 133.3 Nm^{-2}, between 22 and $140^{\circ}C$. The constants

in this case were found to be temperature - independent.

Read[96], Gay and Tompkins[97] have suggested that the retarding

effect on the rate with an increase in the initial pressure of

nitrous oxide is caused by the deactivation of a fraction of

surface sites with atomic oxygen, derived on the surface from the

decomposition of nitrous oxide. The deactivation may also result

from a physical effect by an increased surface coverage. This

effectively would reduce sites needed for 0 atom - mobility on

a surface which is already considered to have a low oxygen

mobility[98]. The fact that reproducibility of consecutive runs

was obtained indicates that the deactivation is reversible when the system is evacuated.

Effect of initially-added gases.

Figures 41 and 42 on pages 131 and 132 represent the results of a series of experiments in which 2.8 k Nm^{-2} oxygen were added initially to 5.5 k Nm^{-2} nitrous oxide.

Figure 41 shows the amount of nitrous oxide decomposed with time for a reaction with and without added oxygen. The effect of added oxygen is greatest at the latter end of the curve where nitrous oxide pressures are approximately 0.4 k Nm^{-2}. A first order relationship of the results given in Figure 41 are shown in Figure 42. The first order relationship applies equally well for each reaction. The rate constant decreases from 0.6 to 0.47 min^{-1} for the decomposition with added oxygen.

Added nitrogen, or carbon dioxide did not produce any marked effect on the rate of decompositions.

Under the conditions employed in this work added oxygen was found not to influence the first order decomposition of nitrous oxide significantly. This result is similar to those obtained by Read[96] and Winter[93] for the decomposition of nitrous oxide on lanthanide oxides at pressures up to 13.3 k Nm^{-2}. These authors have suggested that in the case of those metal oxides which are relatively insensitive to added oxygen the decomposition of nitrous oxide is confined to special areas of the surface. These areas being not readily accessible to gaseous oxygen.

The reaction scheme given by equation 1 to 3, section 3.3.

outlines a probable mechanism for the decomposition of nitrous oxide. These equations are compatible with the following

$$- d \frac{P_{N_2O}}{dt} = \frac{k_s \; b_{N_2O} \; P_{N_2O}}{1 + b_{N_2O}P_{N_2O} + (b_{O_2} \; P_{O_2})^{\frac{1}{2}}} \qquad - 3$$

Equation 3 reduces to a simple first order relationship when $(1 \gg b_{N_2O} \; P_{N_2O} + (b_{O_2} \; P_{O_2})^{\frac{1}{2}})$. For completeness, mechanisms which include molecular or atomic oxygen were considered[93,99,100] these expressions did not give as good a fit as the first order relationship.

FIGURE 35

PLOT OF a). INITIAL RATE AGAINST INITIAL PRESSURE OF N_2O
b). A DOUBLE LOGARITHM PLOT OF THE ABOVE
DATA : FOR THE DECOMPOSITION OF N_2O OVER
0.5% w/w $Ru-Al_2O_3$, (0.48g); AT 500°C.
(SLOPE ~ 0.76 ± 0.07)
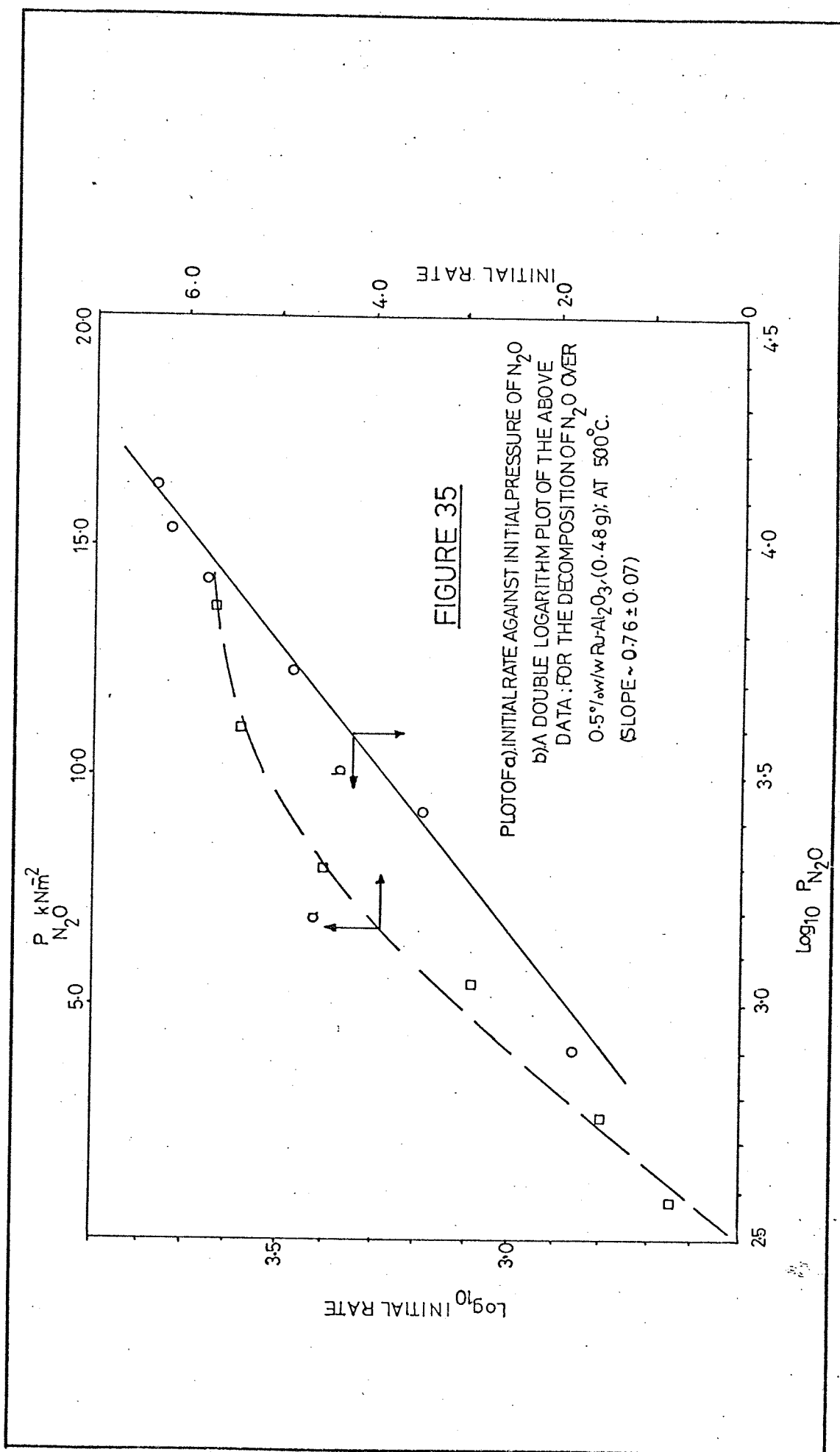
FIGURE 36

PLOT OF Ln RATE AGAINST Ln UNREACTED N_2O FOR THE DECOMPOSITION OF $5.5\,kN\,\bar{m}^2$ N_2O OVER 0.5% w/w $Ru\text{-}Al_2O_3$, $(0.48g)$; AT $500°C$. (calculated in torr for conversion to S.I. units add 4.89).
INITIAL SLOPE ~ 0.8.

Ln $-dP_{N_2O}/dt$

Ln UNREACTED N_2O

FIGURE 37

FIRST ORDER PLOTS FOR THE DECOMPOSITION OF N_2O OVER 0.5% w/w Ru-Al_2O_3, (0.48 g); 500°C.
× = P_{N_2O} = 0.8 kNm^{-2}; □ = P_{N_2O} = 27 kNm^{-2}; ○ = P_{N_2O} = 13.9 kNm^{-2}.
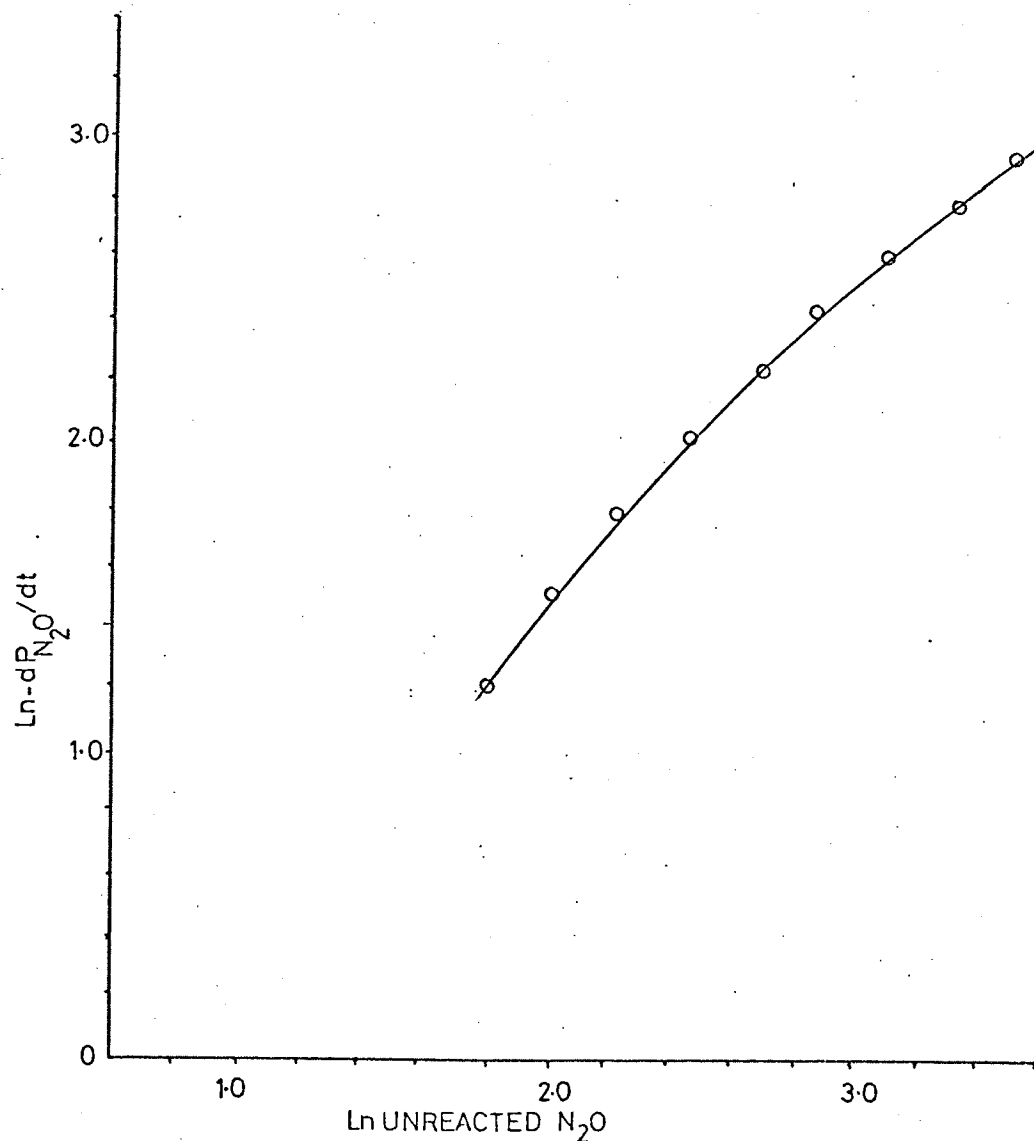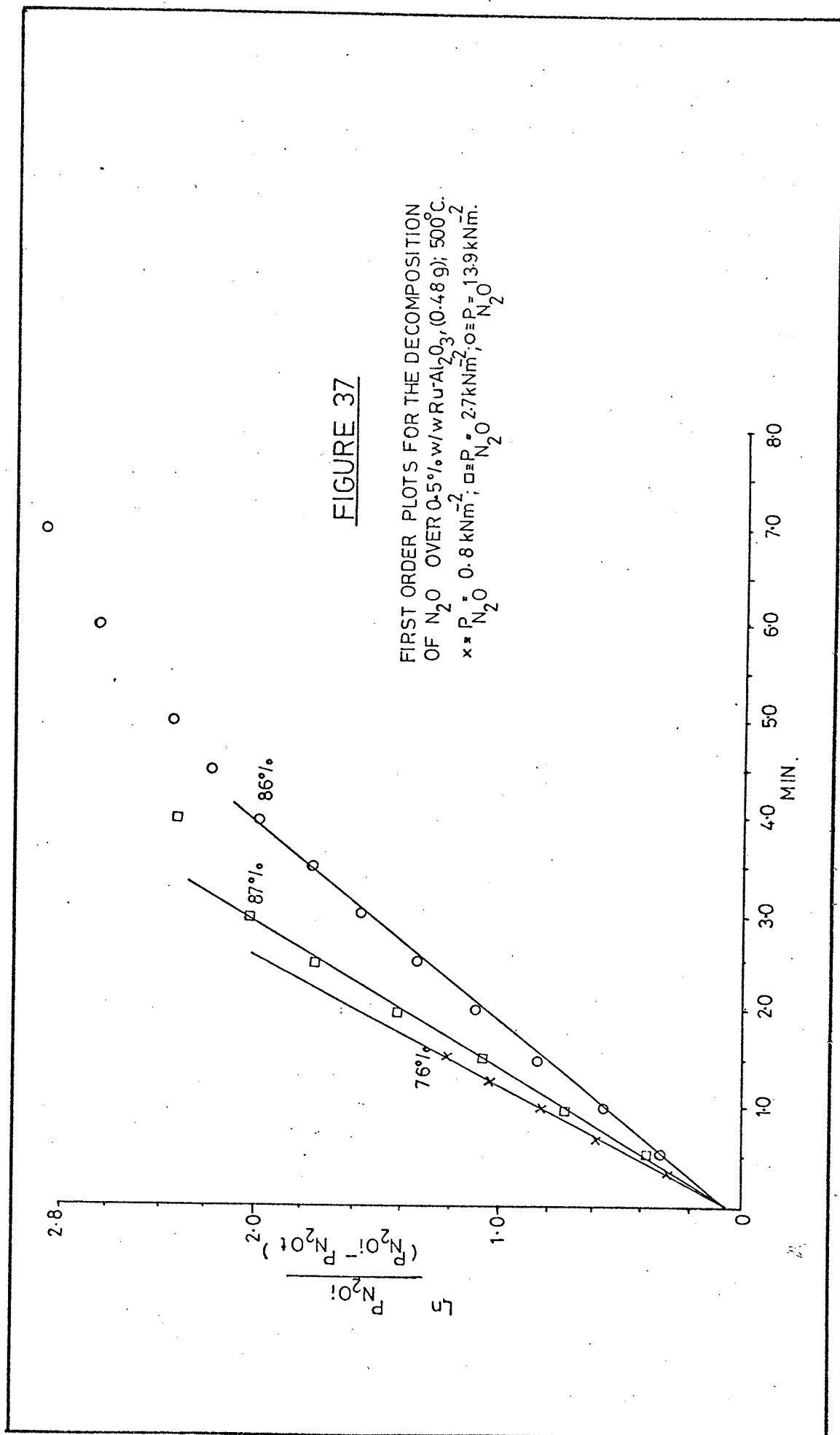
FIGURE 38

FIRST ORDER PLOTS FOR THE DECOMPOSITION
OF N_2O (5·4 kNm^{-2}) OVER 0.5%ow/w Ru-Al_2O_3,
(0.48g). BETWEEN 300-500°C.
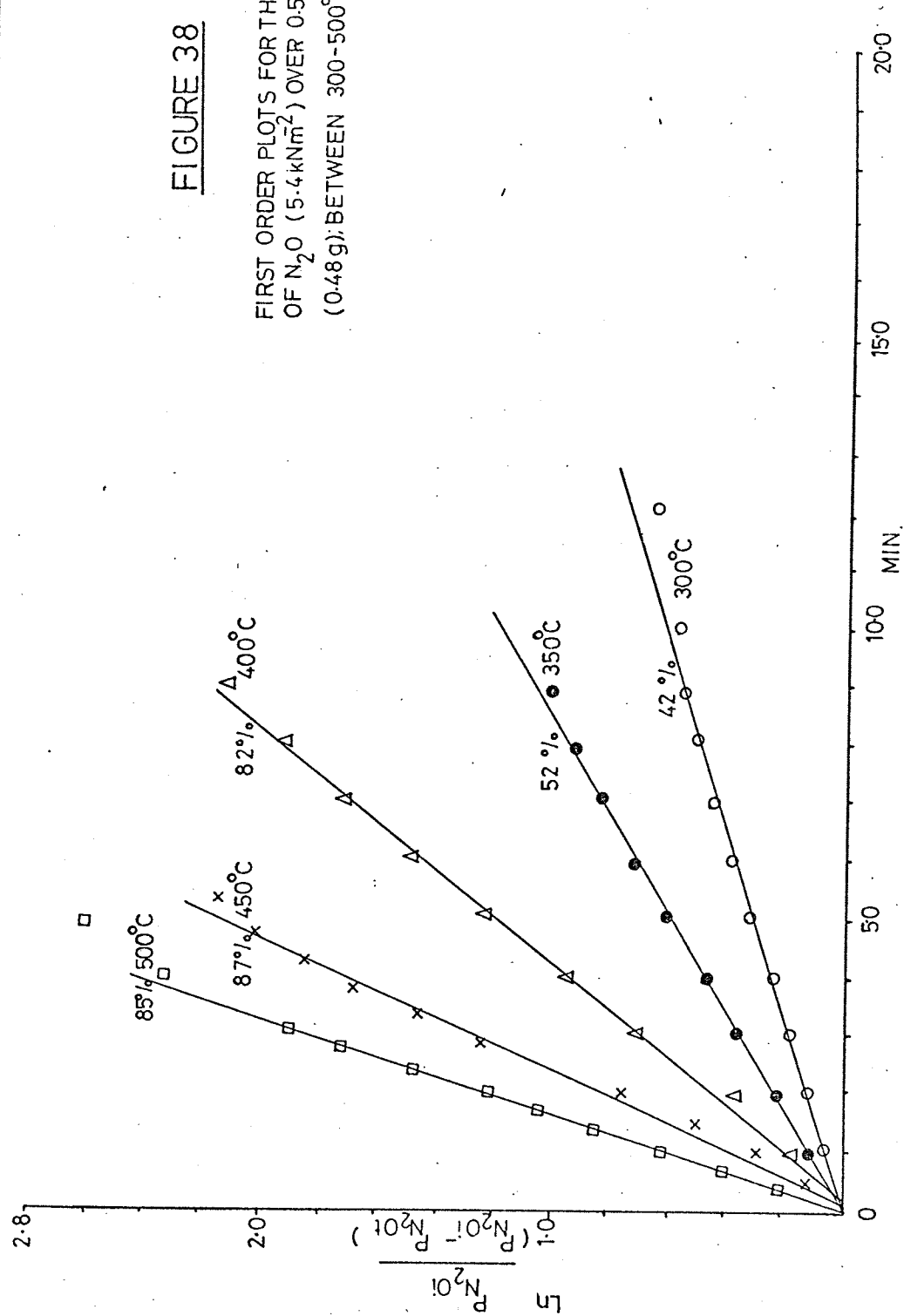
FIGURE 39

ARRHENIUS PLOT FOR THE DECOMPOSITION
OF N_2O (5.4 kN$\bar{m}^2$) OVER 0.5°/o w/w Ru-Al$_2O_3$.
(0.48g).

FIGURE 40

PLOT OF Log kobs AGAINST Log INITIAL PRESSURE OF
N_2O FOR THE DECOMPOSITION OF N_2O OVER 0.5°/ow/w
$Ru-Al_2O_3$,(0.48 g); AT 500°C: CORRELATION COEFFICIENT
-0.995.

FIGURE 41

PLOT SHOWING THE EFFECT OF ADDED O_2 ($2.8\,kNm^{-2}$) ON THE DECOMPOSITION OF N_2O OVER $0.5\%\,w/w\,Ru-Al_2O_3$, ($0.48g$):AT $500°C$. $\square = P_{N_2O} = 5.5\,kNm^{-2}$; $o = P_{N_2O} = 5.5 + P = 2.8\,kNm^{-2}$ O_2

FIGURE 42

FIRST ORDER PLOTS OF THE DATA SHOWN
IN FIGURE 41; □ ≡ $P_{N_2O} = 5.5\,kNm^{-2}$, o ≡ $P_{N_2O} = 5.5 + P_{O_2}\,2.8\,kNm^{-2}$.
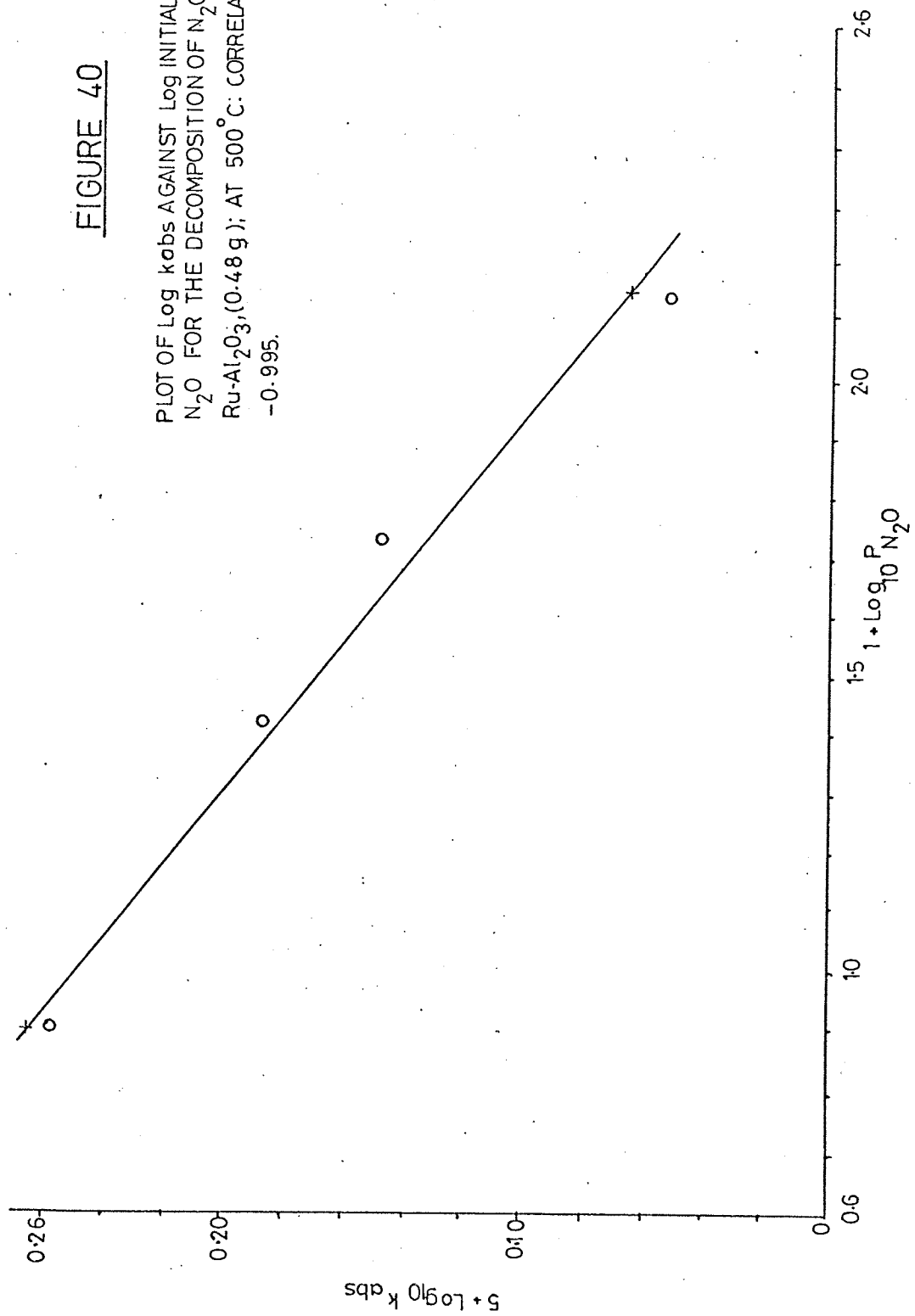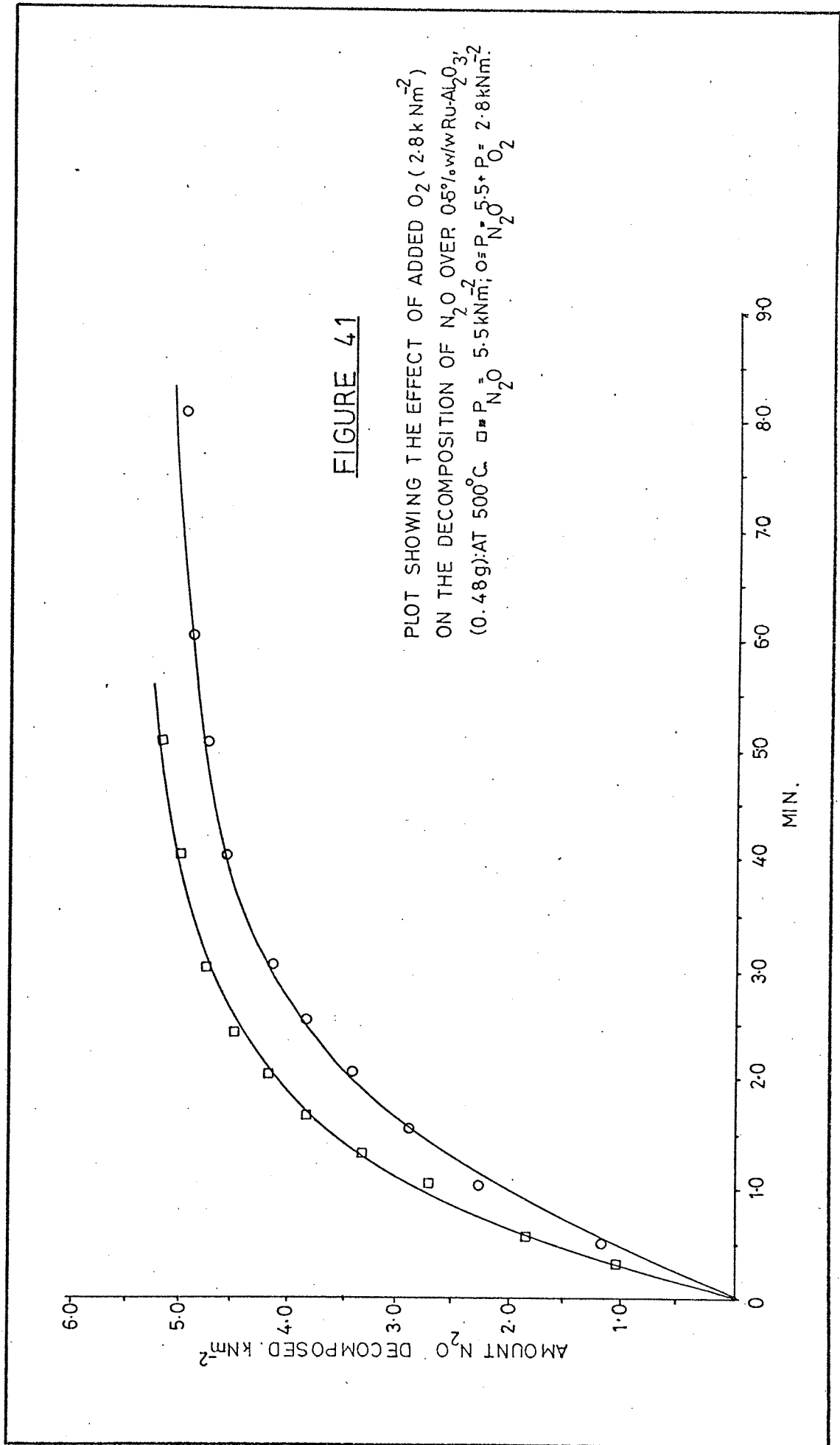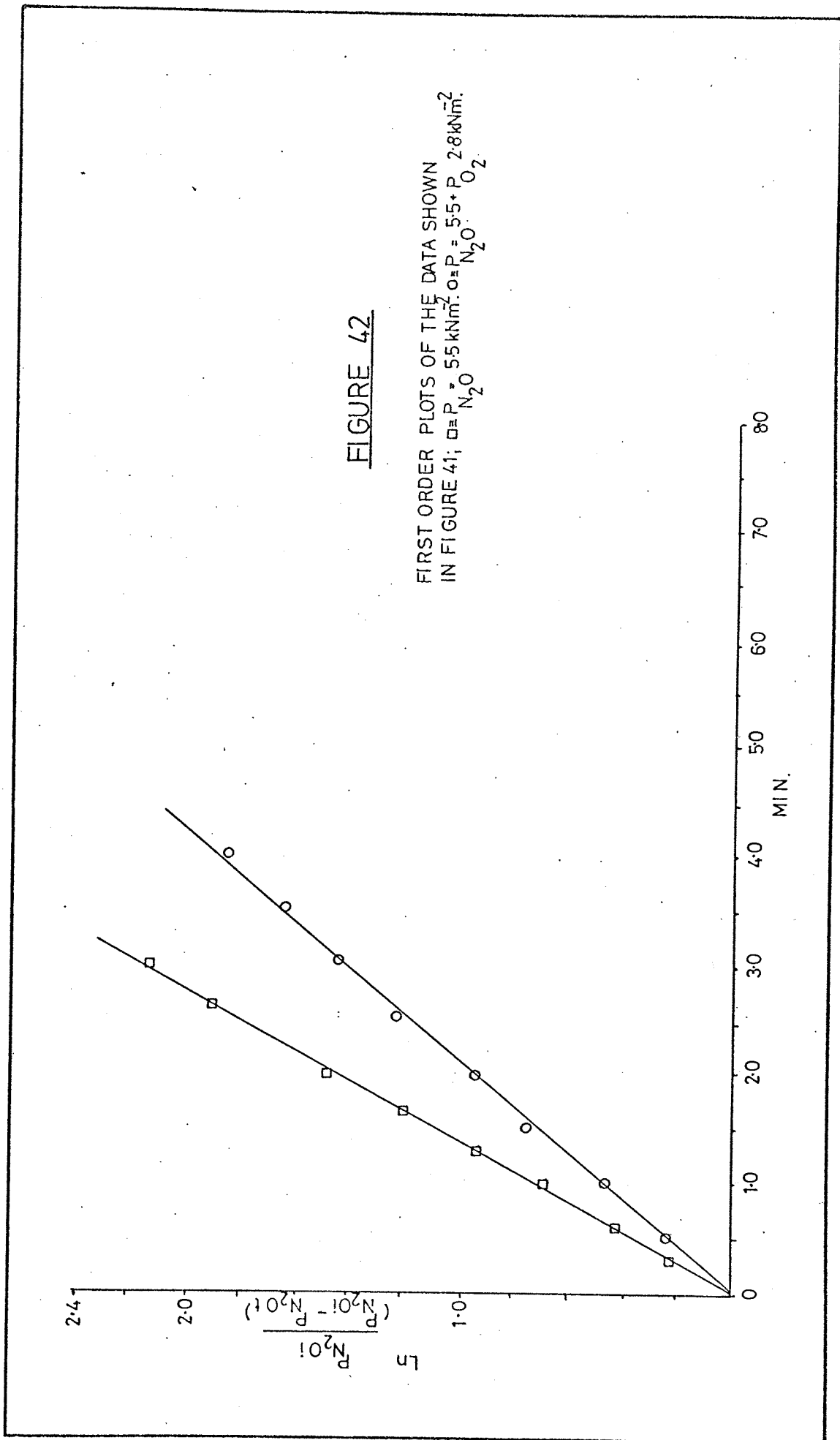
3.3.2. THE CATALYTIC REACTION OF NITROUS OXIDE AND CARBON MONOXIDE

OVER 0.5% w/w Ru- Al_2O_3 CATALYST

A study of the catalytic reaction between nitrous oxide and carbon monoxide was carried out in the manner described in section 2.6.1.

Figures 43 and 44 on pages 138 and 139 are double logarithm plots of the results obtained from the initial rate data. The effect of nitrous oxide pressure on the initial rate is represented by Figure 43. The Figure shows deviation from linearity below nitrous oxide pressures of 1.0 k Nm^{-2}. The order with respect to nitrous oxide determined from the linear portion of the graph was 1.3$\pm$0.3.

A time course plot obtained from a single run having 1.0 k Nm^{-2} and 5.2 k Nm^{-2} pressure of nitrous oxide, and carbon monoxide respectively is shown by Figure 45 page 140. The plot shows linearity for 80% of the reaction. The slope of this portion, which represents the order with respect to time was 1. This result is consistent with the order obtained from the initial rate method.

The effect of carbon monoxide pressure upon the initial rate Figure 44 shows a large scatter of points. A similar result was obtained for the initial rate dependence of carbon monoxide pressure for the reaction with nitric oxide and hydrogen[57] respectively. For these cases the order with respect to carbon monoxide was taken to be zero.

A time course plot obtained for a single rate having 0.9k Nm^{-2}

and 4.8 k Nm^{-2} pressure of carbon monoxide and nitrous oxide
is shown by Figure 46 page 141. This plot shows no strong
dependence for carbon monoxide up to 55% completion, after which
the order with respect to time tends to one. The initial zero
order pressure dependence for carbon monoxide is consistent
with the interpretation made from the initial rate method.

For equal reactant pressures the overall order with respect
to time is one, Figure 47 page 142. This result is in line
with the interpretation made from the initial rate and time
course plots for the pressure dependence of carbon monoxide and
nitrous oxide. For equal reactant pressures the order with
respect to time should be equal to the overall order with respect
to concentration.

The empirical rate law which describes the carbon monoxide –
nitrous oxide reaction over ruthenium is given by

$$Rate = k \ P_{N_2O}^{\sim 1} \ P_{CO}^{\sim 0} \qquad\qquad - \ 1$$

Equation 1 implies that carbon monoxide exhibits a high surface
coverage and is relatively strongly adsorbed. This is in line
with the nature of chemisorption of carbon monoxide on ruthenium
and of the results obtained for the reduction of nitric oxide
by carbon monoxide (section 3.1.).

In comparison nitrous oxide exhibits a first order pressure
dependence which is consistent with its first order decomposition
described in the previous section. This suggests that the
reaction proceeds through the decomposition of nitrous oxide,
for example, by the equations 1 to 8 given in section 3.3. Since

carbon monoxide has a relatively strong affinity for ruthenium its reaction with atomic oxygen is most likely to be a rapid surface one. A surface mechanism which is compatible with this scheme is given by the Langmuir - isotherm for a bimolecular reaction in which the reactants are adsorbed on two different types of surface site. This is in line with Winter[94] and Reads[96] proposal that the decomposition of nitrous oxide is confined to special areas. A zero order pressure dependence for carbon monoxide will obtain when the surface other than these special areas is completely covered by carbon monoxide. This scheme is given by

$$\frac{d\,P_{CO_2}}{dt} = k_s \frac{b_{N_2O}\,P_{N_2O}\,b_{CO}\,P_{CO}}{(1 + b_{N_2O}\,P_{N_2O})(1 + b_{CO}\,P_{CO})} \qquad - 2$$

The notations in equation 2 are the same as those used previously. First order kinetics were obtained for the decomposition of nitrous oxide, then $1 > b_{N_2O}\,P_{N_2O}$. When carbon monoxide has a high surface coverage $b_{CO}\,P_{CO} > 1$. By substitution equation 2 becomes

$$\frac{d\,P_{CO_2}}{dt} = k\,P_{N_2O}\,P_{CO}^{\,0} \qquad - 3$$

where $k = k_s\,b_{N_2O}$

Equation 3 is of the same form as that obtained from the initial rate method.

Experimental results plotted as a first order relationship for the reaction between carbon monoxide and nitrous oxide are

shown in Figure 48 and 49 on pages 143 and 144. Figure 48
shows that for the reactant pressures indicated, straight lines
were obtained to at least 70% of the reactions. The rate
constant decreases with an increase in the initial pressure
of carbon monoxide and nitrous oxide. The rate law was also
found to hold between a temperature range of $350°$ to $500°C$ for
equal reactant pressures (4.6 k Nm^{-2}), Figure 49 page 144

The apparent activation energy determined from an Arrhenius
plot, Figure 50 page 145 was found to be $72.3^{\pm}10$ k J mol^{-1}.
The fact that this value is approximately twice that obtained
for the decomposition of nitrous oxide suggests that the activa-
tion energy is associated with the reaction between carbon mono-
xide and oxygen.

The empirical rate law for the reaction of nitrous oxide
and carbon monoxide over ruthenium has been verified graphically.
A retarding effect on the reaction rate constant with an increase
in initial pressure of nitrous oxide or carbon monoxide was
noted. This effect may be caused by the deactivation of a
fraction of surface sites by (a) atomic oxygen and (b) carbon
monoxide for each reactant respectively (see section 3.3.1.).

The decomposition of nitrous oxide in the presence of carbon
monoxide is probably the rate limiting step in the two stage
reaction process (see equation 1 to 8 in section 3.3.). Evid-
ence to support this proposal is shown in Figure 51 page 146.
Figure 51 was obtained by monitoring the positive ion currents
due to carbon dioxide, nitrous oxide and oxygen in three identical

reactions respectively. The Figure 51 indicates that for a
reaction mixture which contains an excess of nitrous oxide,
oxygen production occurs only after the depletion of carbon
monoxide. This means that carbon monoxide affects the decom-
position of nitrous oxide which is slower than the reactions
between carbon monoxide and atomic oxygen.

In summary the reaction between nitrous oxide and carbon
monoxide over ruthenium proceeds by a two stage (a) the decom-
position of nitrous oxide and (b) the reaction between carbon
monoxide and atomic oxygen. The first order decomposition of
nitrous oxide is the rate limiting step; this stage is retarded
by an excess of carbon monoxide.

138

FIGURE 43

PLOT OF Log INITIAL RATE AGAINST Log INITIAL PRESSURE OF N_2O FOR THE REDUCTION OF N_2O BY CO OVER 0,5%w/w Ru-Al_2O_3,(0·48g); AT 500°C; CONSTANT CO 5·2 kNm². SLOPE α≈1·3 ±0·3.

Log_{10} P_{N_2O}
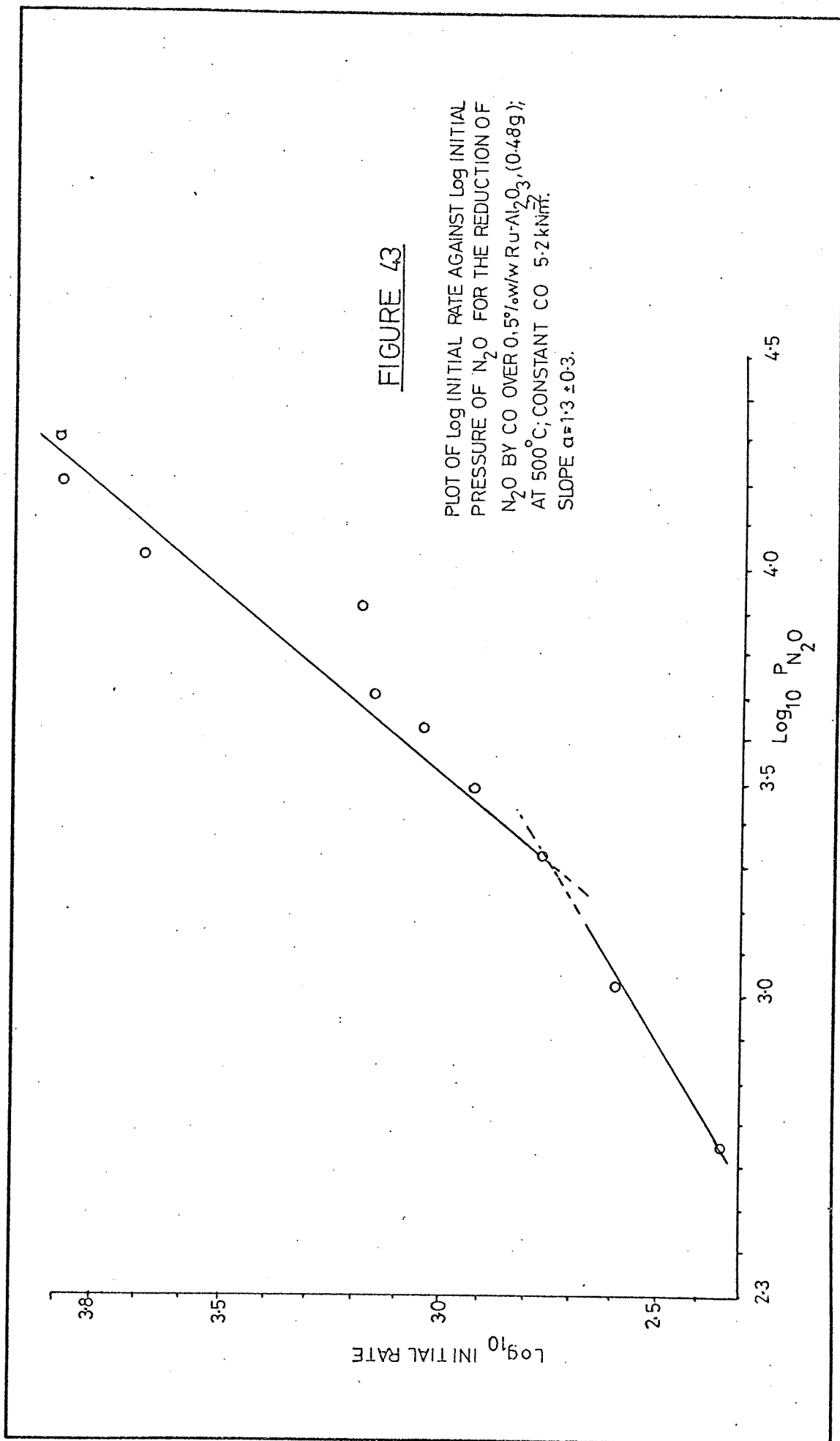
Log_{10} INITIAL RATE

FIGURE 44

PLOT OF Log INITIAL RATE AGAINST Log INITIAL PRESSURE OF CO FOR THE REDUCTION OF N_2O BY CO OVER 0.5% w/w $RuAl_2O_3$, (0.48g); AT 500°C; CONSTANT N_2O 5.2 kNm^{-2}.
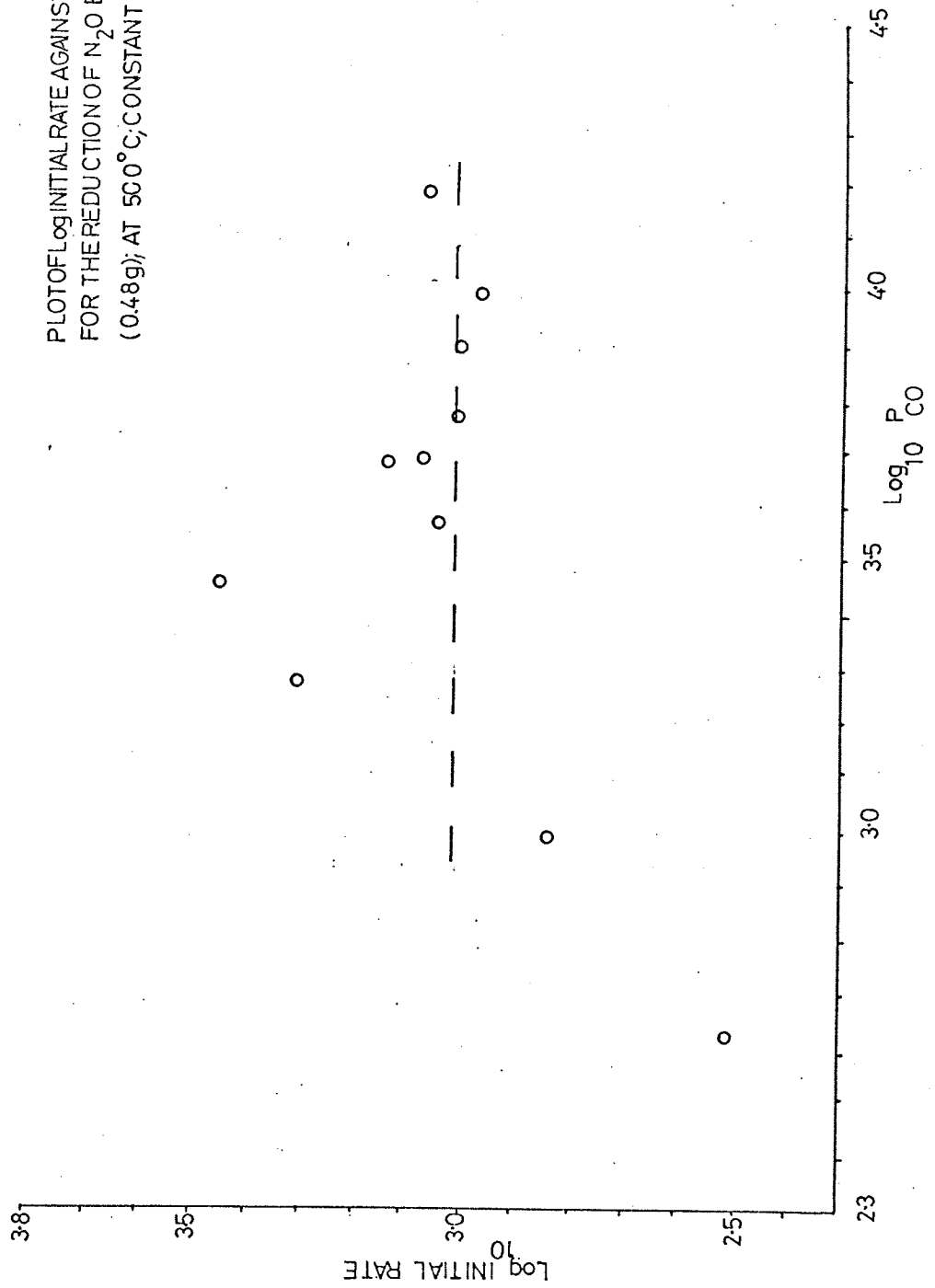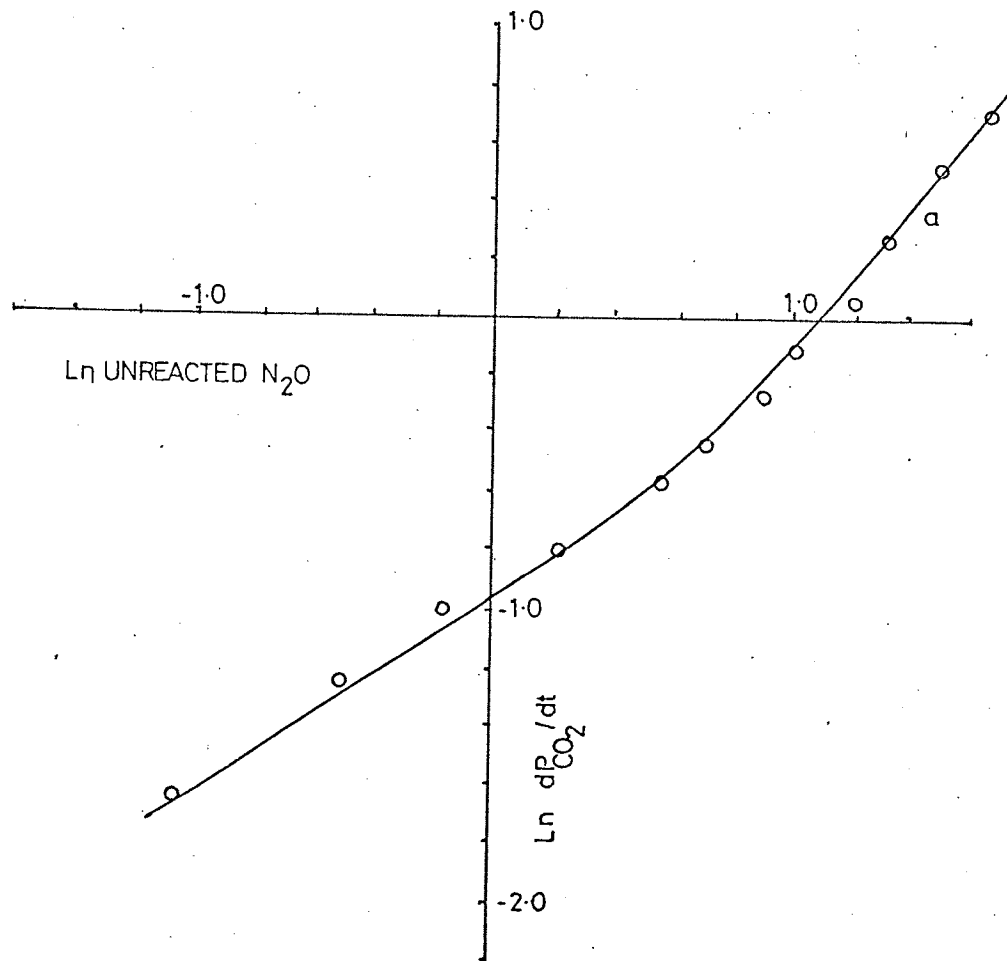
FIGURE 45

PLOT OF Ln RATE AGAINST Ln UNREACTED N_2O FOR A SINGLE
RUN WITH $1.0 \, kNm^{-2} \, N_2O$, $5.2 kNm^{-2} CO$, OVER 0.5% w/w $Ru-Al_2O_3$,
$(0.48g)$; AT $500°C$. INITIAL SLOPE $a \sim 1$ (calculated in torr for
conversion to S.I. units add 4.89)
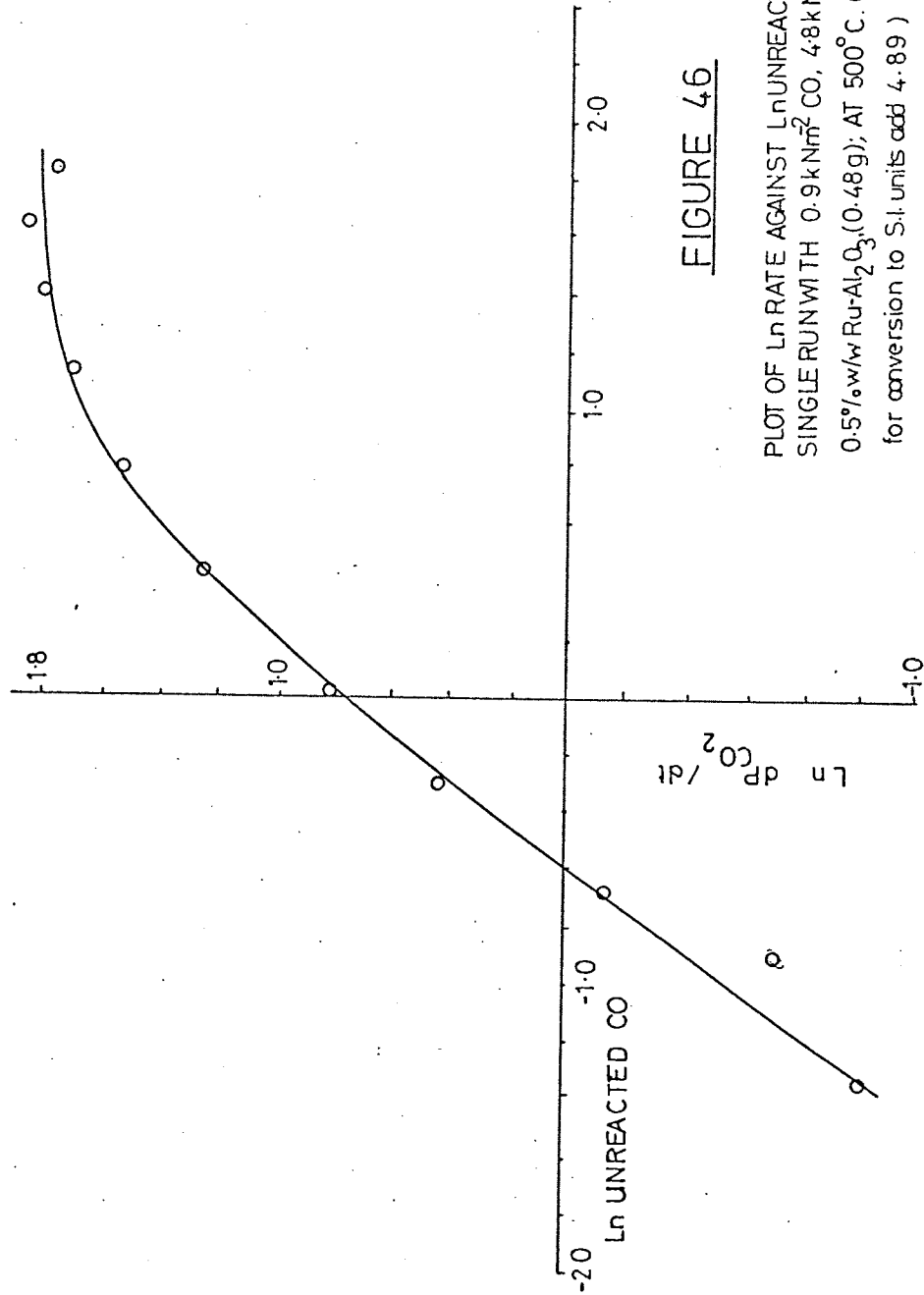
FIGURE 46

PLOT OF Ln RATE AGAINST Ln UNREACTED CO FOR A
SINGLE RUN WITH 0.9 kNm^{-2} CO, 4.8 kNm^{-2} N$_2$O OVER
0.5% w/w Ru-Al$_2$O$_3$,(0.48g); AT 500°C. (calculated in torr
for conversion to S.I. units add 4.89)

FIGURE 47

PLOT OF Ln RATE AGAINST Ln UNREACTED CO
(OR N_2O) FOR A SINGLE RUN WITH EQUAL
REACTANT PRESSURES (4.9 kNm^{-2}) OVER
0.5%/w/w Ru-Al$_2$O$_3$; (0.48g); AT 500°C.
INITIAL SLOPE ≈ 1 (calculated in torr for
conversion to S.I. units add 4.89)
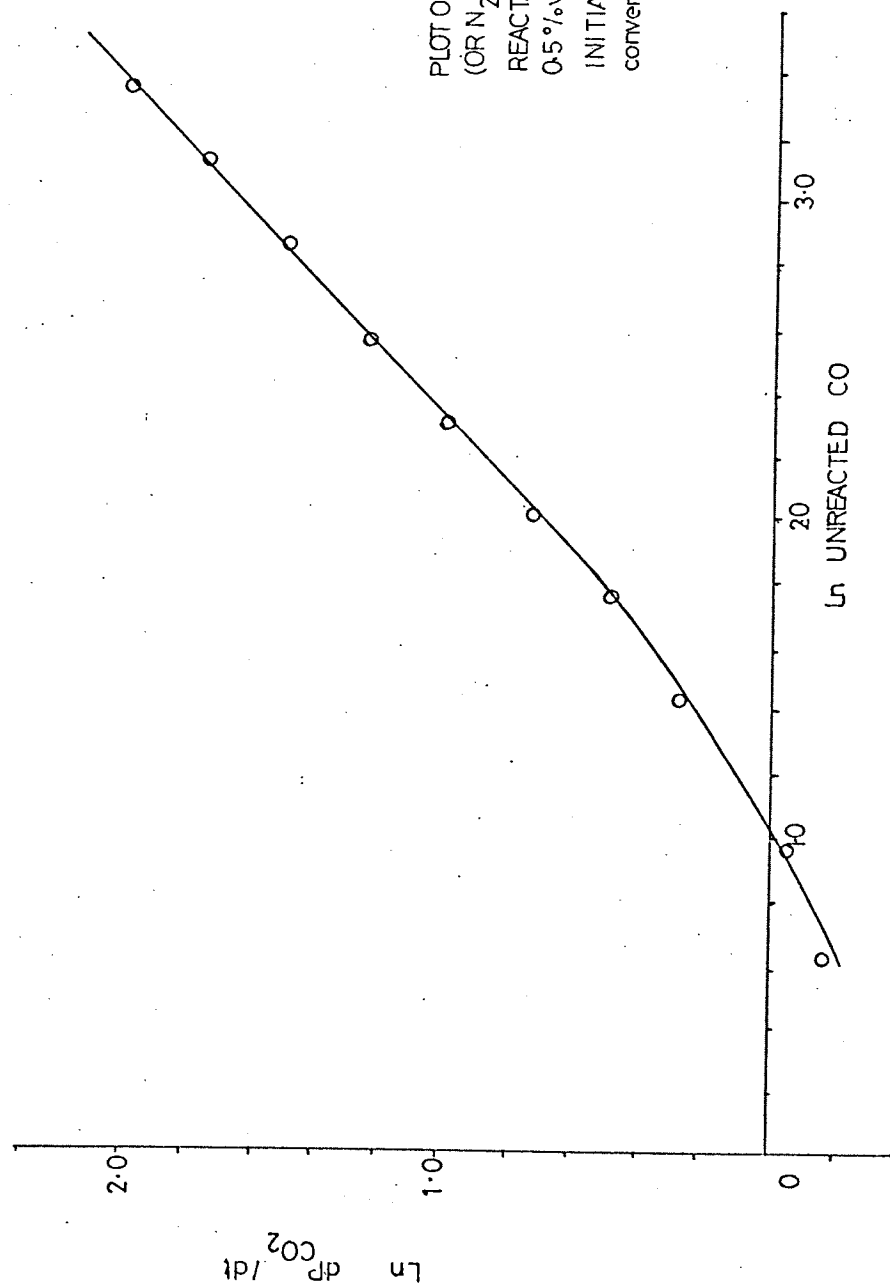
FIGURE 48

FIRST ORDER PLOTS FOR THE REACTION BETWEEN N_2O AND CO OVER $0.5\%w/wRu-Al_2O_3$,$(0.48g)$; AT $500°C$.
O $= P_{N_2O} = 4.8 \, kN \, m^{-2}$, $P_{CO} = 2.7 \, kNm^{-2}$: □ $= P_{N_2O} = 2.2 \, kNm^{-2}$, $P_{CO} = 5.3 \, kNm^{-2}$
● $= P_{N_2O} = 5.8 \, kNm^{-2}$, $P_{CO} = 4.9 \, kNm^{-2}$: △ $= P_{N_2O} = 8.0 \, kNm^{-2}$, $P_{CO} = 5.2 \, kNm^{-2}$
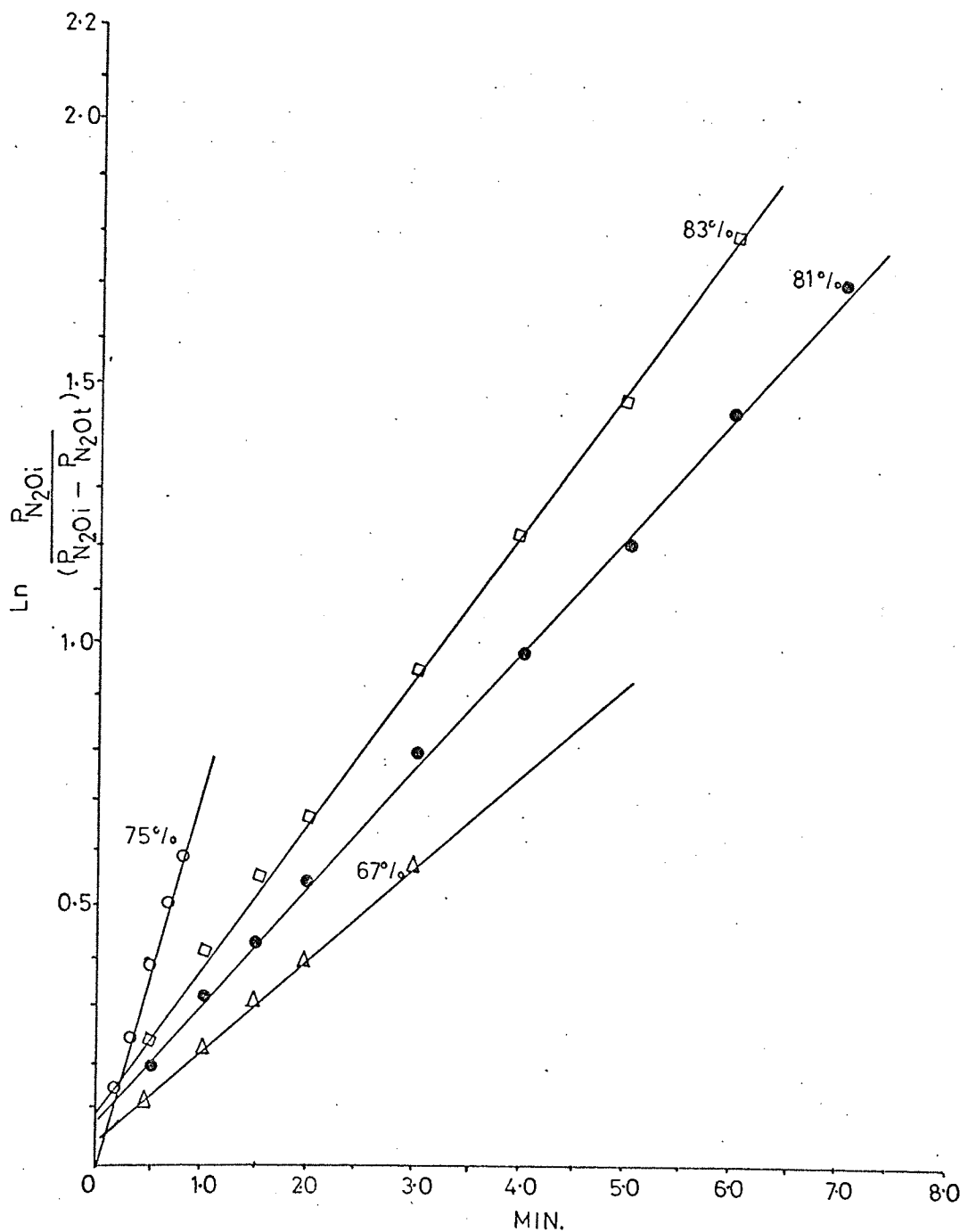
FIGURE 4.9

FIRST ORDER PLOTS FOR THE REACTION
BETWEEN N_2O AND CO OVER 0.5% w/w
Ru·Al_2O_3, (0.48g): BETWEEN 300-500°C.
$P_{N_2O}^= P_{CO}^= 4.6 \, kNm^{-2}$.
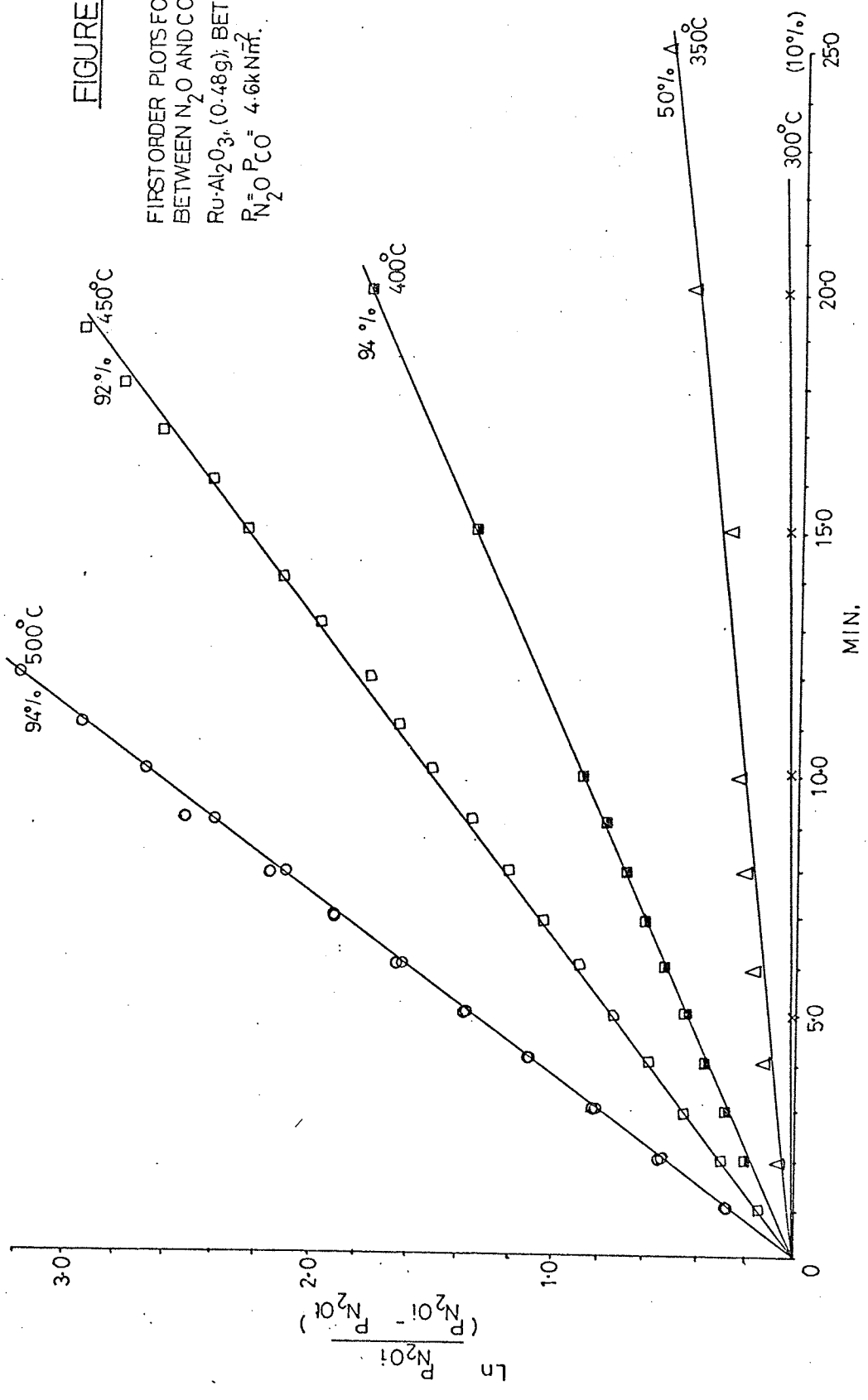
FIGURE 50

ARRHENIUS PLOT FOR THE REACTION BETWEEN N_2O AND CO OVER 0.5% w/w Ru Al_2O_3 (0.48g); $P_{N_2O} = P_{CO} = 4.6 \, kNm^{-2}$.
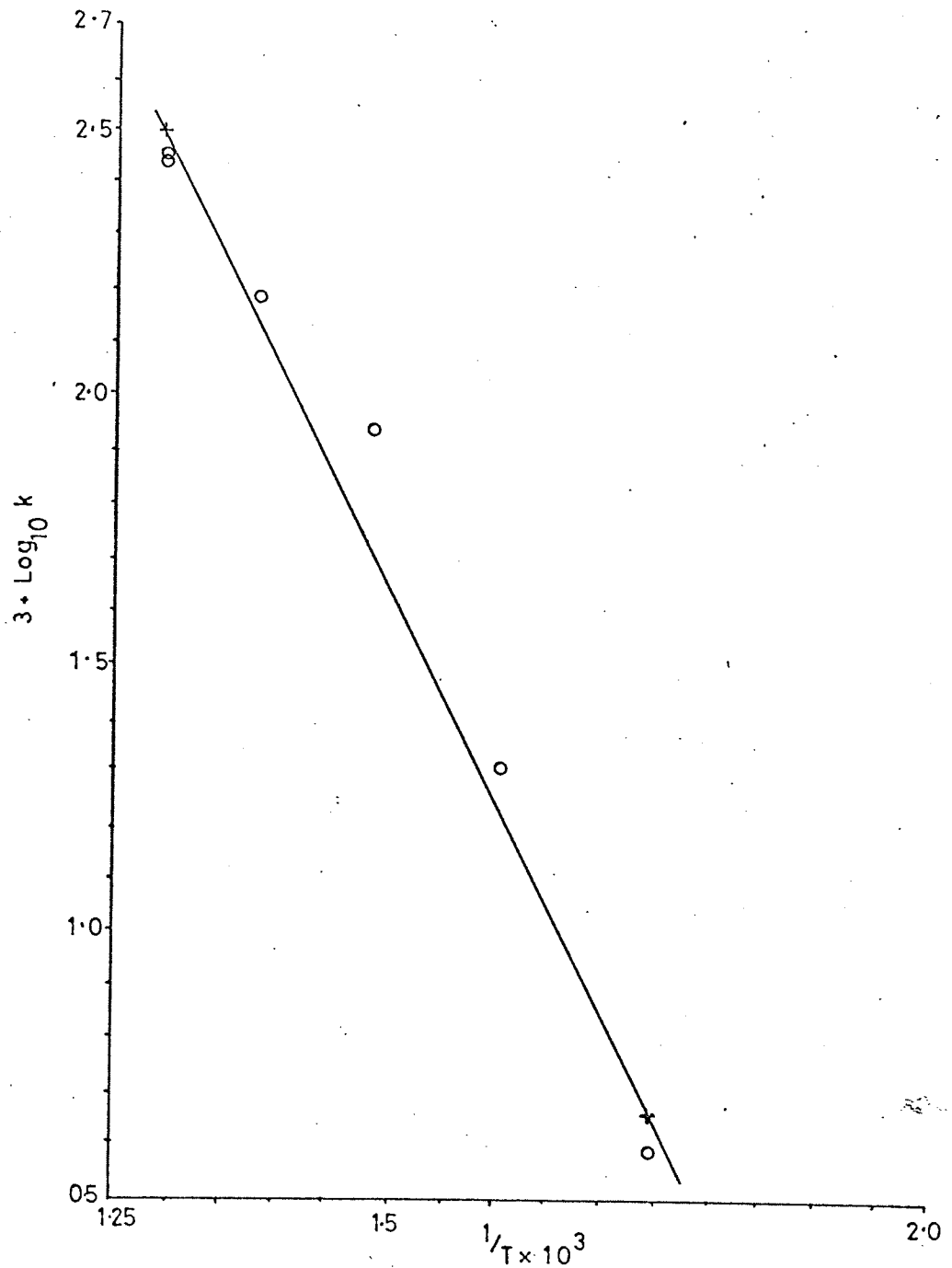
FIGURE 51

COMPOSITION/TIME PLOT FOR THE REACTION BETWEEN $5.0 kNm^{-2}$ N_2O AND $2.1 kNm^{-2}$ CO OVER 0.5% w/w $Ru-Al_2O_3$ (0.59g) AT $400°C$
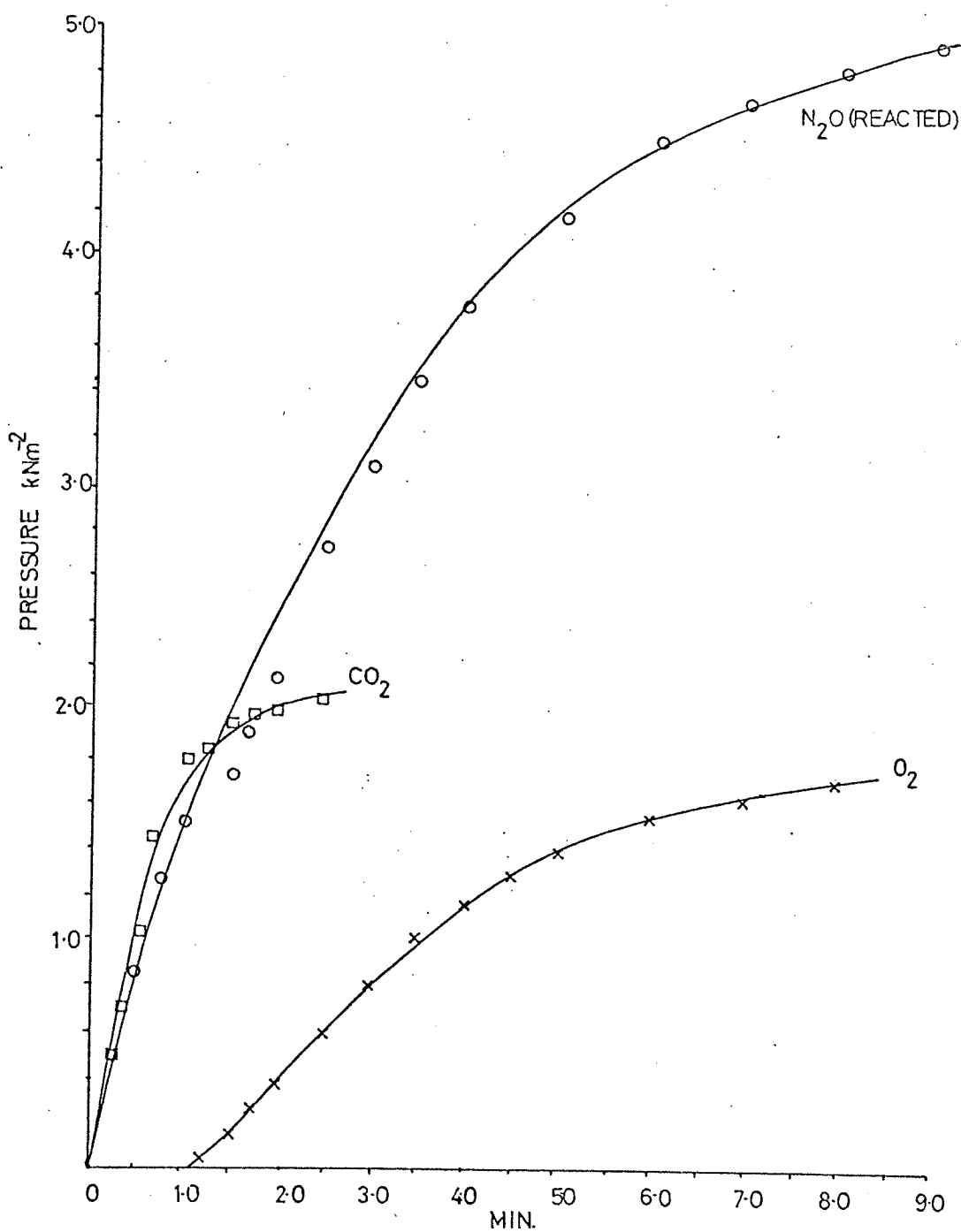
3.4. A COMPARISON OF Pd and Ru-Al$_2$O$_3$ CATALYSTS FOR THE REDUCTION

OF NITRIC OXIDE AND NITROUS OXIDE BY CARBON MONOXIDE

Comparison with noble metals.

Some of the physical properties and chemical activities of the group VIII metals have been considered so that they may be related to the results and discussions of this work. Palladium, platinum, rhodium, iridium and ruthenium were chosen for this comparison since they have been widely used as catalysts for the reduction of nitric oxide by carbon monoxide and hydrogen, for the methanation reaction and hydrogenolysis of hydrocarbons. Table 19 on page 152   compares this noble metal series with their activity for the above reactions and their ability to form nitrous oxide, isocyanates and ammonia.

For the reduction of nitric oxide by carbon monoxide Table 19 shows a correlation between the catalytic activity and the formation of nitrous oxide and isocyanates. The difference in activity may be attributed to the increasing inhibiting nature of carbon monoxide from ruthenium up to palladium[101]. Whereas, nitrous oxide and isocyanate formation is associated with the nitric oxide - catalyst stability (which is coupled with the ability of the catalyst to convert nitric oxide to nitrogen in the reduction process). The difference in activities may also be due to an additive affect associated with surface isocyanate formation. Infrared studies (chapter 5) have shown that surface isocyanates are relatively stable, when formed they reduce the number of sites available for reaction which effectively reduces the nitric oxide conversion rate.

This is not the case when the reducing agent is changed to
hydrogen. Under these conditions it would be expected that
the catalyst sequence would remain unchanged for nitrous oxide
formation. Furthermore, the ability of the catalyst to form
ammonia should be in the same sequence as that for isocyanate
formation. Table 19 shows correlation between the formation
of isocyanate, nitrous oxide and ammonia; ruthenium forming
the least amount in each case. These correlations support
the proposals made in chapter 1, section 1.3. and chapter 3,
section 3.0.2. that the formations of nitrous oxide, ammonia,
and isocyanates during the reduction of nitric oxide by hydrogen
and carbon monoxide respectively are interrelated mechanistically.

Electronic properties of the catalyst series have also been
related to catalytic activity. Sinfelt[102] has found a correlat-
ion of catalyst activity with the percentage "d" character of
the noble metal series for the hydrogenolysis of ethane. Table
19 shows that there is a weak correlation of catalyst activity
with the percentage " d" character for the reduction of nitric
oxide. A correlation between nitric oxide - catalyst stability
(i.e. the catalysts ability to form nitrous oxide isocyanates
and ammonia) and the percentage "d" character also exists, albeit
weak. Sinfelt however, pointed out that the electronic property
the catalyst is only one of the factors involved in determining
the activity of catalysts; since in relating catalytic activity
to percentage "d" character one is assuming that a relation
exists between bond strength in the surface layer and bond strength
inside the crystal.

Comparison of results.

Tables 20 and 21 on pages 153 and 154 represent a comparison of data for the reduction of nitric oxide and nitrous oxide by carbon monoxide over palladium and ruthenium catalysts.

NO - CO reaction.

One of the principal differences between the two catalysts for this reaction is that ruthenium has the ability to switch between two metastable states; this has a major effect on the reaction mechanism and product distribution. For example, the ability of these catalysts to promote nitrous oxide and isocyan-ates[48] is ordered Pd>Ru. The main difference in the surface mechhanism lies with the proposal that for the ruthenium catalyst, in state 2, the adsorption of nitric oxide is modified so that the oxygen of the nitric oxide molecule also interacts with the surface. Under these conditions nitrogen may be formed by the N - N coupling of adjacent surface nitric oxide molecules. Conversely, in state 1 (and for the palladium catalyst) the mechanism is based on the formation of a nitrogen atom through a linearly adsorbed NO - CO complex.

Thermodynamic feasibility for oxide formation is in the order Ru>Pd[103,104] indicating that ruthenium is the "least - noble" in this respect. As already mentioned, during adsorption of nitric oxide on ruthenium, if both the nitrogen and oxygen atoms interact with the catalyst surface so that when bond rupture eventually occurs ruthenium can accommodate oxygen atoms then specificity for production of molecular nitrogen follows. Specificity for formation of molecular nitrogen will also be favoured for the

ruthenium catalyst because of the greater surface coverage by nitric oxide. This will ensure an increased probability of nitric oxide adsorption on adjacent surface sites.

Palladium, on the other hand, favours adsorption of carbon monoxide, so that in this case nitric oxide covers only a minority of sites. Since there is little tendency for surface oxide formation, albeit transient, rupture of nitrogen oxygen bonds will occur through the interaction of an adjacently adsorbed carbon monoxide molecule to give surface isocyantes or nitrous oxide dependent upon reaction conditions as already described.

The activity of these catalysts for the reduction of nitric oxide is not significantly different; ruthenium is approximately twice as active as palladium. Although, ruthenium is more susceptible to changes in reactant stoichiometry and temperature. The order of activity and the chemisorption properties of the reactants have been noted in a number of studies[59,101]. Hitherto, there has not been any kinetic evidence to support the proposals of these authors.

N_2O - CO reaction.

The relative activities of the catalysts for the reduction of nitrous oxide by carbon monoxide is in the order of Pd>Ru (Table 21). This is the reverse of that for the nitric oxide - carbon monoxide reaction. The decomposition of nitrous oxide over ruthenium is significant for this reaction. This decomposition, which may be the rate limiting step is inhibited by the presence of carbon monoxide. In comparison, palladium does

not promote the decomposition significantly ($< 500^{\circ}C$) and the
reaction is not inhibited by carbon monoxide.

Apparent activation energies.

The apparent activation energies for the reduction of nitric
oxide and nitrous oxide by carbon monoxide are similar for each
catalyst this suggests in the broad sense that the reactions all
have the same energy limiting step.   This step may be associated
with the carbon monoxide – oxygen reaction.   Evidence which
supports the above can be obtained by comparing the apparent
activation energies for the carbon monoxide – oxygen reactions
over noble metals for similar temperature and pressure ranges.
Baddour et al.[105] obtained an apparent activation energy of 92
k J mol^{-1}. Interestingly, these authors also found that the rate
of production of carbon dioxide was inversely proportional to the
pressure of carbon monoxide.

In summary, it has been possible through the interpretation
of kinetic and infrared data to explain the reactivity of the
catalysts for these reactions.   Furthermore,this activity series
correlates with the known reactant chemisorption properties.

TABLE 19

152

Represents some of the physical properties and relative activities
of catalytic reactions for a noble metal series.

NOBLE METAL SERIES						REFERENCE
	Pd	Pt	Rh	Ir	Ru	
1) PHYSICAL PROPERTIES						
Atomic radius nm	0.137	0.138	0.134	0.135	0.132	106
Normal lattice structure	f.c.c.	f.c.c.	f.c.c.	f.c.c.	c.p.h.	106
Percent "d" bond character	46	44	50	49	50	106
Work function e.v.	4.49	4.52	4.65	4.57	4.52	106
2) REACTIONS **NO – CO**						
1) Activity (Ex's CO)	Pt < Pd < Rh < * < Ru					101
2) Isocyanate formation relative to Ru	Pd 4.4 Pt 3.5 Rh 3.5 Ir 2.8 Ru 1					47-48
3) Nitrous oxide formation relative to Pd (Ex's NO)	Pd > Pt > * > * > Ru					59-57
NO – H$_2$						
1) Activity (Ex's H$_2$)	Pd > Pt > Rh > * > Ru					101
2) Nitrous oxide formation relative to Pd	Pd > Pt > * > * > Ru					59
3) Ammonia formation relative to Pd	Pd > Pt > * > * > Ru					
CO – H$_2$						
1) Activity	Pd ~ Pt < Rh ~ Ir ≪ Ru					67
HYDROGENOLYSIS OF,						
1) ETHANE, activity	Pd ≲ Pt < Rh ≲ Ir < Ru					102
2) PENTANE, activity	Pd < Ir < Pt < Rh < Ru					107
(C)n + H$_2$						
1) Activity	Pd ≲ Pt < Rh ~ Ir < Ru					108
M + O$_2$ OXIDE FORMATION	Pd < Pt ~ Rh < Ir < Ru					104
	Pd ~ Pt < Rh ~ Ir < Ru					103

* proposed order of activity

TABLE 20

Lists the rate laws and predominant mechanisms for the reduction
of nitric oxide and nitrous oxide by carbon monoxide over 0.5%
w/w Pd- Al_2O_3 and 0.5% w/w Ru-Al_2O_3.

CATALYST	CONDITIONS	RATE LAW	MECHANISM
Pd	NO + Excess CO	$r = k\, P_{NO}^{2} P_{CO}^{-1}$	L - H
Pd	N_2O+ Excess CO	$r = k\, P_{N_2O} P_{CO}^{\frac{1}{2}}$	R - E
Pd	N_2O+ CO	$\propto P_{N_2O}^{\frac{1}{2}} P_{CO}^{\frac{1}{2}}$	L - H
Pd	Excess N_2O+CO	$\propto P_{N_2O}^{\frac{1}{2}} P_{CO}$	L - H
Ru	NO + Excess CO	$r = k\, P_{NO}^{0} P_{CO}^{0.2}$	L - H
Ru	NO + 2 Excess CO	$\propto P_{NO}^{1} P_{CO}^{0.2}$	L - H
Ru	N_2O	$r = k\, P_{N_2O}$	L - H
Ru	N_2O+ CO	$\propto P_{N_2O} P_{CO}^{0}$	L - H

TABLE 21

Represents a comparison of data obtained for the reduction of

nitric oxide, and nitrous oxide by carbon monoxide over palladium

and ruthenium catalysts.

CATALYST 0.5% w/w Al_2O_3	REACTION		
	NO − CO	N_2O − CO	N_2O
1) Rate equations describing the above reactions for equal reactant pressures to 500°C			
Pd	$Rate = k \, P_{NO}^{2} P_{CO}^{-1}$	$Rate = k \, P_{N_2O}^{+\frac{1}{2}} P_{CO}^{+\frac{1}{2}}$	−
Ru	$Rate = k \, P_{NO}^{0} P_{CO}^{0.22}$	$Rate = k \, P_{N_2O}^{1} P_{CO}^{+0}$	$Rate = k \, P_{N_2O}^{1}$
2) Reaction rates at 350°C molecules. $cm^{-2} \, sec^{-1}$			
Pd	6.1×10^{14}	6.5×10^{15}	−
Ru	1.2×10^{15}	3.3×10^{13}	2.0×10^{14}
3) Apparent activation energies, for a temperature range between 250 − 500°C, and equal reactant pressures of $\simeq 4.7 \, k \, Nm^{-2}$ ($k \, Jmol^{-1}$)			
Pd	91.2 (Log_{10} A 6.3)	65.1 (Log_{10} A 4.6)	− −
Ru	82.4 (E_0) (Log_{10} A 10.8)	72.3 (Log_{10} A 4.4)	42.5 (Log_{10} A 2.6)

SECTION 2

CHAPTER 4

INFRARED SURFACE STUDIES

4.0 INTRODUCTION

This investigation continues the study of the kinetics and mechanism of the reduction of nitric oxide by carbon monoxide over a palladium catalyst: Chapter 3 section 3.0 A comparative study of the infrared spectra of reaction intermediates and chemisorbed species during the nitric oxide- carbon monoxide reaction over platinum, palladium, rhodium, indium, and ruthenium on alumina has been made by Unland[48]. A strong band was observed in 2260-2270 cm^{-1} region and was attributed to a surface isocyanate species. This band was observed when the reaction contained an excess of carbon monoxide at temperatures above $300^{\circ}C$.

The discovery of the presence of a surface isocyanate has led to the postulation of new mechanistic pathways for the nitric oxide - carbon monoxide reaction. Unland[44] proposed for example, that the isocyanate acts as a true reaction intermediate and offered the following mechanisms:—

$$NO \xrightarrow[300^{\circ}C]{Pt/Al_2O_3} N_{ads} + O_{ads}$$

$$N_{ads} + CO \longrightarrow NCO_{ads}$$

$$O_{ads} + CO \longrightarrow CO_2$$

$$NCO_{ads} + NO \longrightarrow N_2 + CO_2$$

Total Reaction

$$2NO + 2CO \longrightarrow N_2 + 2CO_2$$
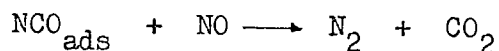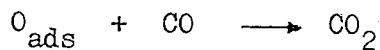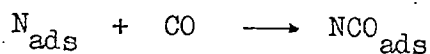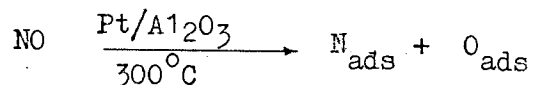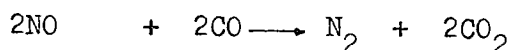
The object of this study was to independently substantiate

Unlands observations and assignments; 2) to establish the stability of the isocyanate species, and thus establish if the mechanistic postulate that isocyanate acts as an intermediate in the carbon monoxide – nitric oxide reaction is correct; and 3) to relate the assignments and conclusions to the kinetic study.

4.1 EXPERIMENTAL TECHNIQUE USED FOR INFRARED SURFACE STUDIES

The technique used for the infrared study of the surface a palladium – alumina was similar to that used by Unland[46].

One of the major problems associated with such a study lies in sample preparation. The sample must have the following characteristics because of the need to obtain suitably intense spectra.

1) The sample must have a high surface area.

2) The sample must have a particle size below the wavelength of infrared radiation, so as to minimize the scattering losses.

3) The metal loading on the support must be such that transmission losses are minimized.

4) The sample must be able to withstand high temperatures without cracking.

Baymal,[109] an alumina powder consisting of boehmite fibrils which swell in water to form a colloidal solution, was used by Unland[46] to support the transition metal catalysts. Baymal produces clear-to-translucent films on smooth surfaces by casting from an aqueous dispersion. Unland[46] observed minimal flaking and crazing of the film after it had been dried and calcined under vacuum at 350 – 600°C. At this temperature the boehmite fibrils dehydrate to give a high surface area γ- alumina.

Baymal was prepared[110] and tested for use as a support for

palladium.   Several difficulties were encountered.   Firstly,
not enough of the palladium — Baymal mixture could be deposited
without severe cracking of the film occurring.   Also, problems
were encountered with regard to sample heterogeneity.   It was
found that powdered γ-aluminium oxide when cast from an aqueous
solution on to a CaF_2 disc (25 x 3 mm), produced a film which
after drying and calcining possessed most of the qualities des-
cribed above.   Patience and a lot of luck were required for the
preparation of the film.

A variety of vacuum cells for supporting the sample in an
infrared beam have been described in the literature [111,112].

These cells consist of essentially two
types: those that enable the sample to be heated at the same
time that the infrared spectrum is recorded, and those in which
the sample is moved to a different portion of the apparatus for
heat treatment.   The latter type was used in this study.

Experimental conditions, and the nature of the reactants
play an important role in the design of an infrared cell.   For
example, the use of high vacuum grease on vacuum joints is pro-
hibited since hydrocarbon contamination of the sample occurs
with relative ease.   Hydrocarbon contamination can also occur
because of reaction between nitric oxide and rubber couplings
or seals.

4.2   INFRARED CELL

Figure 52 on page 162   is a photograph, 1:2.5 scale of the
infrared cell.   This cell is similar to that used by Butler
and Poles [113]

The infrared cell was made from borosilicate glass and con-

sists of a reaction chamber, and an infrared chamber. The reaction chamber, provided with a central thermocouple well was completely enclosed by an electrical furnace. The temperature of the furnace was controlled by a variac transformer and a thermocouple/potentiometer meter. Figure 53 on page 163 represents a scale diagram of the infrared chamber. Sodium chloride windows 50 x 5 mm, were positioned at each end of the infrared chamber by aluminium screw clamps, the base of which was attached by "Araldite" to the glass rims. A silicone rubber washer between the cell and the windows provided for a vacuum tight seal.

A stainless steel wire holder was used to support a CaF_2 disc 25 x 3 mm, and act as a carriage for the transfer of the disc along a glass rod positioned inside the cell.

Greaseless high vacuum valves A and B permit the cell to be isolated from the vacuum and gas mixing system.

4.2.1 VACUUM AND GAS MIXING SYSTEM

The infrared cell could be attached through B-7 joints to a conventional portable vacuum system, and the gas mixing system which was described in chapter 2 sections 2.03. Operational pressures obtained with the cell attached were of the order of 1.3×10^{-4} Nm^{-2}.

The infrared cell could also be attached through the B-7 joint and a length of glass tubing to the gas mixing system at tap D Figure 2 page 44 described in section 2.03.

4.3 SAMPLE PREPARATION, 10% w/w Palladium - Alumina

The catalyst was prepared by stirring 164 mg purified γ-aluminium oxide powder (Hopkins and Williams) with an aqueous

solution of palladium II chloride containing 16.4 mg palladium. The mixture was bought to the boil and the water evaporated off slowly to ensure even impregnation.   After drying at 120°C, the catalyst was crushed to a fine powder in a mortar.

Approximately 80mg of the catalyst was mixed with five drops of water and one drop of acetone.   The resulting slurry was ground to a fine dispersion in a mortar.   With the aid of a teat pipette three to five drops of the dispersion was spread on a preweighed CaF_2 disc.   The slurry was dried slowly in an oven at 70°C to give a fine even dispersion of catalyst on the disc. The sample was heated in air to 360° (6° min^{-1}) for one hour, cooled to room temperature then re-heated for one hour in flowing hydrogen 40ml min^{-1} at 360°C.   On cooling, the weight of the catalyst containing 10% w/w palladium - alumina was determined to be 33 mg.

The disc was mounted in the stainless steel holder and attached to the glass rod in the infrared cell.   With the sodium chloride windows in position the disc was manoeuvred into the reaction chamber.   The cell was then attached to the vacuum line and gas mixing systems and heated for one hour at 420°C under a vacuum of 1.3×10^{-4} Nm^{-2}.   The sample was treated, respectively, for $1\frac{1}{2}$ - 2 hours with 13.3 k Nm^{-2} oxygen and 13.3 k Nm^{-2} hydrogen at 420°C.   After each treatment the sample was evacuated to 1.3×10^{-4} Nm^{-2} for one hour, then cooled to room temperature.

The sample contained 8.4 mg cm^{-2} of the catalyst and was 6.6×10^{-3} cm thick.

4.4 EXPERIMENTAL PROCEDURE FOR INFRARED SURFACE STUDIES

The sample was prepared, introduced into the cell and treated as described in the previous section. The cell was isolated from the vacuum system, and a predetermined mixture of gases allowed into the cell through valve B from the gas mixing system. The pressure of gases was measured manometrically as described in section 2.5.

The cell was isolated, and the sample heated to $400^{o}C$. After a length of time, depending upon the experiment the sample was cooled to room temperature and the reactant gases evacuated to 1.3 Nm^{-2}.

The infrared cell was removed from the vacuum line and tilted so that the CaF_2 disc supporting the catalyst could be manoeuvred into position in the infrared chamber. The cell was then attached to a bracket mounted on a Perkin Elmer 225 spectrometer and the spectrum recorded over a range of 2500 - 1000 cm^{-1} with a normal slit programme.

In certain experiments the gases were not evacuated from the sample cell. In these cases differential spectroscopy was used. Estimated proportions (trial and error) of the gases in the sample cell were introduced into a gas cell of similar path length to that of the sample cell. The absorptions due to the gases in the sample cell were eliminated exactly when the reference cell was placed in the reference beam. Thus using differential spectroscopy the progression of surface bands, if any, in the region of the gas phase absorptions could be monitored without evacuation of the sample cell.

In order to provide a reproducible background spectra

for each experiment the sample was initially treated with
oxygen and hydrogen as described in the previous section.
Details of the experimental procedures used in each experiment
are listed on the individual spectra described in chapter 5.
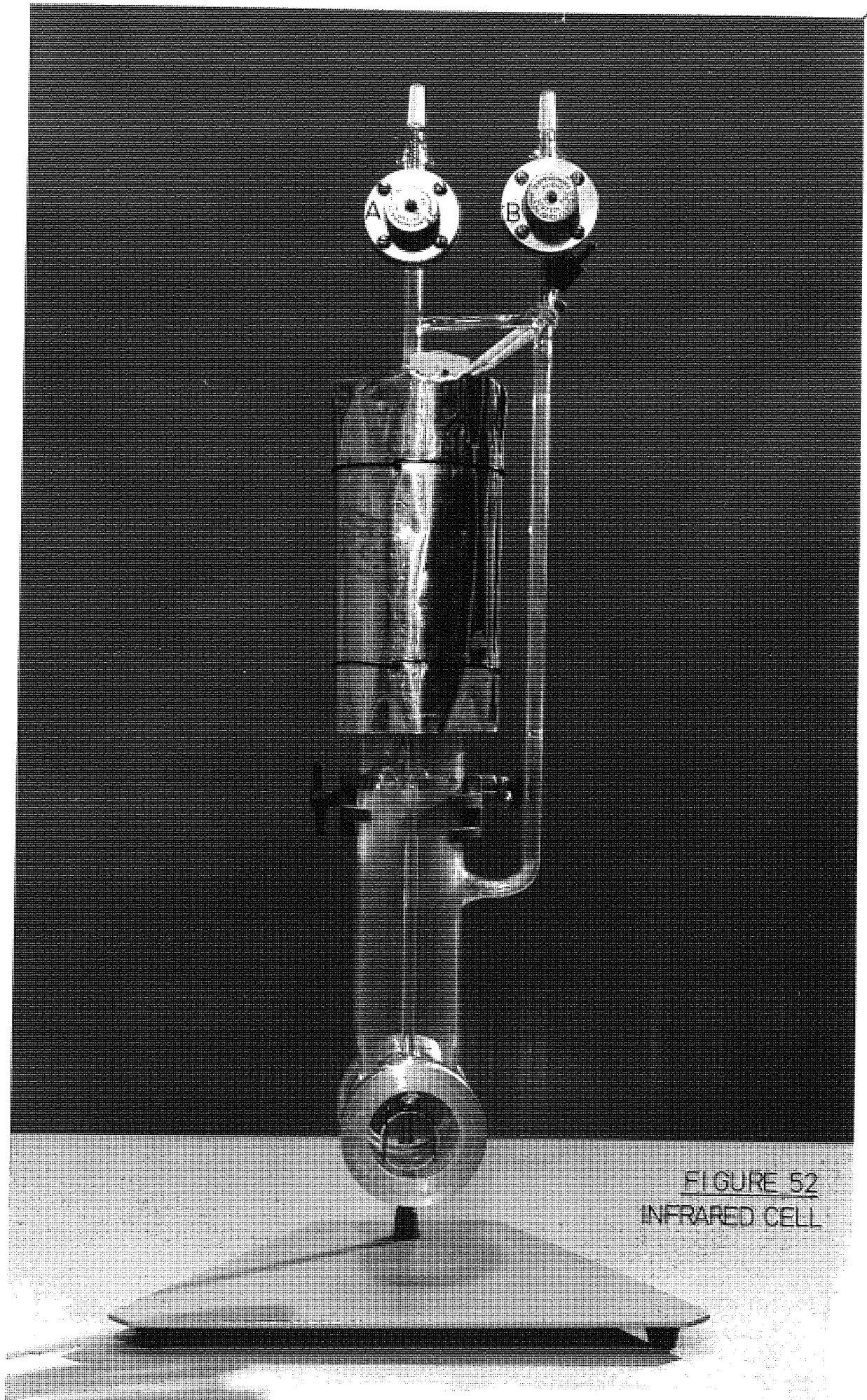
FIGURE 52
INFRARED CELL

FIGURE 53

INFRARED CELL

TO HEATING CHAMBER

GLASS ROD

ALUMINIUM SCREW BASE

NaCl WINDOWS

SILICONE RUBBER WASHER

ALUMINIUM SCREW WINDOW CLAMP

CaF$_2$ DISC

STAINLESS STEEL WIRE HOLDER

HARD RUBBER WASHER
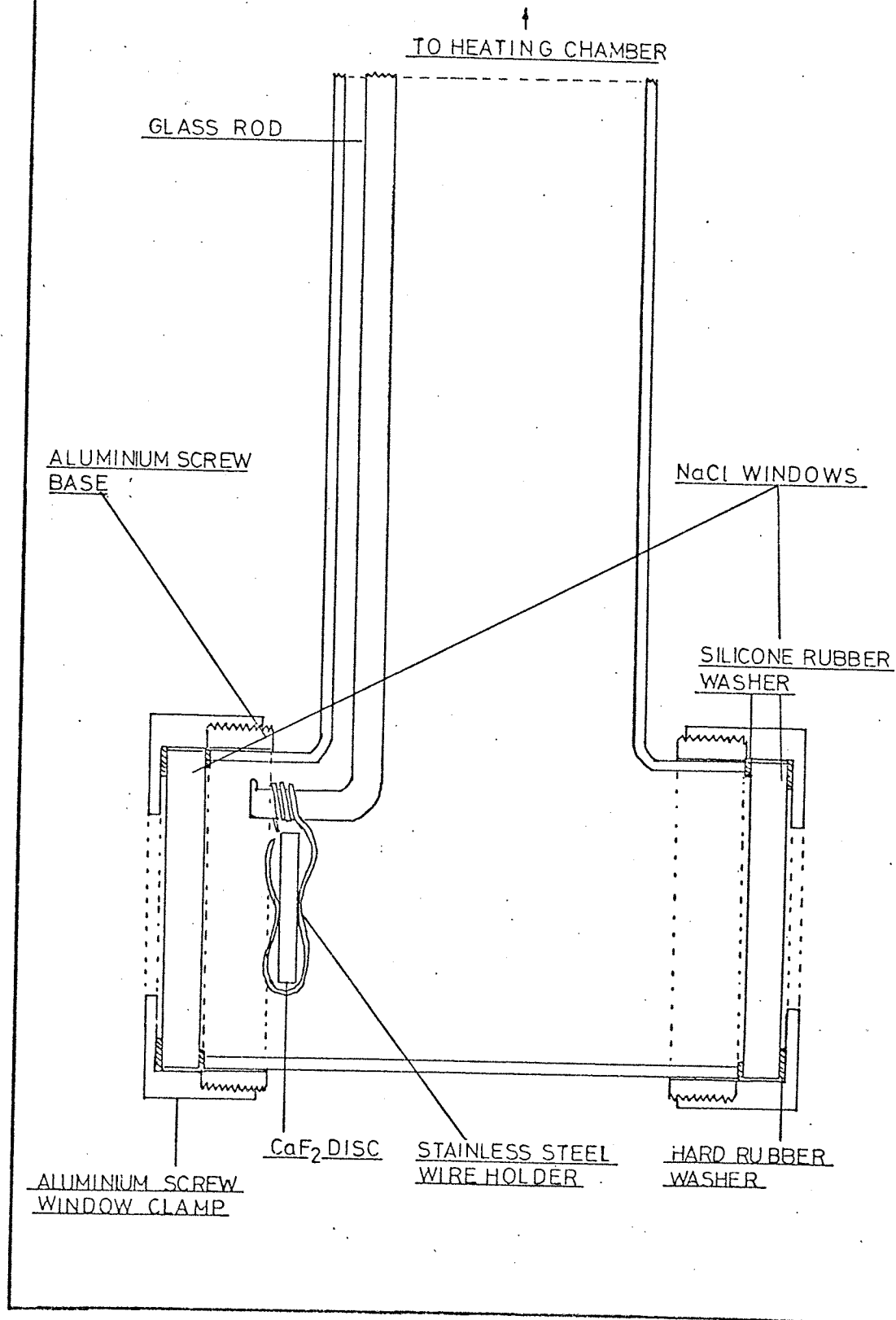
CHAPTER 5

RESULTS AND DISCUSSIONS OF INFRARED STUDIES

5.0 INFRARED SPECTRA OF REACTANTS ADSORBED ON 10% w/w Pd-Al$_2$O$_3$

Reference spectra from individual adsorptions of carbon

monoxide, carbon dioxide, nitric oxide and nitrous oxide were

obtained by contacting the gases respectively on a pre-treated

surface at 400°C.   The absorptions due to the reactant-surface

interactions were assigned by comparison with the absorption

band frequencies of analogous inorganic complexes.   It is

important to bear in mind, however, that the surface of the

catalyst is heterogeneous and due allowance of the whole surface

interaction must be taken into account when comparing the catalyst

surface spectra to inorganic complex spectra.

5.0.1 ABSORPTION BANDS DUE TO CARBON MONOXIDE AND CARBON DIOXIDE

(a) Carbon monoxide

Figure 54 on page 178   reports the infrared absorption bands

which develop when the catalyst was treated with carbon monoxide.

Carbon monoxide gave three main bands in the 1590, 1465 and 1390-

1375 cm^{-1} region.   Small bands were also observed in 2200- 1800

cm^{-1} region (spectra not shown).   Studies[75] have shown absorption

bands in this region are mainly due to two types of surface species

a bridged and a linear form of adsorbed carbon monoxide.   These

were discussed in chapter 3, section 3.0.

Absorption bands in the 1800 - 1000 cm^{-1} region may be attri-

buted to carbonate type structures.   These have been classified

according to their co-ordination[111]and are represented in Table

22   on page 184.

Using Table 22 the bands 1590 and 1390 - 1375 cm^{-1} shown in Figure 54 are attributed to a bidentate carbonate type II structure. The band at 1465 cm^{-1} is assigned to a carbonate ion vibration.

(b) Carbon dioxide

Carbon dioxide when brought into contact with the catalyst surface at $400^{\circ}C$ produced three main absorption bands, 1645, 1455 and 1225 cm^{-1} (figure not shown). Those at 1645 and 1225 are assigned to a bidentate type 1 structure and the band at 1455 cm^{-1} to a symmetrical carbonate ion vibration, Table 22.

The background peak at 1365 cm^{-1} which remains even after the reconditioning process has been observed before on alumina[114,115] This band is associated with the support and arises from a carbonate ion vibration.

The absorption bands which appear after the surface has been treated with carbon monoxide and carbon dioxide cannot be unequivocally assigned to reactant - palladium interactions since reactant-alumina interactions give bands in a similar region[116,117]. Table 23 on page 184.

5.0.2 ABSORPTION BANDS DUE TO NITRIC OXIDE AND NITROUS OXIDE

(a) Nitric oxide

Figure 54 shows that the chemisorption of nitric oxide on a pre-treated surface gave rise to absorption bands at 1635, 1575, 1560 cm^{-1}, a shoulder at 1515 cm^{-1} and a broad band at 1220 cm^{-1}. These bands are due to nitric oxide-surface interactions since the nitric oxide was evacuated from the cell before recording the spectrum.

A general description of the common forms of bonding of nitric oxide on metal surfaces was given in the introduction,

chapter 1, section 1.2.2. Sidwick[118], Lewis et al.[16] and others[18] have classified the absorption frequencies obtained from transition metal nitrosyl complexes according to cationic NO^+ or NO^- stretching frequencies. Table 24 on page 184 represents the range of the absorption frequencies of these ionic groups made by the above workers. Nakamoto[119] has suggested that the classification may need revision since no monomeric nitrosyl complexes are known to exhibit NO^- stretching in the anionic region. Gans[120] has suggested that the anionic NO^- stretching frequencies should include the $1700 - 1500$ cm^{-1} region. The Table 24 also shows that covalent nitric oxide - metal bonding gives rise to absorption frequencies in the $1800 - 1500$ cm^{-1} region.

On the basis of the classification of nitric oxide absorption frequencies shown in Table 24 it is not possible to positively assign the bands due to nitric oxide absorptions shown in Figure 54 The absorption bands could arise from ionic or covalent structures. Included in this spectrum are absorption bands which could arise from dinitrosyl or bridged nitrosyl stretching frequencies; these structures could be formed whilst the catalyst is cooling to room temperature since it is unlikely that they are formed at catalytic temperatures.

Examples of metal complexes containing nitric oxide together with the nitrosyl stretching frequencies are listed in Table 25 on page 185.

Unland[48], and London and Bell[44] have obtained similar spectra for nitric oxide adsorbed on palladium and copper oxide.

Unland[48],however, did not discuss the nature of these bands. London and Bell[44] considered the possibility of these bands aris-

ing from anionic NO^- stretching frequencies but were more inclined to attribute bands between 1600-1500 cm^{-1} to monodentate and bidentate nitrato structures.

(b) Nitrous oxide

Nitrous oxide adsorption on the catalyst surface produced a number of small bands.   The frequencies of these bands were situated at 1710, 1690, 1655, 1650, 1580, 1510, 1465 and 1380 cm^{-1} (figure not shown).   The bands at 1710, 1690, 1655 and 1650 were removed on evacuation of the cell to 1.3 x 10^{-2} Nm^{-2} at room temperature.   This suggests that they arise from weakly adsorbed species.   The bands which remain are consistent with nitric oxide stretching frequencies, as mentioned previously.   Nitric oxide could be formed as a result of the dissociation of nitrous oxide, for example, $2N_2O \rightleftharpoons 2NO + N_2$.

5.1   INFRARED SPECTRA OF REACTION MIXTURES ADSORBED ON 10% w/w
       Pd - Al_2O_3

(a) Nitrous oxide-carbon monoxide reaction mixtures.

A series of nitrous oxide – carbon monoxide reaction mixtures containing 1) excess nitrous oxide, 2) excess carbon monoxide and 3) stoichiometric reactant mixtures, were admitted to the infrared cell containing the sample at 400°C (spectra not shown).

The results of this set of experiments revealed absorption bands due to surface carbonates; bands 1645, 1455 and 1225 cm^{-1}. These bands diminished on evacuation at room temperature but re-appeared upon the re-introduction of carbon dioxide.   This result suggests that carbon dioxide, a product of the reaction, is comparatively weakly held to the surface and does not inhibit

the main reaction.

b) i Nitric oxide – carbon monoxide reaction mixtures.

In order to reproduce Unlands[46-48] experimental conditions a series of reactions containing 1) excess nitric oxide, 2) excess carbon monoxide, and 3) stoichiometric reactant mixtures, were admitted to the infrared cell containing the sample at $400^{o}C$.

After evacuation of the infrared cell to 1.3×10^{-2} Nm^{-2} at room temperature, absorption bands due to surface carbonates were identified for the reaction mixtures containing an excess of nitric oxide and stoichiometric reactant mixtures. For the reaction mixture which contained an excess of carbon monoxide in a 2:1 ratio ($4.3:2.1$ kNm^{-2}), four major absorption bands were noted. These bands differed in intensity from any others described so far; they were broad and centred around 2250, 1640, 1575 and 1290 cm^{-1}, Figure 55 page 179. Figure 55 shows the spectra due to surface interactions only since the products of the reaction, carbon dioxide and nitrogen have been removed by evacuation at room temperature. The bands appeared concurrently, suggesting that the structures which give these absorptions are interdependent. The formation of the bands at 2250, 1640 and 1575 cm^{-1} in reducing conditions is consistent with the work of Unland[46-48].

Figure 55 also shows that the exposure of the major bands to a further 2:1 ratio of carbon monoxide – nitric oxide mixture produced little enhancement of the bands. The gas spectrum showed that the reaction had reached completion after one hour implying that the reaction is still catalyzed in the presence

of these four major surface bands.

The effect of temperature on the bands in vacuo at $400^{\circ}C$
resulted in their diminution; complete disappearance occurred
only after continual heating in vacuo for 4 to 5 hours.

The fact that the major bands do not increase in size to
any extent after the re-introduction of the reaction mixture
and that the reaction is catalyzed in the presence of a surface
exhibiting these bands implies: 1) the structure giving rise to
the bands are formed only on selective surface sites, or 2)
that this structure has attained a surface equilibrium.

b) ii Reaction of carbon monoxide with pre-adsorbed nitric oxide.

Figure 56 on page 180   reports the results obtained when
carbon monoxide was introduced to a surface which had been
previously exposed to nitric oxide.   Figure 56 shows: 1)
the spectrum obtained after the surface had been exposed to 5.3
kNm^{-2} nitric oxide at $400^{\circ}C$ for 30 minutes.   The spectrum was
recorded at room temperature after the cell had been evacuated
to 1.3×10^{-2} Nm^{-2}.   The Figure shows that the chemisorption
of nitric oxide on the surface gave rise to absorption bands
similar to those described for the nitric oxide - reference
spectrum, section 5.0.2 (a); 2) the spectrum obtained after the
surface had been exposed to 6.0 kNm^{-2} of carbon monoxide at $400^{\circ}C$
for 30 minutes, cooled to room temperature and the cell evacuated
to 1.3×10^{-2} Nm^{-2}.   The spectrum shows the appearance of the
bands 1590, 1465 and 1390 - 1360 cm^{-1} which are associated with
carbonate structures, section 5.0.1 (a).

It is interesting to note that the bands produced are only those associated with carbon monoxide, carbon dioxide - surface interactions. There is no evidence of the formation of the four major bands at 2250, 1640, 1575 and 1290 cm^{-1} described previously. This result implies that the nitric oxide structures which give rise to absorptions in the region of 1635 - 1515 cm^{-1} are not responsible for the formation of the four major bands on reaction with carbon monoxide.

London and Bell[45] using a flow system and a feed of nitric oxide over a copper oxide catalyst found that the introduction of carbon monoxide produced a band at 2140 cm^{-1} (attributed to an isocyanate species) at the expense of the adsorptions due to nitric oxide. The reason for the production of the isocyanate band may be due to the fact that nitric oxide was not only adsorbed on the surface but also present in the gaseous phase together with carbon monoxide.

Experimental evidence obtained in this work and by London and Bell[45] implies that 1) there is more than one form of nitric oxide - surface absorption, and/or 2) that carbon monoxide has same modifying influence towards nitric oxide - surface adsorption, for example, making its adsorption more favourable so that a carbon monoxide - nitric oxide - surface complex may be formed in the manner described in chapter 3 section 3.0.2.

5.2 A COMPARATIVE INTERPRETATION OF ABSORPTION BANDS DUE TO ISOCYANATE STRUCTURES

Table 26 on page 185 compares the results obtained by Unland[46-48] with those of this study.

The Table 26 shows that the frequencies of the bands 2250, 1640 and 1575 cm^{-1} are consistent with those obtained by Unland. The excess carbon monoxide will account for the band at 1465 cm^{-1} which has been assigned to a carbonate ion vibration. The band at 1290 cm^{-1} has not been observed before.

Unland[46] assigned the band 2264 cm^{-1} to an isocyanate species by analogy with inorganic complexes $[W(CO)_5 NCO]^-$ and $[(C_6H_5)_3P]_2 Pt(NCO)_2$. The band at 1635 cm^{-1} was attributed to an imine structure, and the 1571 cm^{-1} band to contributions arising from a carbonate and nitrate species. These assignments were made after isotopic labelling experiments showed that bands 2264, 1635 and 1571 cm^{-1} contained both carbon and nitrogen atoms.

There is no dispute of the fact that Unlands[46-48] assignments of the bands can exist to a greater or lesser extent but there are some inconsistencies. Firstly, if Unlands[46-48] assignment of the band 2264 cm^{-1} to an isocyante is correct then one would expect a secondary band associated with pseudosymmetrical out of phase stretching[124-127] $\nu(NCO)$ in the region of 1550 - 1300 cm^{-1}. The band at 1575 cm^{-1} could arise from this mode of isocyanate stretching. Secondly, the fact that the bands 2250, 1640, 1575 and 1290 cm^{-1} appear concurrently and are larger than any of the reference spectra suggest that they arise from inter-related structures. Therefore, the assignment of the 1575 cm^{-1} band to contributions arising from carbonate and nitrate species alone seems unlikely.

The bands 2250 and 1575 cm^{-1} have been assigned to an iso-cyanate structure, leaving the bands at 1640 and 1290 cm^{-1} to be

assigned.   Since the experimental evidence suggests that the
bands are interrelated then it is not unreasonable to propose
that the bands in part could be due to polymeric isocyanate
structures [124,128].   The following represents some of the numer-
ous polymeric structures which could occur on the surface.
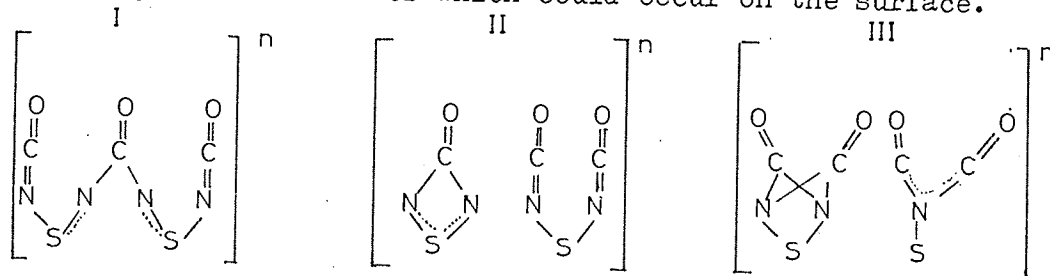
These structures are similar to those found in inorganic com-
plexes [119,124,128].   They give rise to absorption bands in the
regions of 1660 - 1590 cm^{-1}, and 1328 - 1245 cm^{-1}, corresponding
to $\nu(CO)$ and $\nu(C-N)$ stretching frequencies respectively.   The
fact that the four major bands are more intense than any of the
reference spectra supports the proposal for the formation of
polymeric isocyanate species.

The Table 26 shows that the assignments of the bands at
2250, 1640 and 1575 cm^{-1} are similar to those of Unlands [46-48]
with the exception that the major contribution of the 1575 cm^{-1}
is assigned to an isocyanate stretching frequency.   It is im-
possible to distinguish absorptions due to carbonyl "amide"
type structures from those of imine ($>C=N$) structures, both
structures could exist in a polymeric form.

The assignment of the major bands in Table 26 were made
after considering alternative structures which could give rise
to infrared bands in the 2300 - 2100 cm^{-1} region.   The most
probable structures being 1) OCN cyanato, 2) CN and NC, cyano

and isocyano, 3) CNO and ONC fulminate and isofulminato complexes.

5.3 STABILITY OF THE SURFACE ISOCYANATE SPECIES

The major bands at 2250, 1640, 1575 and 1290 cm^{-1} have been assigned to a surface isocyanate species.   Unland[46] has proposed that the surface isocyanate species acts as a reaction inter- mediate during the reduction of nitric oxide by carbon monoxide (chapter 4 section 4.0).   If this is the case then the surface isocyanate would be expected to react easily with one or both of the reactants, and thus diminishing the bands assigned to iso- cyanate as a consequence.   If not, then all the bands would be expected to remain.   (This assumes that the bands arise from an interrelated structure.).   One other possibility is that if the bands are not interrelated then one or more bands would disappear.

In order to try and establish which of the above possibili- ties occurs a catalyst surface exhibiting the surface bands 2250, 1640, 1575 and 1290 cm^{-1} was subjected to the following series of experiments.   Before each experiment the bands were regener- ated on a pre-treated surface in the manner described in section 5.1.

5.3.1 EFFECT OF CARBON MONOXIDE

Figure 57 on page 181 reports the results obtained when a surface exhibiting the four major bands were heated with 8.0kNm^{-2} carbon monoxide at $400^{\circ}C$.   Before recording the spectra the infra- red cell was evacuated to 1.3×10^{-2} Nm^{-2} at room temperature. The Figure 57   shows that the interaction of carbon monoxide produced a broading of the band at 1575 cm^{-1} and a shift to 1590cm^{-1}. This implies that carbonate species are formed without otherwise influencing the isocyanate bands.   Carbonate bands were also

noted at 1465 and 1390 cm^{-1}; these are described in section 5.0.1.

Unlands[46,48] work on a platinum catalyst has revealed a further band at 2130 cm^{-1}. This band was attributed to either an anionic $(NCO)^-$ or a cyano $-(C\equiv N)$ species. A compatible mechanism for the formation of a cyano species was offered whereby carbon monoxide might attack the surface isocyanate to give carbon dioxide and an isocyano intermediate, which could rearrange to a cyano species as follows,

$$Pt - NCO \ + \ CO \ \longrightarrow \ Pt - NC \ + \ CO_2 \qquad\qquad (1)$$

$$Pt - NC \ \rightleftharpoons \ Pt - CN$$
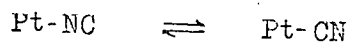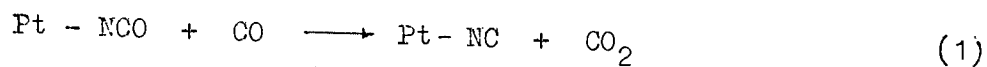
Cyano absorptions in the 2150 cm^{-1} region are generally sharp which is not the case for the broad bands centred at 2150 - 2050cm^{-1}. These bands are attributed to carbon monoxide adsorbed by dipolar interaction[112,129]. The formation of a cyano species by the above mechanism can be ruled out, since if this was the case a diminution in one or all the bands would be observed.

5.3.2 EFFECT OF NITRIC OXIDE

The catalyst exhibiting the four major surface bands was heated in the presence of 6.0kNm^{-2} nitric oxide to 1) 50°, 2) 150°, 3) 250°, 4) 300°, 5) 400° and 6) 400°C respectively. After each treatment the catalyst was allowed to cool to room temperature before recording the spectrum. In this case differential spectroscopy was used to eliminate the gas spectra due to nitric oxide in the manner described in chapter 4 section 4.4.

Figure 58 on page 182 reports the results of these experiments. The Figure 58 shows that above 300°C, nitric oxide had a marked effect on all the major bands. New bands at 1635, 1565,

1425 and 1310 cm^{-1} appeared, and the sample turned yellow. These bands remained even after the cell had been evacuated to 1.3×10^{-2} Nm^{-2} at room temperature. Figure 58 also shows that the major bands disappear concurrently, leaving small bands at 1635 and 1565 cm^{-1}. These bands are similar to those described for the reference spectrum of nitric oxide section 5.0.2. The fact that the bands disappear concurrently supports the proposal that they are interrelated.

The large bands produced at 1425 and 1310 cm^{-1} are consistent with the formation of a nitro complex, in particular the appearance of a band in the region of 1330 cm^{-1} is characteristic of a metal – nitrogen bonded group[119,130]. Inorganic metal nitro complexes which are generally yellow have absorption frequencies in the 1420 and 1330 cm^{-1} regions[119,130]. These frequencies correspond to asymmetric $\nu(NO_2)$ and symmetric $\nu(NO_2)$ stretching, respectively. The route to the production of a surface nitro complex is difficult to reconcile for no absorption bands in this region were obtained for the nitric oxide – surface reference spectra section 5.0.2. This evidence indicates that nitro species are formed by reaction of the isocyanate with nitric oxide. One such route may be represented by the following equations:-

$$S\ NCO\ +\ NO \rightleftharpoons S\ N_2O\ +\ CO \qquad (1)$$

$$SN_2O\ +\ NO \rightleftharpoons S\ NO_2\ +\ N_2 \qquad (2)$$

$$or \quad SN_2O\ +\ SNO \rightleftharpoons S\ NO_2\ +\ N_2 \qquad (3)$$
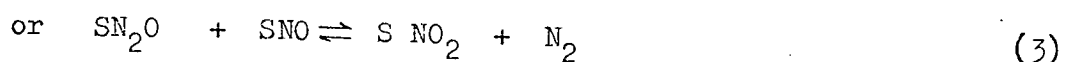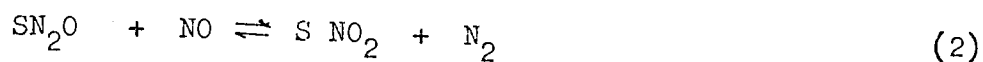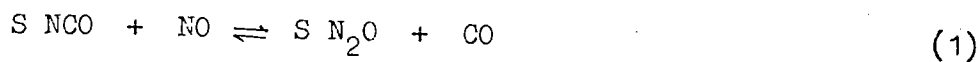
Under these conditions equation 1 indicates that the isocyanate species could act as a reaction intermediate in the formation

of nitrous oxide. This being an alternative route to that which was described in chapter 3, section 3.0.2.

5.3.3 EFFECT OF HYDROGEN

Figure 59 on page 183 represents the results obtained when a surface exhibiting the four major bands was heated in the presence of 6.0 k Nm^{-2} hydrogen at $400^{o}C$. Figure 59 shows that after the third heating the band at 2250 cm^{-1} was removed; the 1640 cm^{-1} band was reduced in intensity and appeared as a shoulder at 1620 cm^{-1}; the 1575 cm^{-1} band shifted to 1585 cm^{-1}, and the appearance of a new sharp band at 1450 cm^{-1} was noted.

Interaction of surface isocyanate species with hydrogen will develop surface ammonium structures through reactions 1, 2 and 3.

$$S\ NCO\ +\ H_2\ \rightleftharpoons\ S\ NH_2\ +\ CO \tag{1}$$

$$S\ NCO\ +\ 2H_2\ \rightleftharpoons\ S\ NH_4^+\ +\ CO \tag{2}$$

$$S\ N_2CO\ +\ H_2\ \rightleftharpoons\ S(NH)_2CO \tag{3}$$
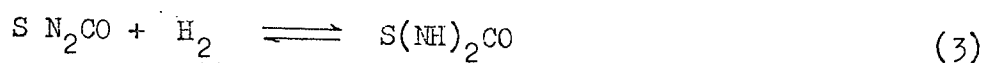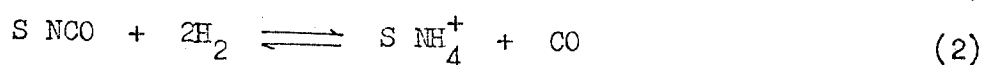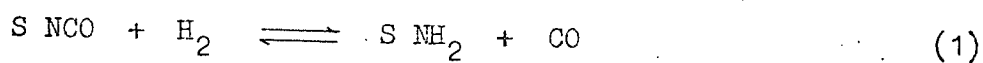
It is well known[112,131] that these structures give rise to absorptions in the 1620 and 1459 cm^{-1} region. The equations show the simultaneous formation of carbon monoxide which will produce bands at 1585 and 1450 cm^{-1}. The enhancement of the 1450 cm^{-1} band may arise from a contribution of a N-H deformation[112] or NH_2 rocking vibrations[132].

The Figure 59 shows that carbonate structures exist in the presence of hydrogen without the methanation reaction taking place. This result is consistent with the fact that palladium is relatively inert for this reaction[67]. One of the main reasons why this reaction does not occur to any extent could be due to the fact that carbon monoxide displaces hydrogen from the

surface [133] and that it is also strongly adsorbed on palladium. The mutual interactions of these reactants on palladium was found by Conrad et al.[133] to be weak. In contrast, these reactants have a strong mutual interaction on ruthenium [134] which is in agreement with the known catalytic activity of this metal for the methanation reaction [67].

5.4 SUMMARY

The formation and the stability of the principal absorption bands 2250, 1640, 1575 and 1290 cm^{-1} indicates that:-

1) The bands which have been assigned to a surface isocyanate species are only formed when there is an excess of carbon monoxide in the reaction mixture.

2) An isocyanate covered surface still catalyses the carbon monoxide - nitric oxide reaction.

3) The isocyanate is more likely to be formed as a bi-product of the reaction on selective sites rather than as an intermediate.

4) In the presence of nitric oxide the isocyanate species reacts to give additional bands at 1425 and 1310 cm^{-1} attributable to surface nitro formation.

5) In the presence of hydrogen there is evidence of the formation of surface carbonates and ammonium complexes after reaction with the isocyanate species.

6) The surface isocyanate species is not affected by carbon monoxide.

7) Carbon dioxide is weakly adsorbed on the surface whereas carbon monoxide is relatively strongly adsorbed.

FIGURE 54
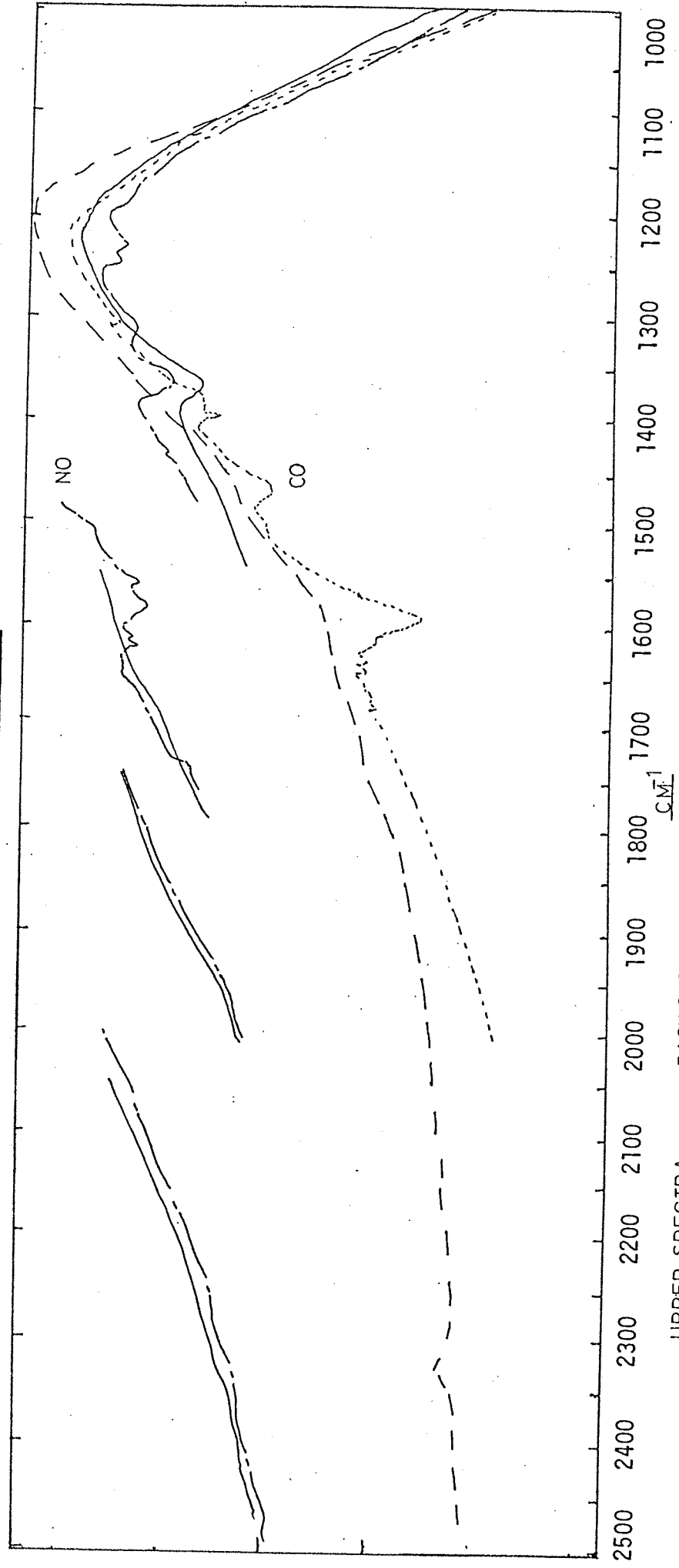
UPPER SPECTRA, ——— BACKGROUND,   10% w/w Pd-Al₂O₃.
              —·—·— 6·0 kNm⁻² NO ADDED; HEATED TO 400°C; COOLED TO R.T.; EVACUATED TO 1·3×10⁻² Nm⁻².

LOWER SPECTRA —··—··— BACKGROUND.
              -------- 7·3 kNm⁻² CO ADDED;   HEATED TO 400°C; COOLED TO R.T.; EVACUATED TO 1·3×10⁻² Nm⁻².

FIGURE 55

1) —————— SPECTRUM AFTER HEATING THE SAMPLE WITH A (4.3 : 2.1 k Nm⁻²) RATIO OF CO-NO TO 400°C FOR 2 HOURS; COOLED TO R.T.; EVACUATED TO 1.3×10⁻² Nm⁻².

2) — — — REINTRODUCTION OF A(2:1)RATIO OF CO-NO; HEATED FOR 1 HOUR AT 400°C.; COOLED TO R.T.; EVACUATED TO 13×10⁻² Nm⁻².

3) ———— AFTER HEATING SAMPLE AS SHOWN IN SPECTRUM (2) FOR 4 HOURS AT 400°C.
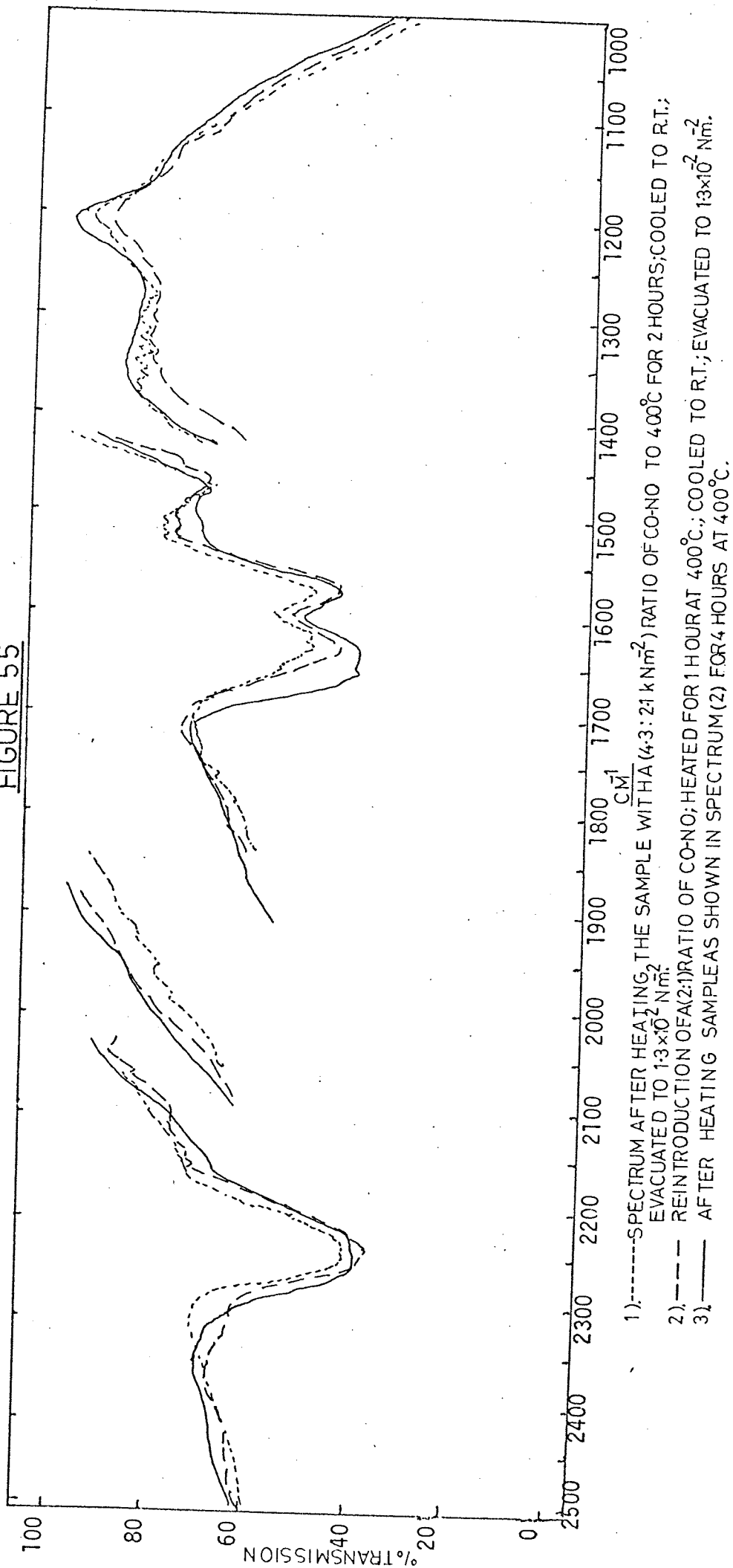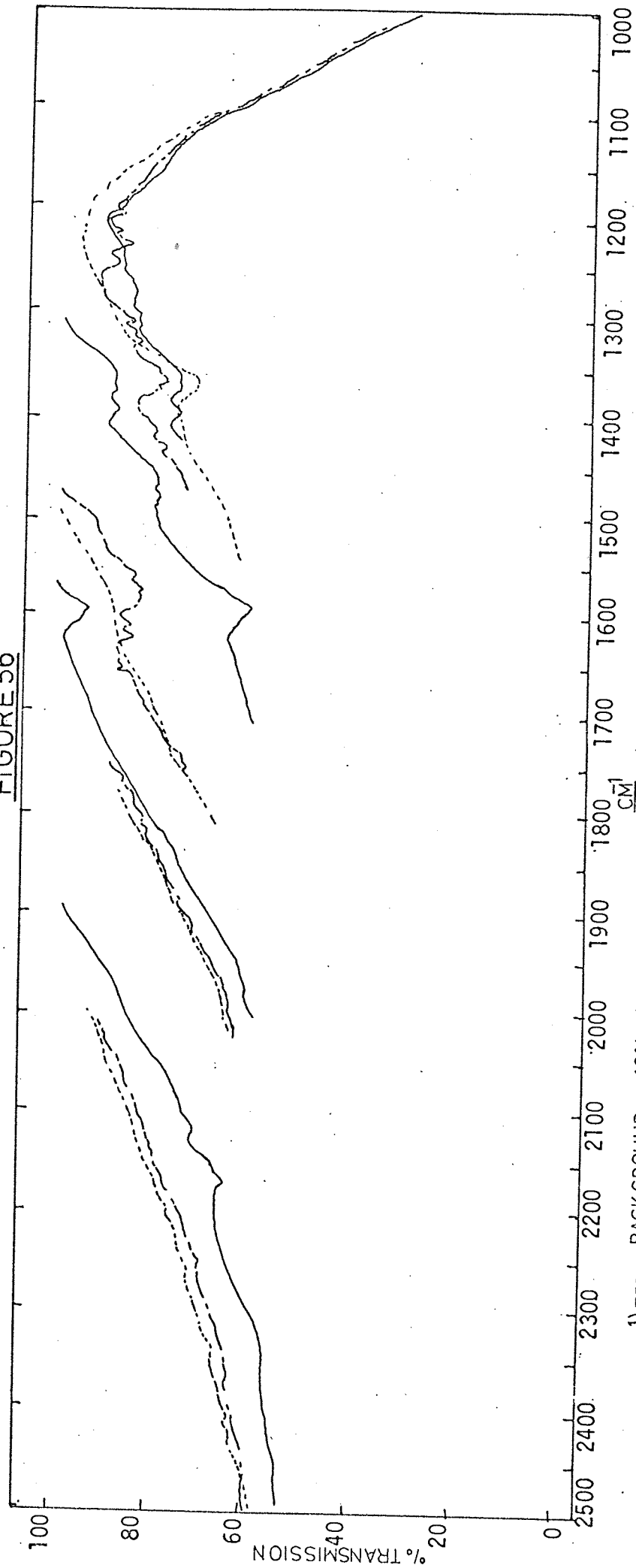
FIGURE 56

1). ------ BACKGROUND, 10% w/w Pd-Al_2O_3.

2). — — — $5.3 kNm^{-2}$ NO ADDED; HEATED FOR 30 MINUTES AT $400°C$; COOLED TO R.T.; EVACUATED TO 1.3×10^{-2} Nm^{-2}.

3). ——— $60 kNm^{-2}$ CO ADDED; HEATED FOR 30 MINUTES AT $400°C$; COOLED TO R.T.; EVACUATED TO 1.3×10^{-2} Nm^{-2}.

FIGURE 57
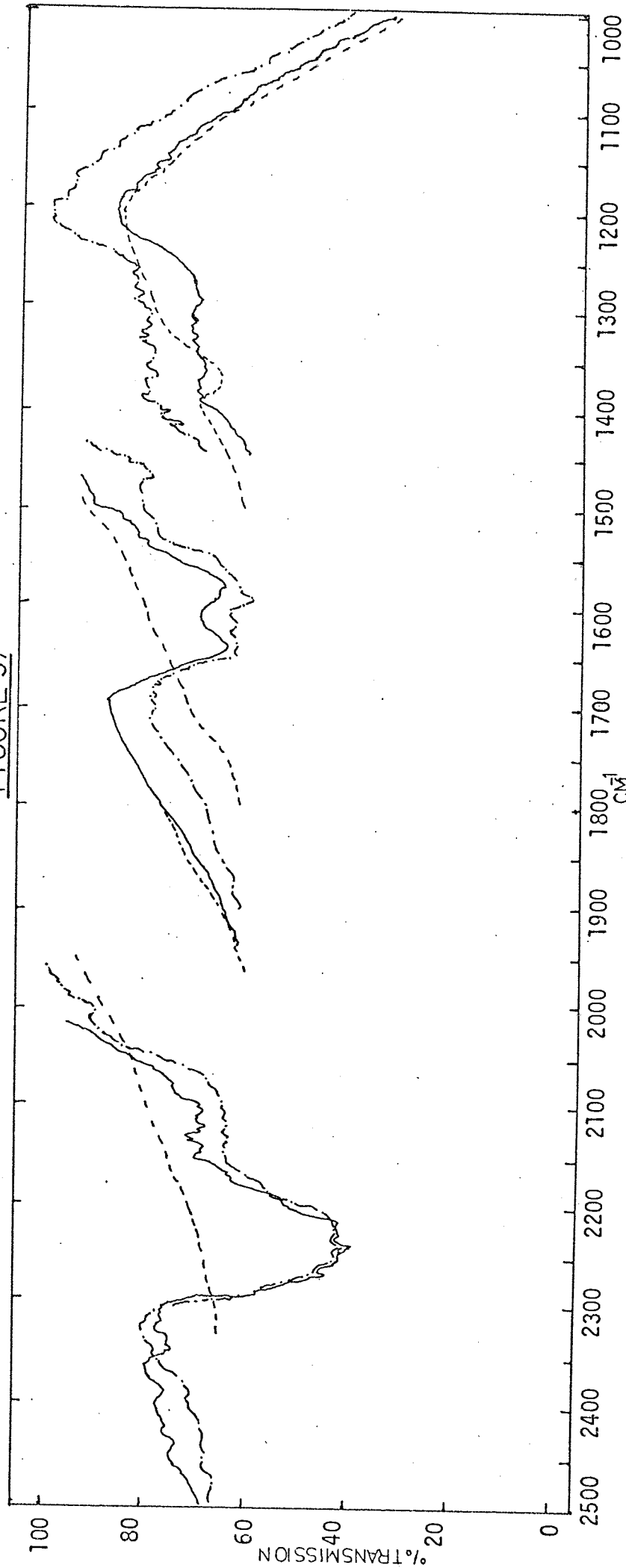
EFFECT OF CO ON BANDS at 2250, 1640, 1575, AND 1290 CM^{-1} AT 400°C.

1). ─ ─ ─ ─ BACKGROUND.

2). ────── BANDS REGENERATED; COOLED TO R.T.; EVACUATED TO 13×10^2 N$\bar{m}^2$.

3). ─ · ─ · ─ 80 k.N$\bar{m}^2$ CO ADDED; HEATED TO 400°C; COOLED TO R.T.; EVACUATED TO 13×10^2 N$\bar{m}^2$.

FIGURE 58

EFFECT OF NO ON BANDS at 2250, 1640, 1575, AND 1290 CM^{-1}.

1). ----- BANDS REGENERATED; COOLED TO R.I.; EVACUATED TO $1 \cdot 3 \times 10^2$ Nm^{-2}.
2)i. ——— 60 k Nm^{-2} NO ADDED; HEATED TO 300°C; COOLED TO R.I. ; DIFFERENTIAL SPECTROSCOPY USED,
2)ii, ——— AS 2.i.   ''   ''   400°C;   ''   '' ;   ''   ''   ;
2)iii. —·— AS 2ii   ''   ''   ''   ''   ''   FOR THE THIRD TIME; COOLED TO R.I., EVACUATED TO $1 \cdot 3 \times 10^2$ Nm^{-2}.

FIGURE 59

EFFECT OF H₂ ON BANDS at 2250,1640,1575 AND 1290 CM⁻¹

1). ——— BANDS REGENERATED; COOLED TO R.T.; EVACUATED TO 1·3×10⁻² Nm⁻².
2)i. ------ 60 kNm⁻² H₂ ADDED; HEATED TO 400°C; COOLED TO R.T.
2)ii. — — AS 2i   ;   "   "   ;   "   "
2)iii. —··— AS 2ii   ;   "   "   ;   "   "

%.TRANSMISSION

CM⁻¹
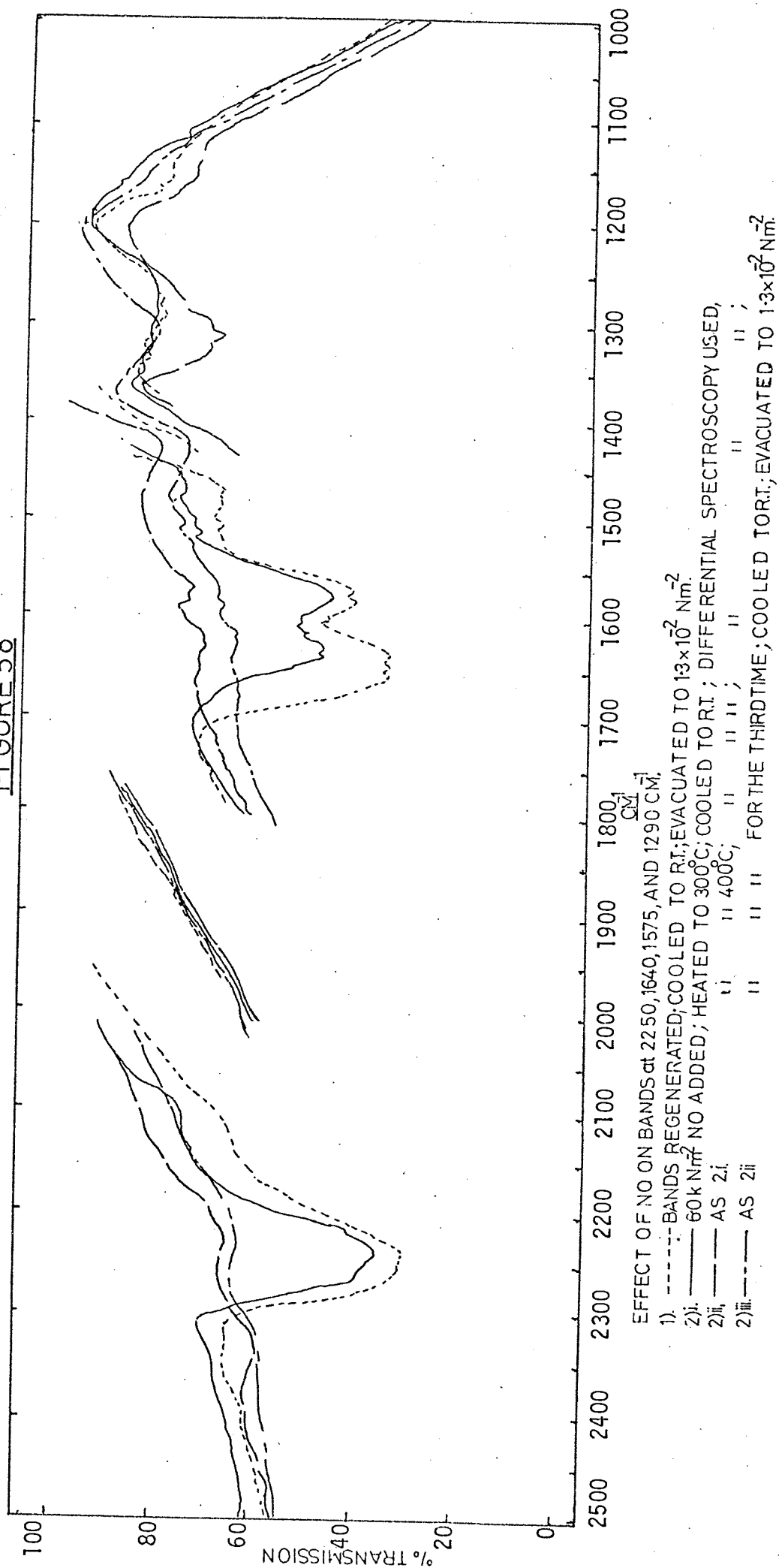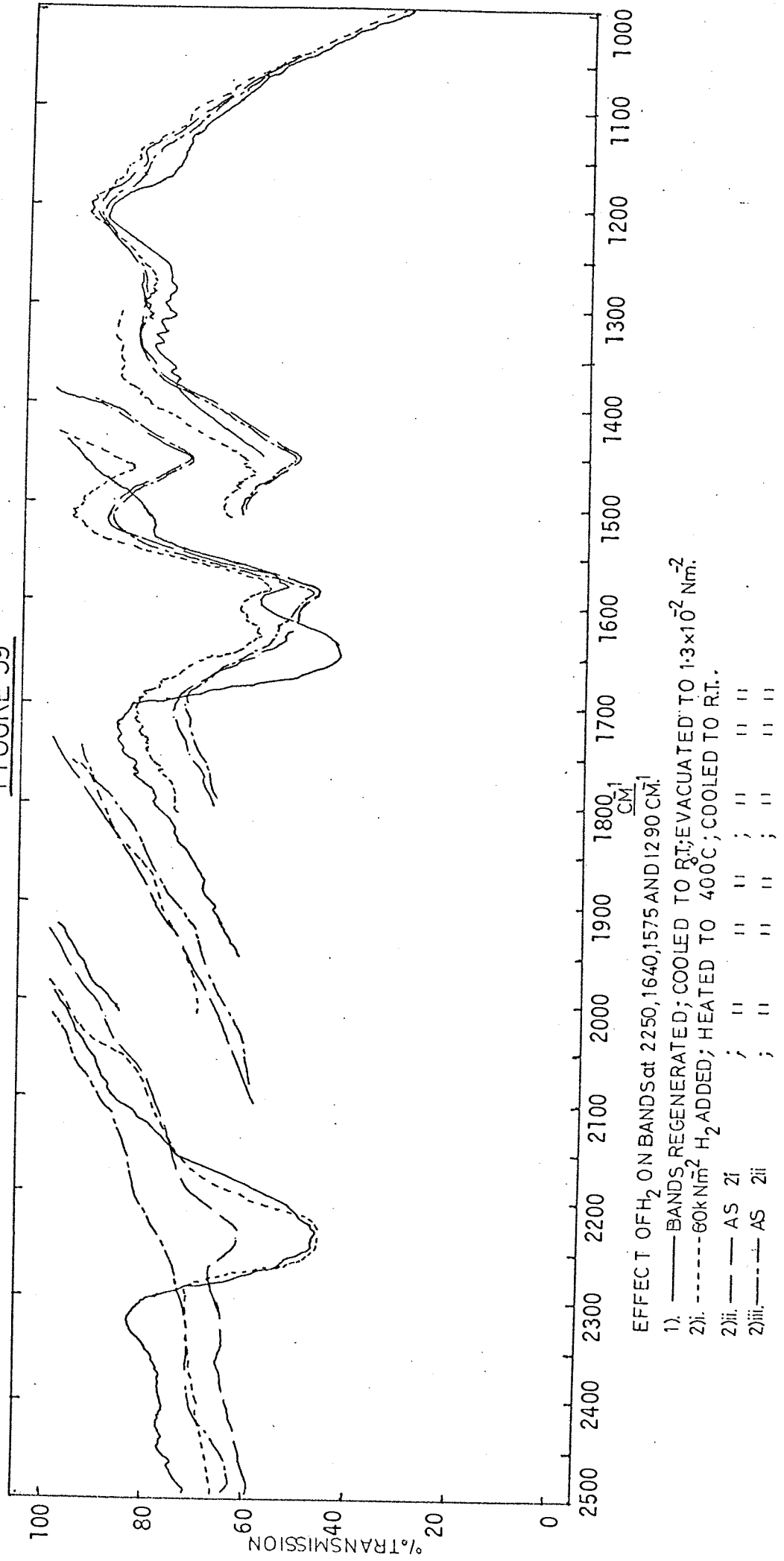
TABLE 22

REPRESENTS EXAMPLES OF THREE MAIN TYPES OF CARBONATE STRUCTURES
TOGETHER WITH THEIR ABSORPTION FREQUENCIES
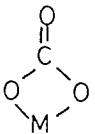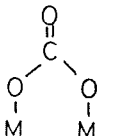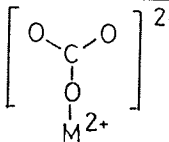
FREQUENCY cm^{-1}	STRUCTURE	CLASSIFICATION
1560 - 1580 cm^{-1} and 1320 - 1380 cm^{-1}		bidentate carbonate type II
1620 - 1640 cm^{-1} and 1220 cm^{-1}		bidentate carbonate type I
1440 - 1350 cm^{-1}		symmetrical carbonate ion

TABLE 23

SHOWS THE INFRARED ABSORPTION BANDS WHICH HAVE BEEN REPORTED FOR THE
ADSORPTION OF CARBON MONOXIDE AND CARBON DIOXIDE ON ALUMINA

	FREQUENCY cm^{-1}	REFERENCE
CO/Al_2O_3	2200,1820,1780,1640,1480,1233	116 117
CO_2/Al_2O_3	1770,1640,1480,1232	116 117
Background peak	~1370	114 115

TABLE 24

LISTS THE RANGE OF INFRARED ABSORPTION FREQUENCIES DUE TO NITRIC OXIDE
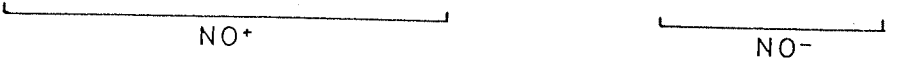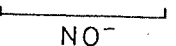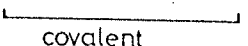
FREQUENCY cm^{-1}						REFERENCE
2100	1900	1700	1500	1300	1000	
NO^{+}				NO^{-}		16 18
	NO^{-}					120
covalent						18 85

TABLE 25

REPRESENTS EXAMPLES OF METAL NITROSYL COMPLEXES WHICH HAVE NO STRETCHING

FREQUENCIES IN THE REGION OF 1650 - 1500 cm^{-1}

NITROSYL COMPLEXES	(NO) cm^{-1}	REFERENCE
$Os(NO)_2(OH)L_2^+$	1632 dinitrosyl	121
$Ir(NO)Cl_2L_2$	1560	122
$Ir P(NO)_2 Br$	1540 1500 dinitrosyl	85
$[V(NO)(CN)_5]^{5-}$	1575 $(NO)^-$	16
$[Cr(NO)(CN)_5]^{4-}$	1515 $(NO)^-$	123
$(C_5H_5)_3 Mn_2(NO)_2$	1515 bridged	16
$NO - Al_2O_3$ interactions	1700 - 1600	18

TABLE 26

SHOWING UNLANDS ASSIGNMENTS OF THE MAJOR ABSORPTION BANDS (cm^{-1}) WHICH
ARE FORMED ON THE CATALYST SURFACE DURING THE REDUCTION OF NITRIC OXIDE
BY AN EXCESS OF CARBON MONOXIDE AND THOSE OBTAINED IN THIS STUDY. THE
ASSIGNMENTS MADE IN THIS STUDY ARE BASED ON THE ASSUMPTION THAT ALL THE
BANDS WITH THE EXCEPTION OF 1465 cm^{-1} ARE INTERRELATED:
* = MINOR CONTRIBUTIONS

Unlands Bands Obtained For 5% Pd-Al_2O_3 cm^{-1}	2264	1635	1571	-	-
Assignments	NCO	$(>C=N)$	CO_3^{2-}, NO_3^-	-	-
This study Bands Obtained For 10% w/w Pd-Al_2O_3	2250	1640	1575	1465	1290
Assignments	$\nu(NCO)$	1) $\underset{N}{\overset{N}{>}}(C=O)$ 2) $>(C=N)$	$\nu_s(NCO)$ *CO_3^{2-}, NO_3^-	CO_3^{2-}	$(C-N)$

CHAPTER 6

6.0 GENERAL CONCLUSIONS OF THE KINETIC AND INFRARED STUDIES

The catalytic reduction of nitric oxide by carbon monoxide has been investigated using kinetic and infrared studies (sections 1 and 2). The following outlines the general conclusions of this study.

(a) For reaction mixtures containing an excess of nitric oxide amounts of nitrous oxide are formed. Under these conditions the formation of nitrous oxide is common to both palladium and ruthenium catalysts; the ability of these catalysts to promote nitrous oxide formation is in the order Pd>Ru.

(b) The reaction between nitrous oxide and carbon monoxide is catalyzed by palladium and ruthenium in the order Pd>Ru.

(c) Under the experimental conditions used the catalytic decomposition of nitrous oxide is significant on ruthenium. The decomposition is not strongly poisoned by oxygen and obeys first order kinetics. The decomposition of nitrous oxide may be the rate limiting step for the reaction between nitrous oxide and carbon monoxide.

(d) The empirical rate laws which describe the reduction of nitric oxide and nitrous oxide by carbon monoxide over palladium and ruthenium show carbon monoxide is strongly adsorbed on palladium relative to ruthenium, and conversely nitric oxide is more strongly adsorbed on ruthenium than palladium. In the empirical rate laws low orders of reaction were found for which-

ever gas molecule was strongly adsorbed or present in a large excess.

(e) For the reduction of nitric oxide by carbon monoxide over palladium a surface scheme based on the kinetic and infrared data was proposed. The mechanism shows how two molecules of nitric oxide are involved in the reaction. Initially, a carbon monoxide – nitric oxide surface complex is formed; this gives carbon dioxide, leaving a single nitrogen atom on the surface which reacts with a second nitric oxide molecule to give a surface nitrous oxide species. This may react with an adjacent carbon monoxide molecule to give carbon dioxide and nitrogen or in an excess of nitric oxide desorb to form gaseous nitrous oxide. The mechanism also shows how an isocyanate species may be formed from the reaction between a nitrogen atom and carbon monoxide, (in an excess of carbon monoxide).

In the case of the ruthenium catalyst the predominant mechanism depends upon the oxidation state of the catalyst and upon the reactant concentrations. When the catalyst is in a reduced state evidence indicates that the reaction occurs in a similar manner to that envisaged for the palladium catalyst, in that it requires a nitrogen atom intermediate. In the oxidized state, nitrogen is formed by the interaction of two adjacent nitric oxide surface molecules (N – N coupling) and not through an isolated nitrogen atom. It has been suggested that the ruthenium surface interacts with both the nitrogen and oxygen atoms of the nitric oxide molecule.

(f) The relative activity of palladium and ruthenium for the reduction of nitric oxide by carbon monoxide was calculated from the appropriate rate law i.e. for

1) Pd, $r = 2 \times 10^6 (e^{-91.2/RT}) P_{CO}^{-1} P_{NO}^{2}$ molecules. $cm^{-2} sec^{-1}$

2) Ru, $r = 6.3 \times 10^{10} (e^{-82.4/RT}) P_{CO}^{\sim 0.22} P_{NO}^{\sim 0}$ molecules. $cm^{-2} sec^{-1}$

The order activity for this reaction agrees with the order found in the literature[59,101].

(g) Surface isocyanate species are formed on palladium catalysts during the reduction of nitric oxide by an excess of carbon monoxide. This substantiates Unlands[46] work. The following absorption bands are attributed to the isocyanate (or polymeric isocyanate) species 2250, 1640, 1575 and $1290 cm^{-1}$.

The surface isocyanate species are relatively stable and are more likely to be formed as a bi-product on selected sites rather than act as an intermediate during the reduction.

6.0.1. SUGGESTIONS FOR FURTHER WORK

For the reduction of nitric oxide by carbon monoxide over the ruthenium catalyst it has been suggested that the adsorption of nitric oxide involves the interaction of nitrogen and oxygen atoms with the surface. Experiments designed to examine the implication of the oxygen with the surface may further the case for the reaction mechanism described previously. An infrared study of adsorbed nitric oxide on ruthenium, and palladium would show if there are frequencies due to metal – oxygen interactions: these occur between $600 - 350$ cm^{-1}. By comparison of the infrared spectra of ruthenium and palladium surfaces in this spectral region it may be possible to demonstrate that metal – oxygen bonds are formed after exposure to nitric oxide atmospheres in the case of ruthenium. The infrared apparatus used in this work (see chapter 4) has a limited range ($3500 - 1100$ cm^{-1}) and would require modification so that frequencies down to 350 cm^{-1} could be observed. This would entail replacing the NaCl windows and the CaF_2 supporting disc with ones made of CsBr. Furthermore, it is suggested that the "evaporated metal" technique[111] is used for the deposition of the metal onto the CsBr supporting disc.

NO^{18} tracer techniques coupled mass spectrometric analysis could also be used to obtain evidence for Ru-O interactions. In this case it is envisaged that labelled nitric oxide is brought into contact with the surface at reaction temperatures; then pumped off and carbon monoxide added. The observation of a molecular ion 46 (CO_2^{18}) would indicate that Ru-O interactions had taken place. The existing apparatus, and technique could be used for this experiment.

LIST OF FIGURES

FIGURE NO.   DESCRIPTION   PAGE NO.

LIST OF TABLES

REFERENCES

1. The Clean Air Amendment of 1970, Public Law 91-602 U.S.A.

2. J. J. Brogan, "Air Pollution control in transport engines", I. Mech. E., Solihull, November 1971, paper C141/71

3. H. K. Newhall, 12th Internat. symposium on combustion, Pittsburg, 1969, 603.

4. W. E. Bernhardt, ref. 2, paper 149/71.

5. R. Shinnar, Science, 1972, 175, 1357.

6. C. D. Haynes and J. H. Weaving, ref. 2, paper 144/71

7. R. S. Lunt, L. S. Bernstein, J. G. Hansel and E. L. Holt, Society Automotive Engineers, Trans., 1972, 81, paper 720209.

8. D. R. Ashmead, J. S. Campbell, P. Davies and K. Farmery, Society Automotive Engineers, Automotive Engineering Congress, Detroit, Mich., 1974, February 25 - March 1, paper 740249

9. D. M. Yost, H. Russell "Systematic inorganic chemistry of the fifth and sixth - group non metalic elements", Prentice - Hall, New York, 1944.

10. H. Wise and M. F. Frech, J. Chem. Phys., 1952, 20, 22.

11. F. Kaufman and J. R. Kelso, J. Chem. Phys., 1955, 23, 1702.

12. C. S. Howard and F. Daniels, J. Phys. Chem., 1958, 62, 360

13. P. J. Durrant and B. Durrant, "Introduction to advanced inorganic chemistry", Longmans, London, 1962

14. C.A.Coulson, "Valence" 2nd Ed, Oxford University Press, London, 1961.

15. C.C.Addison and J.Lewis, Quart. Rev., 1955, 9, 115.

16. J.Lewis, R.J.Irving and G.Wilkinson, J. Inorg. Nuclear Chem., 1958, 7, 32.

17. W.P.Griffith, J.Lewis and G.Wilkinson, J. Inorg. Nuclear Chem., 1958, 7, 38.

18. A.N.Terenin and L.M.Roev, Spectrochim. Acta, 1959, 15, 274, 946.

19. M.Shelef and J.T.Kummer, Amer. Inst. Chem. Engineers Symp. series, 1971, 67, 115.

20. J.P.Melia, J. Inorg. Nuclear Chem., 1965, 27, 95.

21. G.K.Boreskov, Discuss. Faraday Soc., 1966, 41, 263.

22a. K.J.Laidler, in "Catalysis", P H Emmet, Ed, 1954, 1, Reinhold, New York.

22b. A.Wheeler in "Catalysis", 1955, 2,

23. I.Langmuir, Trans. Faraday Soc., 1921, 17, 607.

24. C.N.Hinshelwood, "Kinetics of chemical change", 1940, 187, Clarendon Press, Oxford.

25. G.E.Green and C.N.Hinshelwood, J. Chem.Soc., 1926, 129, 1709.

26. P. W. Bachman and G. B. Taylor, J. Phys. Chem., 1929, 33, 447.

27. J. Zawadski and G. Perlinsky, Compt. rend., 1934, 198, 260.

28. R. R. Sakaida, R. G. Rinker, Y L Wang and W H Corcoran, Amer. Inst. Chem. Engineers J., 1961, 7, 658.

29. J. M. Fraser and F. Daniels, J. Phys. Chem., 1958, 62, 215.

30. W. E. Addison and R M. Barrer, J. Chem. Soc., 1955, 757.

31. E. L. Yuan, J. I. Slaughter, W. E. Koerner and F. Daniels, J. Phys. Chem., 1959, 63, 952.

32. M. Shelef, K. Otto, and H. Gandhi, Atmos. Environ., 1969, 3, 107.

33. D. R. Cooper, A. M. G. Law and B. J. Tighe, Brit. Polymer J., 1973, 5, 163

34. D. R. Cooper, Ph.D Thesis, University of Aston in Birmingham 1974.

35. F. R. Taylor, "Elimination of oxides of nitrogen from automobile exhaust", Air pollution foundation report, 1959, Rept 28.

36. S. Sourirajan and J. L. Blumenthal, Internat. J. Air Wat. Pollut., 1961, 5, 25.

37. J. F. Roth and R. C Doerr, Ind. and Eng. Chem., 1961, 53, 293.

38. R.J.Ayen and Yu-Sim. Ng, Internat. J. Air Wat. pollut., 1966, 10, 1.

39. M.Shelef, K.Otto and H.Gandhi, J. Catalysis, 1968, 12, 361

40. R.A.Baker and R.C.Doerr, Ind. and Eng. Chem., (Process Design), 1964, 4, 189.

41. M.Shelef and K.Otto, J. Catalysis, 1968, 10, 408.

42. E.L.Force and R.J.Ayen, Chem.Eng. Progr., Symp., 1973, 31, 32.

43. J.R.Kittrell, R.Mezaki, and C.C.Watson, Ind. and Eng. Chem., 1965, 57, 18, IBID Brit. Chem.Eng., 1966, 11, 15.

44. J.W.London and A.T.Bell, J. Catalysis, 1973, 31, 32.

45. J.W.London and A.T.Bell, J. Catalysis, 1973, 31, 96.

46. M.L.Unland, J. Phys. Chem., 1973, 77, 1952.

47. M.L.Unland, Science, 1973, 179, 567.

48. M.L.Unland, J. Catalysis, 1973, 31, 459.

49. C.E.H.Bawn, Trans. Faraday Soc., 1935, 31, 461.

50. R.F.Strickland-Constable, Trans. Faraday Soc., 1938, 34, 1074, and 1374.

51. D.G.Madley and R.F.Strickland - Constable, Trans. Faraday Soc., 1953, 49, 1312.

52. K.Tanaka, G.Blyholder, J. Phys. Chem., 1972, 76, 1807.

53. C.A.Leach and M.S.Peters, Amer. Inst. Chem. Engineers Symp. series, 1973, 68, 75.

54. S.Weller, Amer. Inst. Chem. Engineers J., 1956, 2, 59, and 62.

55. "Gmelins Handbuch of Anorg. Chemie", 8 ed. Verlag. Chemie., Weinheim and Berlin, Syst. 4, Stickstoff 1936, 719.

56. R.G.Kokes, J. Phys. Chem., 1966, 70, 296.

57. M.Shelef and H. Gandhi, Ind. and Eng. Chem. (Product Res. and Development), 1972, 11, 1, and 393.

58. J.C.Varuli and R.D.Gonzalez, Ind. and Eng. Chem. (Product Res. and Development), 1973, 12, 171.

59. K.C.Taylor and R.L.Klimisch, J. Catalysis, 1973, 30, 478.

60. R.J.Ayen and M.S.Peters, Ind. and Eng. Chem. (Process Design), 1962, 1, 204.

61. K.Otto, M.Shelef and J.T.Kummer, J. Phys. Chem., 1970, 74, 2690.

62. K.Otto, M.Shelef and J.K.Kummer, J. Phys. Chem., 1971, 75, 875.

63. K.Otto and M.Shelef, 7, Phys. Chem., (Frankfurt), 1973, 85, 308.

64. R.L.Klimisch and K.C.Taylor, Environ.Sci.Technol., 1973, **7**, 127.

64b. IBID, Ind. and Eng.Chem.(Product Res.and Development), 1975, **14**, 26.

65. J.W.Ault and R.J.Ayen, Amer.Inst.Chem.Engineers, J., 1971, **17**, 265.

66. M.Shelef and H.S.Gandhi, Ind. and Eng. Chem.(Product Res. and Development), 1974, **13**, 80.

67. D.W.McKee, J. Catalysis, 1967, **8**, 240.

68. K.C.Taylor, R.M.Sinkevitch, and R.L.Klimisch,J.Catalysis, 1974, **35**, 34.

69. J.D.Butler, J. Chem.Soc.(B), 1968, 905.

70. A.I.Vogel, "Quantitative inorganic analysis", 2nd Ed. Longmans.

71. J.C.Russ "Energy dispersion x-ray analysis; x-ray and electron probe analysis", Amer.Soc.for testing and materials; Special technical publication, 485 04-485000 - 39, 73rd meeting June 1970, 21, Toronto, Canad.

72. S.Brunauer, "The adsorption of gases and vapours", 1945, 1, Oxford University Press.

73. S. *Brunauer* and P. H. Emmett, J. Amer. Chem.Soc., 1937, 59, 1553.

74. D. D. Eley and C. F. Knights, Proc. Roy.Soc.,1966,(A)294,1.

75. R. P. Eischens, S. A. Frances, and W. A. Pliskin, J. Phys.Chem., 1956, 60, 194.

76. R. L. Park and H. H. Madden, Surface Sci.,1968,11, 188.

77. A. Palazov, C. C. Chang and R. J. Kokes,J.Catalysis,1975,36, 338.

78. H. Dunken and H. Hobert, Z. Chem., 1963, 3, 398.

79. N. W. Cant and P. W. Fredrickson, J. Catalysis,1975,37, 531.

80. R. Eisenberg and C. D. Meyer,Accounts Chem.Res.,1975,8, 26.

81. J. B. Peri, J. Phys. Chem., 1974, 78, 588.

82. E. L. Kugler and R. J. Kokes, J. Catalysis, 1975, 36, 142.

83. E. L. Kugler and J. W. Gryder, J. Catalysis, 1975,36, 152.

84. S. Bhaduri, B. F. G. Johnson, C. J. Savory, J. A. Segal, and R. H. Walter, Chem. Comm., 1974, 809.

85. B. L. Haymore and J. A. Ibers, J. Amer.Chem.Soc.,1974,96,3325.

86. F. S. Karn, J. F. Shultz and R. B. Anderson, Ind. and Eng. Chem. (Product Res.Development), 1965, 4, 265.

87. R. A. Della Betta, A. G. Piken and M. Shelef, J. Catalysis, 1974, 35, 54.

88.   R.J.H.Voorhoeve and L.E.Trimble, J. Catalysis,1975,
       38, 80.

89.   M.Kobayashi and T.Shirasaki, J.Catalysis,1974, 32,254.

90.   H.P.Bonzel and T.E.Fischer, Surface Sci.,1975, 51,213.

91.   S.A.Isa and J.M.Saleh, J. Phys.Chem., 1972,76, 2530.

92.   R.Suhrmann, Adv.Catalysis, 1955, 7, 339.

93.   E.R.S.Winter, J. Catalysis, 1969, 15, 144.

94.   E.R.S.Winter, J. Catalysis, 1974, 34, 431.

95.   M.Onchi and H.E.Farnsworth, Surface Sci., 1969,13,425.

96.   J.F.Read, J. Catalysis, 1973, 28, 428.

97.   I.D.Gay and F.C.Tompkins, Proc.Roy.Soc.,1966,(A)293,19.

98.   E.R.S.Winter, J. Chem.Soc. (A), 1968, 2889,

99.   C.N.Hinshelwood and C.R.Prichard, J. Chem.Soc.,1925,
       127, 327.

100.   J.P.Redmond, J.Phys. Chem., 1963, 67, 788.

101.   T.P.Kobylinski and B.W.Taylor,J.Catalysis,1974,33,376.

102.   J.H.Sinfelt,Catalysis Rev.,1969,3,175, H Heinemann Ed.

103.   L.Brewer, Chem. Rev., 1953, 52, 1.

104.   G.V.Samsonov Ed. "The oxide Handbook",1973,Plenum, New
       York, London.

105.   R.F.Baddour, M.Model and U.K.Heusser,J.Phys. Chem.,1968,
       72, 3621

106.   G.C.Bond, "Catalysis by Metals," 1962, Academic Press,
       London and New York.

107.   E.Kikuchi, M.Tsurumi and Y.Morita, J. Catalysis, 1971, 22, 226.

108.   A.Tomita and Y.Tamai, J. Catalysis,1972, 27, 293.

109.   J.Bugosh, R.L.Brown, J.R.McWhorter, G.W.Sears and R.S. Sippel, Ind. and Eng. Chem. (Product Res. and Development), 1962, 1, 157.

110.   J.Bugosh, U S Patent 2,915,475, December 1959.

111.   M.L.Hair, "Infrared spectra in surface chemistry", 1967, Edward Arnold.

112.   L.H.Little, "Infrared spectra of adsorbed species", 1966, Academic Press, London and New York.

113.   J.D.Butler and T.C.Poles, J. Chem. Soc. Perkin Trans. II, 1973, 41.

114.   A.Zecchina, S.Coluccia, E Gugielminotti and B.Ghiotti, J. Phys. Chem., 1971, 75, 2790.

115.   L.H.Little and G.H.Amberg, Canad. J. Chem., 1962, 40, 1997.

116.   N.D.Parkyns, J. Chem. Soc.(A), 1967, 1910.

117.   N.D.Parkyns, J. Chem. Soc.(A), 1969, 410.

118.   N.V.Sidewick and R.W.Bailey, Proc.Roy.Soc.,1934,A 144, 521.

119.   K. Nakamoto, "Infrared spectra of inorganic and co-
       ordination compounds", 1970, 2nd Ed.

120.   P. Gans, Chem. Comm., 1965, 144.

121.   J. M. Walters and K. R. Whittle, Chem. Comm. 1971, 518.

122.   D. M. P. Mingos and J. A. Ibers, Inorg. Chem. 1971, 10, 1035.

123.   W. P. Griffith, J. Lewis and G. Wilkinson, J. Chem. Soc.,
       1959, 872; 1635; 1775.

124.   V. Horn and P. Pretzold, Spectrochim. Acta, 1974, 30A,
       1489.

125.   D. Forster and D. M. L. Goodgame, J. Chem. Soc., 1965, 1286.

126.   F. A. Miller and G. L. Carlson, Spectrochim. Acta, 1961,
       17, 977.

127.   A. N. Norbury and A. I. P. Sinha, J. Chem. Soc.(A), 1968,
       1598.

128.   R. G. Arnold and J. A. Nelson, Chem. Rev., 1957, 57, 47.

129.   J. H. Taylor and G. H. Amberg, Canad. J. Chem., 1961, 17,
       953.

130.   J. J. Levison and S. D. Robinson, J. Chem. Soc. (A), 1971,
       762.

131.   L. J. Bellamy, "The infrared spectra of complex molecules",
       1958, Methuen Co, London.

132.   A.Yamaguchi, R.B.Penland, S.Mizushima, T.S.Lane,
       C.Curran and J.V.Quagliano, J. Amer.Chem.Soc.,1958,
       80, 527.

133.   H.Conrad, G.Ertyl, E.Latta, J. Catalysis, 1974, 35,
       363.

134.   K.Kraemer and D.Menzel, Verh. Deut. Phys. Ges., 1973,
       8, 441 (VI).   [as quoted by reference 133]